

Ergonomic Risk Assessment in Construction Manufacturing Facilities

by

Xinming Li

A thesis submitted in partial fulfillment of the requirements for the degree of

Doctor of Philosophy

in

Construction Engineering and Management

Department of Civil and Environmental Engineering
University of Alberta

© Xinming Li, 2017

ABSTRACT

The construction manufacturing industry in North America has a disproportionately high number of lost-time injuries due to the high physical demand of the labour-intensive tasks it involves. It is essential to investigate the physical demands of body movement in the construction manufacturing workplace in order to proactively identify worker exposure to ergonomic risk. This research thus analyzes the primary ergonomic risk factors that cause work-related injuries: awkward body posture, overexertion, and repetitive motion.

This research first develops a framework to approach an improved physical demand analysis for risk identification, evaluation, and mitigation by providing modified work. The framework is implemented in a manufacturing industry facility, and four main ergonomic risk identifications, together with the corresponding modified work, are recommended. Second, a framework of assessing muscle force and muscle fatigue development due to manual repetitive lifting tasks using surface electromyography (sEMG), kinematic motion capture, and human body modelling is also proposed. The results show that sEMG is capable of visualizing muscle activity. However, it is limited to identifying muscle fatigue development of bulkier and superficial muscle bundles in low fat areas. Physiological measurements also have technical, ethical, cost, and real-life implementation limitations. This research thus further investigates an innovative framework for converting observational or video-captured body movements in an actual construction manufacturing plant into 3D modelling for ergonomic risk assessment of continuous motions. The proposed 3D motion-based risk assessment methodology is validated through the aforementioned motion capture experiment to prove the reliability of the framework. The integration between the first and third framework is also proposed and implemented in modular construction operations. Thus the capability of 3D modelling is extended to support the

optimization of human body movement and the re-design of the workplace accordingly to mitigate the ergonomic risks inherent in operational tasks. Modified work recommendations are expected as a result of this research, which facilitates the establishment of a more robust return-to-work program for various industries. Ultimately, the goal is to proactively curtail workplace injuries and claims and thereby reduce workers' compensation insurance costs.

PREFACE

This thesis is the original work of the author, Xinming Li. Three journal papers and three conference papers related to this thesis have been submitted or published and are listed as below.

This thesis is organized in paper format following the paper-based thesis guidelines.

1. Li, X., Gül, M. and Al-Hussein, M. “A risk assessment framework based on an improved physical demand analysis for the building and manufacturing industries.” *International Journal of Industrial Ergonomics* (Under review).
2. Li, X., Han, S., Gül, M., Al-Hussein, M. and El-Rich, M. “3D motion-based rapid ergonomic risk assessment framework and its validation method.” *Journal of Construction Engineering and Management* (Under review).
3. Li, X., Komeili, A., Gül, M., and El-Rich, M. (2017). “A framework for evaluating muscle activity during repetitive manual material handling in construction manufacturing.” *Automation in Construction*, 79, pp. 39–48.
4. Li, X., Han, S., Gül, M., and Al-Hussein, M. (submitted). “Automated ergonomic risk assessment based on 3D visualization.” *Proceedings, 34th International Symposium on Automation and Robotics in Construction*, Taipei, Taiwan, June 28-July 1, 2017 (under review).
5. Li, X., Han, S., Gül, M., and Al-Hussein, M. (2016). “3D motion-based ergonomic and body posture analysis in construction.” *Proceedings, Modular and Offsite Construction (MOC) Summit*, Edmonton, AB, Canada, Sep. 29-Oct. 1, pp. 215–223.
6. Komeili, A., Li, X., Gül, M., Lewicke, J., and El-Rich, M. (2015). “An evaluation method of assessing the low back muscle fatigue in manual material handling.” *Proceedings, Modular and Offsite Construction Summit*, Edmonton, Alberta, Canada, May 19-21, pp.

467–475.

7. Li, X., Fan, G., Abudan, A., Sukkarieh, M., Inyang, N., Gül, M., El-Rich, M., Al-Hussein, M. (2015). “Ergonomics and physical demand construction manufacturing facility analysis.” *Proceedings, 5th International/11th Construction Specialty Conference*, Vancouver, British Columbia, Canada, Jun. 8-10.

The research project of which this thesis is a part received research ethics approval from the University of Alberta Research Ethics Board, Project Name “3D Motion-Based Ergonomic and Physical Demand Analysis in Construction”, No. Pro00069136, Feb. 1st, 2017.

ACKNOWLEDGEMENTS

First and foremost, I would like to thank my supervisors, Dr. Mohamed Al-Hussein and Dr. Mustafa Gül, for their immense support, inspiration, visionary guidance, and great patience throughout my studies. I am also grateful to my supervisory and examining committee, Dr. Yasser Mohamed, Dr. Carl Haas, Dr. Marwan El-Rich, Dr. Hossein Rouhani, and Dr. Rafiq Ahmad, for their review of my dissertation and their invaluable comments.

In addition, I would like to express my thanks to Jonathan Tomalty and Claire Black for editing my thesis and for valuable suggestions on my publications. I would also like to extend acknowledgement to my dear colleagues and friends, Sang, Youyi, Xiaoxi, Hexu, Lei, Sadiq, Hamid, Chelsea, Amin, Tao, Gordon, Hongru, Hongxian, Tanzania, Hamida, Gurjeet, Val, Qusai and Jacek for their continuous moral support.

Especially, my deepest gratitude is given to my parents, Qingyi Li and Yanfei Li, as well as my family, who have been an immense support behind me over the years. They have always encouraged me during this journey. My husband, Bo Zhang, is also very much appreciated for his kind and continuous company through this phase of my life.

TABLE OF CONTENTS

ABSTRACT.....	ii
PREFACE.....	iv
ACKNOWLEDGEMENTS.....	vi
TABLE OF CONTENTS.....	vii
LIST OF FIGURES	xi
LIST OF TABLES.....	xiii
LIST OF ABBREVIATIONS.....	xv
Chapter 1: INTRODUCTION	1
1.1 Background and Motivation	1
1.1.1 Physical demand analysis and modified work	3
1.1.2 Risk assessment tools.....	4
1.1.3 Physical data collection methods	5
1.2 Research Objectives.....	6
1.3 Thesis Organization	8
Chapter 2: PHYSICAL DEMAND ANALYSIS.....	10
2.1 Introduction.....	10
2.2 Current Physical Demand Analysis	14
2.3 Existing Risk Assessment Tools and Guidelines.....	16
2.4 Improved Physical Demand Analysis for Risk Assessment.....	19
2.4.1 Implementation method	21
2.4.1.1 Data collection	23
2.4.1.2 Time study	24

2.4.1.3	Supplementary information	25
2.4.2	Case study	26
2.4.2.1	PDA implementation in a window glazing station	26
2.4.2.2	Assessment and identification of ergonomic risks.....	29
2.5	Limitations	33
2.6	Conclusion	33
2.7	Acknowledgements.....	34
Chapter 3: EVALUATION OF MUSCLE ACTIVITY DURING REPETITIVE MANUAL		
MATERIAL HANDLING		
3.1	Introduction.....	35
3.2	Muscle Fatigue Identification Method.....	38
3.2.1	Motion capture and sEMG.....	40
3.2.1.1	Data acquisition	40
3.2.1.2	Maximum voluntary contraction and test procedure	44
3.2.1.3	Post-processing	46
3.2.2	Human body modelling.....	49
3.2.3	Proactive ergonomic analysis	51
3.3	Results and Discussion	51
3.4	Conclusion	58
3.5	Acknowledgements.....	59
Chapter 4: 3D MOTION-BASED ERGONOMIC RISK ASSESSMENT AND ITS		
VALIDATION		
4.1	Introduction.....	60

4.2	Literature Review.....	61
4.2.1	Existing body motion data collection methods.....	61
4.2.2	3D visualization method.....	62
4.3	3D Motion-based Ergonomic Risk Assessment Method.....	64
4.4	Validation Approach.....	68
4.4.1	Validation methods.....	70
4.4.2	Validation results.....	72
4.4.2.1	Joint angle comparison.....	73
4.4.2.2	REBA/RULA risk rating comparison for body segments.....	74
4.4.2.3	REBA/RULA total risk rating and risk level comparison.....	77
4.4.3	Validation discussion.....	80
4.5	Conclusion.....	84
4.5.1	Validation summary.....	84
4.5.2	Limitations and future study.....	85
4.6	Acknowledgements.....	86
Chapter 5: 3D MOTION-BASED PHYSICAL DEMAND AND ERGONOMIC ANALYSIS		87
5.1	Integration of Physical Demand Analysis and 3D Modelling.....	87
5.2	3D Modelling Data Acquisition and Post-data Processing Algorithm.....	90
5.2.1	3D modelling data acquisition.....	90
5.2.2	3D modelling post-data processing and risk rating algorithm.....	99
5.3	Implementation of 3D Motion-based Physical Demand Analysis in a Case Study....	109
5.3.1	Installation of insulation by four different methods.....	111
5.3.2	Adjust the workstation design.....	117

5.3.3 Case study conclusions	119
5.4 Conclusion	121
Chapter 6: CONCLUSIONS.....	123
6.1 Research Summary	123
6.2 Research Contributions.....	125
6.3 Limitations and Future Research	126
References.....	129
Appendix A.....	150
Appendix B.....	153
Appendix C.....	156
Appendix D.....	157

LIST OF FIGURES

Figure 2.1: Framework for improved PDA-based risk assessment	13
Figure 2.2: Window glazing station motions	27
Figure 3.1: Description of research framework	40
Figure 3.2: (a) sEMG sensors location; (b) Reflective markers attached to specific anatomical locations	42
Figure 3.3: Positions of 36 reflective markers used to drive the AnyBody model	42
Figure 3.4: Body posture and procedures of maximum voluntary contraction test: a. back flexion; b. abdominal extension	45
Figure 3.5: Configuration of a full cycle lifting task with two epochs corresponding to experimental sEMG raw data.....	46
Figure 3.6: Normalized sEMG parameters of CH 1-8 obtained from subject 1 in trial 2. (Curves marked with/without circles represent muscles in the left/right side, respectively)	53
Figure 3.7: Inter-trial variation of sEMG parameters for subject 1 CH6 (left longissimus)	54
Figure 3.8: Comparison of power-frequency curves of CH5 (right longissimus) in trial 1 and trial 2 for subject 3.....	54
Figure 3.9: Comparison between the sEMG RMS and predicted muscle forces obtained from human body model.....	56
Figure 3.10: Comparison of the calculated normalized area related to RMS sEMG and muscle force curves presented in Figure 3.9; C: Correlation Coefficient.....	57
Figure 4.1: Overall methodology and framework of proposed ergonomic risk assessment.....	64
Figure 4.2: Schematic drawings of 41 joint angles.....	67
Figure 4.3: Motion capture lifting task and its five key motions.....	70

Figure 4.4: Joint angle comparisons of body segment3-subject 3	75
Figure 4.5: Trunk flexion comparisons-subject 3	76
Figure 4.6: REBA risk rating for body segments-subject 3	76
Figure 4.7: REBA/RULA total risk rating and risk level comparison for entire motion—subject 3	79
Figure 5.1: 3D motion-based physical demand and ergonomic analysis methodology	90
Figure 5.2: Example file of obtaining joint angles and batch file generation.....	91
Figure 5.3: Developed user interface of the proposed method in 3ds Max	101
Figure 5.4: Risk assessment sample final REBA risk rating and detailed individual rating for each body segment.....	102
Figure 5.5: Joint angle raw data at each time frame with its risk assessment method (REBA or RULA)	103
Figure 5.6: Trunk lateral bending angles from the three subjects in the experiment during lifting tasks.....	107
Figure 5.7: Leg angles from the three subjects in the experiment during lifting tasks.....	108
Figure 5.8: Difference between left and right leg angles among subjects in the experiment during lifting tasks.....	109
Figure 5.9: Four scenarios for placing insulation	113
Figure 5.10: REBA and RULA results from four scenarios of placing insulation	114
Figure 5.11: Three scenarios with different workstation tilt angles	117
Figure 5.12: REBA and RULA risk comparison for the three scenarios.....	119
Figure 5.13: REBA and RULA body segment risk comparison for the three scenarios	119

LIST OF TABLES

Table 2-1: Content of existing PDA templates	16
Table 2-2: Risk assessment tools	18
Table 2-3: Proposed physical demand analysis form	21
Table 2-4: REBA score for glazing task	28
Table 2-5: RULA score for glazing task	28
Table 3-1: Reflective markers position descriptions and marker names in the AnyBody model.	43
Table 3-2: Four pairs of muscle activities recorded by eight sEMG channels.	47
Table 3-3: Heartbeat rates of subjects during lifting task at the end of each trial.	51
Table 4-1: REBA/RULA rating comparison of trunk for all three subjects	77
Table 4-2: RULA total risk rating and risk level comparison for all subjects	80
Table 5-1: List of bones in the biped	91
Table 5-2: List of joint angles in order (batch file).....	92
Table 5-3: Joint angle calculation, schematic drawing, and implementation in REBA and RULA	94
Table 5-4: Implementation of joint angles into REBA and RULA calculations	104
Table 5-5: Adjusted REBA risk level category	110
Table 5-6: Adjusted RULA risk level category	111
Table 5-7: REBA and RULA results from four scenarios of placing insulation with max, min, and mean values	114
Table 5-8: REBA and RULA results from three scenarios of placing insulation with risk ratings of each body segment.....	115
Table A-1: Time study table (60-min)	150

Table B-1: Descriptions of marker positions for motion capture data collection.....	153
Table B-2: REBA/RULA rating comparison of each body segment for all subjects	155
Table C-1: REBA/RULA rating comparison of subject 3-another lifting cycle	156
Table D-1: 41 Joint angle schematic drawings.....	157
Table D-2: Scenarios covered by the proposed 3D modelling	160

LIST OF ABBREVIATIONS

PDA	Physical Demand Analysis
MMH	Manual materials handling
MVC	Maximum Voluntary Contraction
WCB	Workers' Compensation Board
REBA	Rapid Entire Body Assessment
RULA	Rapid Upper Limb Assessment
OWAS	Ovako Working-posture Analysing System
NIOSH	National Institute for Occupational Safety and Health
PEO	Portable Ergonomic Observation
PATH	Posture Activity Tools Handling
3D	Three Dimensional
EMG	Electromyograms
sEMG	Surface electromyograms
RMS	Root-Mean Square
ARV	Average Rectified Value
MNF	Mean Frequency
MDF	Median Frequency
LBP	Low back pain
ASIS	Pelvis-anterior superior iliac
PSIS	Pelvis-posterior superior iliac
CH	Channels
DOFs	Degrees of Freedoms
WMSDs	Work-related Musculoskeletal Disorders
DLL	Dynamic-link Library

CHAPTER 1: INTRODUCTION

1.1 Background and Motivation

A recent study of fatal and nonfatal injury rates in the construction sectors of ten industrialized countries shows fatal injury rates ranging from 3.3 to 10.6 deaths per 100,000 workers and nonfatal injury rates ranging from 1.0 to 10.8 injured per 100 workers. The United States and Canada in particular suffer relatively high fatality rates of 9.7 and 8.7 (The Center for Construction Research and Training 2012). The Association of Workers' Compensation Boards of Canada (2015) reports that the manufacturing and construction industries had the second and third highest number of lost-time claims due to injuries in 2015, accounting for 14% and 11%, respectively, of the total workplace injury claims (232,629) in Canada. In the United States, the manufacturing and construction industries accounted for 11% and 7%, respectively, of all nonfatal occupational injuries and illnesses in 2015 (Bureau of Labor Statistics 2016). Thus, improving workplace safety practice in order to reduce work-related injuries in the manufacturing and construction industries is a top priority.

In this context, modular building construction is becoming a more widely recognized construction paradigm, in which building components are manufactured off site. Benefits of the modular building approach include an environmentally-friendly construction process, reduced construction cycle time, and waste reduction at cost-competitive prices. Although modular manufacturing is evolving with the introduction of automated and semi-automated machinery, considerable physical efforts are still required for the operational tasks in the modular manufacturing process.

Repetition of motion, forceful exertion, and awkward body posture are the three primary factors that may cause work-related musculoskeletal disorders (WMSDs), including injuries and disorders of the muscles, tendons, and nerves (Public Services Health & Safety Association (PSHSA) 2010; Canadian Centre for Occupational Health and Safety 2017; Ontario Safety Association for Community and Healthcare 2010). Given the ergonomic risks inherent in their existing work processes, companies attempt to design injury-free workplaces. It is recommended that high physical demand operational work can be controlled by proper education, job and task rotation, frequent rest breaks, stretching exercises, modification to the work site, and assistive devices (PSHSA 2010). During repetitive work, fatigue is a common sign and symptom of metabolic disorder and neuromuscular disease. In efforts to eliminate the risk of muscle injury, the role of muscle fatigue cannot be overlooked. Fatigue is a key indicator to assist with designing an optimal job rotation program and working schedule. In addition, to avoid forceful exertion and potentially detrimental physical motion for workers, the re-designing of workstations may be necessary; however, changes in the plant may introduce the risk of a decrease in productivity since ergonomic design may not be optimum for productivity, and because time and investment may be required in order to complete renovations in the plant and workers will have to adjust to the new plant layout. Taking into consideration ergonomic factors in the design phase can thus proactively mitigate ergonomic risks and reduce the need for future investment on re-structuring or re-designing the workstations. Therefore, integrating ergonomic assessment in the planning and execution of construction tasks is essential for all physical work-related operations.

1.1.1 Physical demand analysis and modified work

In order to gain knowledge about the tasks involved at each workstation, a systematic approach recommended by workers' compensation boards (WCBs) is to perform a physical demand analysis (PDA). PDA is a procedure used to assess and quantify the physical, sensory, and environmental demands of tasks station by station in a given work environment. Companies utilize PDA as one of the proactive approaches for ergonomic risk identification, injury prevention, employee recruitment, training, and job assignment (Industrial Accident Prevention Association 2009). In the PDA approach, the task information, strength demands of a job, frequency of each motion, sensory demands, and environmental conditions can be recorded. The contents of the PDA are vital inputs for ergonomic risk assessment and for providing modified work. Providing the proposed modified work and the change of task manoeuvres to workers allows them to continue to work and add value to the company with reduced ergonomic risk, especially for injured workers on return-to-work programs. Modified work also helps with retention of experienced workers, reduces return-to-work time, solidifies the worker relationship with the employer, boosts worker morale, improves the employer's reputation, and reduces insurance claims and training costs (WCB-Alberta 2015). However, in current practice PDA does not contain sufficient information for ergonomic risk assessment, a deficiency which also limits the development of modified work and solutions to improve safety and to promote proactively a healthier work environment. Thus, there is potential to establish improved PDA practice by gaining better understanding of the various workstation tasks and to provide organized documentation for review by the WCB. In addition, for the injured worker, health care professionals, physicians, or rehabilitation therapists are also able to review this improved PDA in order to assist the worker to recover, to define whether or not the worker is ready to return to

the previously assigned occupational workstation, and ultimately to streamline the worker's return to work. As a result, an improved PDA with risk assessment also helps to determine if the new occupational workstation assignment is in keeping with the medical restrictions and physical ability of the worker.

1.1.2 Risk assessment tools

Rapid Entire Body Assessment (REBA) and Rapid Upper Limb Assessment (RULA) are commonly used by researchers for ergonomic risk assessment, and they are also selected as the supportive risk assessment methods for the development of the research frameworks presented in this thesis. REBA objectively analyzes body postures for all body segments by assigning scores to every segment in the body (Hignett and McAtamney 2000; Middlesworth 2012; Ansari and Sheikh 2014). RULA focuses on upper limb assessment by recording postures, scoring them, and scaling action levels (McAtamney and Corlett 1993; Agrawal 2011; Plantard et al. 2016; Ansari and Sheikh 2014). Escobar (2006) conducts a sensitivity analysis on both REBA and RULA risk assessment tools by using a Pearson's bi-variate correlation test. The trunk, neck, legs, upper arm, and wrist are identified as critical for REBA, with correlations of 0.56, 0.52, 0.45, 0.32, and 0.14 to the final risk rating, respectively. The upper arm, neck, trunk, and legs are found to be critical for RULA, with correlations of 0.54, 0.49, 0.37, and 0.07, respectively, to the final risk rating. In addition, Levanon et al. (2014) validate the method of modified RULA (which includes minor adjustment of wrist and load rating compared with regular RULA assessment method) for computer workers. Syahril and Sonjaya (2015) also prove the reliability of REBA and RULA methods for geothermal tasks and point out that REBA is more sensitive in risk measurement than are the Quick Exposure Check, RULA, and Strain index methods.

These risk assessment tools, however, require detailed physical data, such as joint angle, in order to complete human body motion analysis. Due to the limitation of obtaining subjective human body posture data from the construction field, Golabchi et al. (2016) develop a method which integrates fuzzy logic with RULA, and which proves to be a more accurate and reliable method than the traditional method, reducing human error from the observation. These risk assessment tools have not been fully implemented in construction cases due to the limitations with respect to the human body posture measurement. Therefore, great potential exists to develop a method by which to obtain body posture data and implement REBA and RULA for risk assessment in order to estimate the body movement magnitude.

1.1.3 Physical data collection methods

Traditional measures to assess work movements during operation rely on direct manual observation and self-report, which are ostensibly subjective, time-consuming, and error-prone. Researchers also invest in both direct and indirect physiological measurements in order to collect human body data for ergonomic and biomechanical analysis, which provide results that are more objective, detailed, and accurate than traditional metrics. Body movements can be obtained by utilizing goniometers, accelerometers, and optimal markers. In order to analyze muscle activity, electromyography (EMG) is commonly used to indicate muscle fatigue (González-Izal et al. 2010; Mathieu and Fortin 2000; Kim et al. 2007; Pah and Kumar 2001). However, these measurements all entail job interruption. The solution here is to conduct indirect physiological measurement by means of a Kinect range camera or computer vision-based approach, which is also commonly used to capture motion and to conduct body posture assessment (Plantard et al. 2016; Khosrowpour et al. 2014; Alwasel et al. 2011; Ray and Teizer 2012; Han and Lee 2013). Some studies (Li and Lee 2011; Han and Lee 2013) use a video-based computer visualization

approach to automatically assess the captured motion. However, all of these measurements have limitations, such as illumination and obstacles in capturing direction, in the real-life implementation in construction manufacturing, and the data post-processing is also time consuming, (David 2005; Li and Buckle 1999). Alternatively, human subjects are commonly utilized to simulate tasks in a laboratory setting in order to imitate the task and utilize direct and indirect measurements to capture the motion and to record physiological data for further ergonomic analysis. It should be noted that laboratory-based simulation can represent tasks with a reasonable level of detail and accuracy (comparing alternative methods), and can thereby facilitate effective ergonomic risk assessment (providing adequate information as the input to these risk assessment tools). However, a laboratory setting will have space limitations compared to the field, and thus can only accommodate the simulation of elemental tasks. In addition, the experimentation in this setting is usually subject to ethical, technical, and cost issues, and it also requires time-consuming data post-processing and a large number of subjects to imitate the motions and activities being evaluated (Spielholz et al. 2001). The need is thus increasing for a new method which can overcome these difficulties and eliminate work interruption on the job in order to automatically identify ergonomic risk is increasing.

1.2 Research Objectives

The research presented herein is built upon the following hypothesis:

“Integrating 3D visualization and physiological measurements in human body motion analysis could assist in analyzing physical demand in order to identify and evaluate ergonomic risks in construction manufacturing operational tasks, and provide modified work to mitigate risk, thus reducing corresponding injuries and workers' compensation insurance costs.”

This research identifies the limitations of current physical demand analysis and physiological measurement experiments. Four systematic methods are proposed which comprehensively assess physical demand, muscle activity, and potential ergonomic risks of continuous motions independently for modular construction activities with the support of physiological measurement and graphical 3D visualization modelling.

This research develops frameworks to assist health and safety personnel to analyze the physical demand on the worker imposed by the existing workstation. By changing the method/posture of completing one task or changing the workstation design, the health and safety manager is able to recommend modified work or to suggest alternative body motions to the worker. These frameworks can also help to mitigate the risk of accidents in the proposed design and ultimately reduce the overall number of plant injuries and corresponding workers' compensation insurance costs. These frameworks can also be implemented in the design phase of a manufacturing plant by means of an ergonomic test/check on workstations to ensure a healthy and safe working environment.

To realize this underlying goal, the research is divided into the following objectives:

- (1) Develop an improved physical demand analysis (PDA) which enables risk identification and evaluation and is also able to provide modified work to mitigate ergonomic risks and reduce injuries.
- (2) Develop a framework to assess muscle force and muscle fatigue development due to manual lifting tasks using surface electromyography (sEMG), kinematic motion capture, and human body modelling.

- (3) Develop a method which enables an automated ergonomic risk assessment with graphical 3D motion-based modelling as a support tool in order to analyze ergonomic risks and hazards.
- (4) Develop a method which enables systematic physical demand and ergonomic risk assessment in order to rapidly analyze ergonomic risks and to provide modified work for modular construction operations.

1.3 Thesis Organization

This thesis consists of six chapters. Chapter 1 presents the background and motivation of this research. The goal and objectives of this research are also outlined in this chapter. In Chapter 2, the research summarizes the input requirements of existing risk assessment tools and proposes an improved PDA form with an integrated framework to facilitate the comprehensive and intelligent use of PDA. The focus covers three aspects in regard to PDA implementation: risk identification, risk evaluation, and risk mitigation. This first framework is implemented in a manufacturing industry facility, and a case study of the assessment of awkward body postures at a window glazing station is described.

Chapter 3 presents, for the purpose of identifying the muscle fatigue from repetitive manual material handling, a framework to assess muscle force and muscle fatigue development due to manual lifting tasks using surface electromyography (sEMG), kinematic motion capture, and human body modelling. Muscle forces are calculated using the human body model and compared qualitatively to sEMG muscle activities. The results indicate that sEMG is capable of visualizing muscle activity. However, sEMG application in identifying muscle fatigue development is limited to bulkier and superficial muscle bundles in low-fat areas. The muscle forces predicted from the human body model are compared with sEMG data from corresponding muscles. In

future research, the developed model will be used to determine optimal task manoeuvres that minimize muscle forces and fatigue by adjusting the workstations, handled load, and working repetitions.

To overcome the difficulties and limitations of existing physical demand analysis practice and physiological measurements, Chapter 4 proposes a methodology for converting observational or video-captured body movements in an actual construction manufacturing plant into 3D motion-based modelling for ergonomic risk assessment. Through 3D modelling, continuous human body data can be obtained (such as joint coordinates, joint angles) for risk assessment analysis using existing risk assessment algorithms. The presented framework enables risk evaluation by detecting awkward body postures and evaluating the handled force/load and frequency that pose ergonomic risks during manufacturing operations. The proposed 3D motion-based risk assessment methodology is validated through the aforementioned motion capture experiment in order to prove the reliability of the framework. It is also compared to the traditional manual observation method. Three human subjects are selected to conduct the experiment and three levels of comparison are completed: joint angle comparison, risk rating comparison for body segments, and REBA/RULA total risk rating and risk level comparison.

In Chapter 5, the integration of physical demand and ergonomic risk assessment with the support of 3D visualization is presented and implemented in a case study for both the existing workstation and the workstation in design. The functionality of the proposed 3D motion-based physical demand and risk assessment modelling is thus proven and expanded. Finally, conclusions and research contributions are summarized in Chapter 6.

CHAPTER 2: PHYSICAL DEMAND ANALYSIS¹

2.1 Introduction

Workers' compensation boards (WCBs) protect employers from lawsuits and allow injured workers to receive benefits (Occupational Health and Safety 2015). WCBs also protect employees against loss of income and provide comprehensive medical and rehabilitation services corresponding risk management. WCB-Alberta requires a report for any injury that necessitates time off work, modified work, or medical treatment, or that may result in permanent disability (WCB-Alberta 2015a). Physical Demand Analysis (PDA), as a systematic method, is commonly recommended to industries in Canada and can also be applied in other jurisdictions to document the physical, cognitive, and environmental demands of essential tasks (WCB-Alberta 2015b; Industrial Accident Prevention Association 2009; Workplace safety North 2016). It also allows the industry to be proactive rather than reactive—taking preventive measures rather than taking action only after a worker suffers an injury that requires them to take time off work (WCB-Alberta 2015b). Thus PDA is a useful method that can be implemented in any industry that involves physical demands.

According to 2013 statistics from the Association of WCBs of Canada (2013), the manufacturing and construction industries have the second and third highest number of lost time injuries/diseases in Canada. Higher physical demands, such as overexertion, repetitive motion, and awkward body posture, are more likely to be placed on workers in the construction and manufacturing industries than in other industries. These physical demands often result in work-related musculoskeletal disorders (WMSDs). The Ontario Safety Association for Community and Healthcare (2010) states that, even if the level of force is low and the movement does not

¹ The manuscript appearing as Chapter 2 of this thesis is under review for publication in the *International Journal of Industrial Ergonomics (Elsevier)*, as of the time of publication of this thesis.

involve any awkward body postures, fatigue, tissue damage, pain, and, ultimately, a WMSD may still be encountered due to high repetition. In the United States, 33% of occupational injuries and illness cases are due to WMSDs (Bureau of Labor Statistics 2014). Ensuring even during the recruitment stage that the job is within the physical capacity of the worker, setting break times to provide employees the opportunity for meals and rest, and shifting construction processes toward automation or semi-automation are core solutions to reduce ergonomic issues. However, certain tasks may still cause WMSDs (Safety and Health Authority 2006). There are three categories of potential issues that may require clinical attention: (1) the least severe case, which can be controlled by advising and guiding the employee, adjusting work load or activity, and prescribing certain medicines; (2) recordable injury, which usually requires more medical treatment and nursing; and (3) severe injury, which may cause the employee to require one day or more away from work (Occupational Safety and Health Administration 1990). These disorders and conditions, in turn, delay the production line due to the lack of immediate replacements for the position.

Evaluation of physical demand is the first step in ergonomic workstation design (Elola et al. 1996). A well-designed workstation that takes ergonomics into consideration can ensure the health and safety of workers while improving the productivity of a manufacturing plant's production line (Deros et al. 2011; Määttä 2007; Elola et al. 1996). On the other hand, workstation design that fails to consider ergonomics, though possibly able to boost operation productivity may often require awkward body postures and activities that are potentially hazardous to workers. In this case, it may contribute to the onset of WMSDs or injuries, and may also threaten workers' mental health, eventually resulting in high compensation costs (Golabchi et al. 2015; Hales 1995). Eight ergonomic hazards—static body posture, overtime work in the

office, manual material handling, WMSDs, poor lighting, usage of tools, slips/trips/falls, and shift work—are identified by the Canadian Centre for Occupational Health and Safety (2016) as candidates for consideration in the design of manufacturing workstations.

Thus, it is vital to review and evaluate the working conditions and physical demands of both existing workstations and workstations still in design, especially in reference to these eight aspects, in order to proactively identify potential ergonomic hazards. This chapter proposes an integrated risk assessment framework based on an improved PDA, as indicated in Figure 2.1, and covers three aspects in regard to PDA implementations: risk identification, risk evaluation, and risk mitigation (modified work). This chapter first presents a comprehensive literature review on current PDA practice and the existing risk assessment tools. Then, in the subsequent sections, any gaps identified through the literature review and addressed with the improved PDA. The methodology of how to implement the improved PDA is also proposed, complete with data collection, time study, and other supplementary information collection. An ergonomic risk assessment and identification framework which can integrate the content in the proposed improved PDA form with existing risk assessment tools is also proposed. Four main aspects—static whole body posture, heavy material handling, sensory risks and awkward body posture—of ergonomic risks are suggested as the focus of this chapter with preliminary modified work to mitigate potential risks.

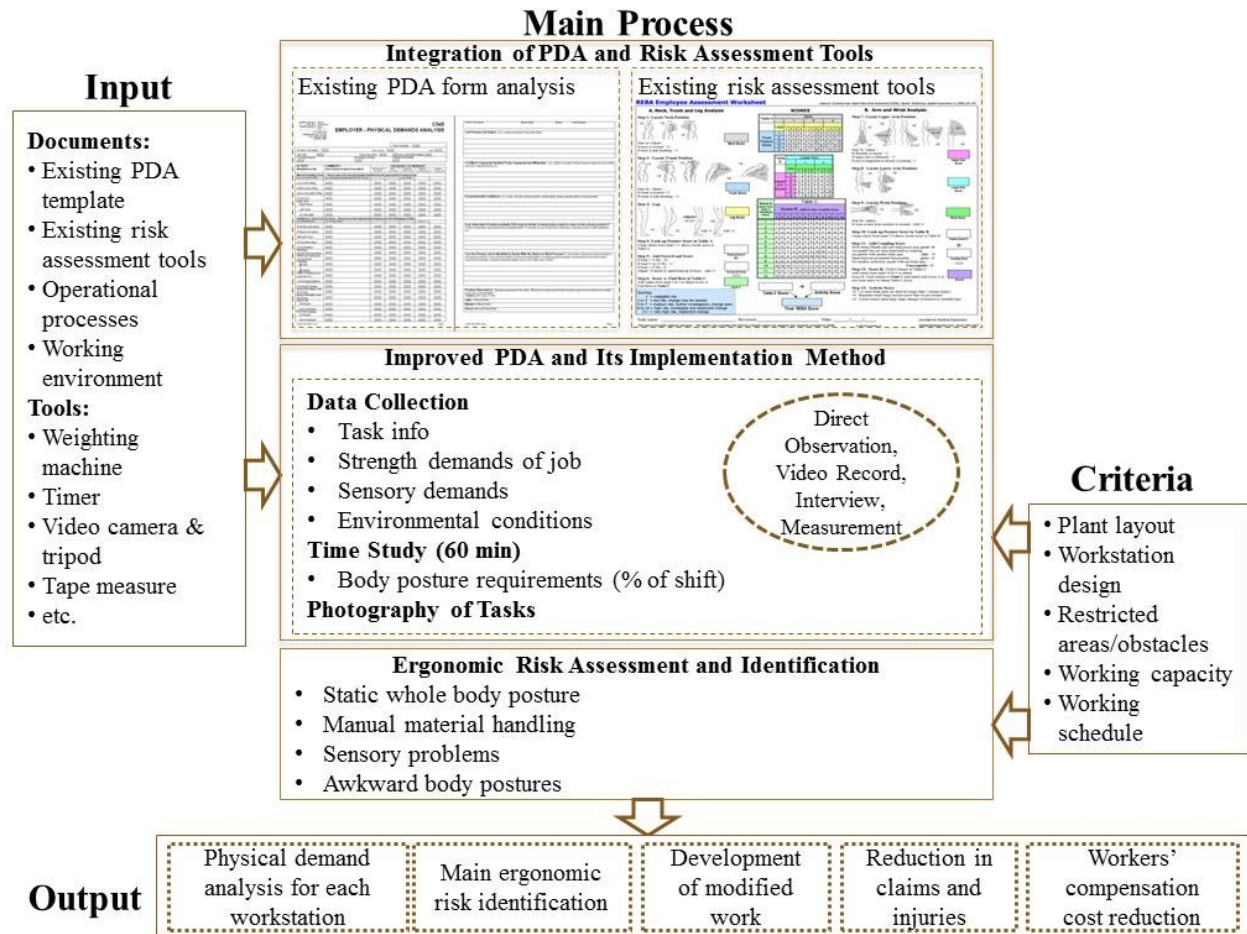


Figure 2.1: Framework for improved PDA-based risk assessment

The inputs to this framework include a literature review of existing PDA and risk assessment tools. Information about plant layout and operation processes of the industry is also vital for risk assessment. Other tools researchers use for collecting data for PDA are listed in the figure. The risk assessment framework, it should be noted, may be constrained by certain criteria, such as working schedule or working capacity, especially during the phase of proposing modified work. As outcomes this framework provides not only a complementary PDA for each workstation and identifies ergonomic risks, but also modified work to mitigate risk, to proactively reduce claims and injuries, and to reduce workers' compensation-related costs.

2.2 Current Physical Demand Analysis

A review of existing physical demand and ergonomic analysis is summarized in this section in order to underscore the need for the present research. An overview of preliminary PDA on the existing manufacturing plant and its limitations is reviewed. Notably, PDA is an integral part of any return-to-work program and provides many benefits (Workplace safety North 2016; Industrial Accident Prevention Association 2009). First, PDA provides a systematic approach to collect data station by station, assisting in identifying tasks for each job, work processes, and equipment used, as well as quantifying and evaluating the physical, sensory, and environmental demands on the worker from the tasks involved in essential and non-essential jobs. Second, this information collected in PDA is useful for job recruitment, training of workers, and job assignment, and will further assist with ergonomic risk identification and injury prevention. Third, PDA assists the WCB representative, the physician, and other health care providers to gain better understanding of the physical requirements of the occupational task that led to the injury claim. When submitting a claim with WCB for an injured worker, PDA of the worker's workstation is requested in conjunction with the claim since the WCB representative and physician must review the PDA in order to provide the injury coverage and treatment, respectively, to the worker. Fourth, PDA can assist and enable the employer to recommend restrictions and strategies for modifying work for the given worker, especially for injured workers, and this serves to further reduce the premium rate paid to WCB. Providing modified work enables the injured worker to continue contributing to the workstation and adding value to the production process, and has a positive effect on production quality (WCB-Alberta 2015c). Thus, PDAs play a vital role in analyzing the job demand and ensuring the effectiveness, efficiency, and quality of return-to-work programs. Having a useful PDA is also beneficial in

that it enables the employer, supervisor, or plant nurse to effectively and efficiently analyze the job demands of the workstation on the injured worker.

PDA has been implemented in several construction industries. WCB provides a PDA template which can be customized for the given industry. Occupational Health Clinics for Ontario Workers Inc. (2012) provides a guideline on how to successfully conduct a PDA. Getty (1994) describes the use of PDA, implementing it at Lockheed Fort Worth Company according to Occupational Safety and Health Administration ergonomic guidelines. Getty's study emphasizes that PDA benefits the productivity and quality of work as well as prevents injuries. Halpern et al. (1997) utilize the job demand and environmental demand approach to confirm the correlation between physical requirements and back injuries. Li et al. (2015) utilize PDAs encompassing strength demand, frequency of activities, sensory demand, and environmental demand in a manufacturing company in Alberta, Canada, and subjectively identify the ergonomic risks. Table 2-1 summarizes the existing PDA templates described in the literature. Other supplementary forms, such as fitness for work form and function ability analysis form, and the offer of modified work also assist in return-to-work programs and facilitate the physical and ergonomic analysis of the worker on each specific occupational workstation.

Table 2-1: Content of existing PDA templates

Organizations	Content in PDA
Workers' Compensation Board, Alberta (2014)	Worker information, job description, primary job duties, manual handling tasks (lifting, carrying, etc.), additional critical job demands (pushing, pulling, bending, etc.), tools, environmental conditions, alternative positions, and modified work.
Workplace safety North (2016)	PDA for mobile equipment: force, work environment, mobility, dexterity, posture/joint position required.
British Columbia Municipal Safety Association (2016)	Physical demand: strength, mobility, sensory/perception, work environment. Cognitive and psychosocial demands: supervision, time pressure, attention, memory, interactions with others, etc.

2.3 Existing Risk Assessment Tools and Guidelines

In the literature prior to 2016, risk evaluations and modified work suggestions have been subjective, with few studies having linked PDA with ergonomic analysis tools. The existing methods for assessing safety risk can provide *a priori* risk estimates and can measure the frequency of unsafe behaviours or conditions, but they do not provide a way to assess the potential for accidents based on the actual execution of the operation (Mitropoulos and Namboodiri 2009). A number of existing risk identification and assessment tools, such as Rapid Upper Limb Assessment (RULA), Rapid Entire Body Assessment (REBA), Ovako Working-posture Analyzing System (OWAS), National Institute for Occupational Safety and Health (NIOSH), Portable Ergonomic Observation (PEO) and ErgoSAM, can be applied to extend the risk assessment capability of PDA. Because of the inherent difficulties of implementing these tools in construction and manufacturing industries, though, adoption has been limited (Golabchi et al. 2015). Also, these existing tools have not been implemented to integrate the PDA information for risk assessment, and some PDAs only provide a guideline for the maximum

external load of a single worker (Minnesota Occupational Health 2012). The comprehensive usage of PDA has therefore been limited.

The detailed risk assessment methods listed above are studied herein in order to test whether or not existing PDA forms solicit sufficient information to serve as the input for the tools summarized below. The Infrastructure Health & Safety Association (IHSA 2014) provides a general guide for identifying ergonomics-related hazards. WISHA Caution/Hazard Checklist (Bernard 2010) is a screening tool to identify whether a given activity requires cautions to avoid risks or if it is already a hazard that may cause WMSDs and thus requires immediate action. RULA focuses on upper limb assessment by recording postures, scoring them, and scaling action levels (McAtamney and Corlett 1993). REBA objectively analyzes body postures for all body segments by assigning scores to each body segment for the entire body (Hignett and McAtamney 2000; Middlesworth 2012). OWAS, a method to identify and evaluate poor postures during work by first using observational technique and then redesigning the working methods and workplaces, is proposed by Karhu et al. (1977). It numbers the posture of each body segment and then combines all the numbers to represent the entire body posture, followed by a reclassification into four categories or “risk levels” (Karhu et al. 1977; Karhu et al. 1981). NIOSH (1981) introduced a tool to assess and guide the lifting weight and proposed a NIOSH lifting equation, which has further been revised and implemented in several cases (Ergonomics Plus Inc. 2015; Nelson et al. 1981; Water et al. 1993; Okimoto and Teixeira 2009). The PEO method relies on real-time continuous observation and is able to record intensity, duration, and frequency of a posture (Fransson-Hall et al. 1995; Murphy et al. 2002; Finnish Institute of Occupational Health 2009). ErgoSAM is a method that can detect musculoskeletal load and physically stressful work situations by estimating in the early planning process the physical demand of work postures,

repetition, forces applied (considering the weight handled), and work zone (Laring et al. 2005; Christmansson et al. 2000). Table 2-2 lists and summarizes these risk assessment methods with the input requirements and outputs. The most important inputs, though not included in the content of existing PDA, are body posture magnitude and amplitude as well as task durations. If the improved PDA contains this information, researchers are able to conduct risk assessment by using these tools.

Table 2-2: Risk assessment tools

Tools	Input		Output
	Information included in existing PDA	Information required for the proposed (improved) PDA	
IHSA	<ul style="list-style-type: none"> ✓ Load/Force ✓ Repetition/Frequency ✓ Moving distance ✓ Handled material 	<ul style="list-style-type: none"> ○ Detail of the body posture ○ Duration 	Level of risk
WISHA	<ul style="list-style-type: none"> ✓ Repetition/Frequency ✓ Load/Force ✓ Tools/Equipment 	<ul style="list-style-type: none"> ○ Detail of the body posture ○ Duration 	Caution/hazard definition
RULA	<ul style="list-style-type: none"> ✓ Load/Force ✓ Repetition/Frequency 	<ul style="list-style-type: none"> ○ Detail of the body posture (Upper arm position, lower arm position, wrist degree, wrist twist, duration, neck bend degree, trunk bend degree, leg bend or not) ○ Duration 	RULA risk rating with four levels
REBA	<ul style="list-style-type: none"> ✓ Load/Force ✓ Repetition/Frequency 	<ul style="list-style-type: none"> ○ Detail of the body posture (Neck bend degree, trunk bend degree, leg bend degree, upper arm position, lower arm position, wrist degree, hand coupling) ○ Duration 	REBA risk rating with five levels
OWAS	<ul style="list-style-type: none"> ✓ Body posture (for back, upper limbs, lower limbs) ✓ Repetition/Frequency ✓ Load/Force 	<ul style="list-style-type: none"> ○ N/A 	Poor working body posture identification and evaluation
NIOSH	<ul style="list-style-type: none"> ✓ Detailed moving distance ✓ Repetition/Frequency (lift/minute) ✓ Weight of the load 	<ul style="list-style-type: none"> ○ Handled material detailed position ○ Coupling multiplier (load coupling, hand position) ○ Asymmetry angle ○ Duration 	Lifting weight recommendation

PEO	<ul style="list-style-type: none"> ✓ Weight/Force ✓ Movements ✓ Repetition/Frequency 	<ul style="list-style-type: none"> ○ Detail of the body posture ○ Duration 	Body posture assessment; Work load evaluation
ErgoSAM	<ul style="list-style-type: none"> ✓ Force/Weight factor (kg) ✓ Repetition/Frequency 	<ul style="list-style-type: none"> ○ Work posture factor (work zone -inner/outer) ○ Duration 	Risk rating (cube value in the range of 1 to 27)

2.4 Improved Physical Demand Analysis for Risk Assessment

The required inputs for existing risk assessment algorithms are reviewed and compared with the content of the existing PDA template, and it is determined that the information in the existing PDA is not sufficient to conduct any objective risk assessments. The inputs for these ergonomic tools vary and the existing PDA does not contain all the information required. The items of information missing in the existing PDA form, and the most important inputs for risk assessment, are the magnitude/amplitude of body posture, the operational moving distance, and the duration of activity. Moreover, the benefits of PDA in providing modified work to reduce risk are not fully realized due to these limitations combined with the low rate of PDA implementation in today's industry. Thus, the existing PDA must be modified and improved in order for it to be more effective. This chapter thus summarizes the required inputs for the tools in Table 2-2, compares them with the content of existing PDA, and integrates all the needed information into a new PDA form, ensuring that this improved PDA is capable of capturing all information required for further risk identification and evaluation. The improved PDA can also be customized based on the unique culture and physical demands inherent in tasks for the given company. Some of the content of the improved PDA, we note, may not be necessary for all companies, so it can be removed from the form in such cases. Each existing risk assessment tool has its limitations. This chapter thus combines different tools for the purpose of practical and comprehensive PDA implementation in the case study facility. Users can choose which tools to employ based on their

own purposes. As a result, the gaps between PDA form and risk assessment tools are seamlessly filled.

The improved PDA form proposed in this chapter, shown in Table 2-3, includes the basic job information, strength demands, body posture demand, sensory demand, environmental demand, handled tools and equipment, and proposed modified work based on the risk assessment results. Different from the existing PDA, the improved PDA also solicits detailed information on the handled force and moving distance under the strength demand, detailed body posture magnitude/amplitude information (especially for back, shoulder, neck, elbow, wrist, ankle) under body posture demand, and detailed sensory demand. As a result, a summary of risk assessment and risk identification is provided together with the corresponding proposed modified work. Thus implementing the improved PDA, potential ergonomic risks can be identified and evaluated proactively, which also facilitates the development of constructive and achievable modified work to mitigate risks, including changes to the tasks, workload, or schedule as well as to working area or equipment (WCB-Alberta 2015a). Other modified work can also be conducted through on-the-job training for the purpose of assigning workers among multiple tasks and staggering tasks between workers in order to establish achievable, safe, constructive, and productive work practices. Health care professionals, physicians, or rehabilitation therapists are also able to review this PDA in order to assist the injured worker to recover, to define whether or not the worker is ready to return to the previously assigned occupational workstation, and ultimately to streamline the worker's return to work. The improved PDA also helps to determine if the new occupational workstation assignment is in keeping with the medical restrictions and physical ability of the worker.

Table 2-3: Proposed physical demand analysis form

PHYSICAL DEMANDS ANALYSIS		Claim Number:
Job Title:	Hours per shift:	
Shifts per week/shift rotation:	Breaks:	
Company Name:	Employer Contact:	Telephone Number:
Overtime Policy if applicable:		

Job Overview: (e.g., list primary job duties)

Responsible for

Job Skills & Training:

Job Primary Tasks with Durations:

- 1.
- 2.

Strength Demands of Job

ACTIVITY	COMMENTS (Description of handled objects, coupling)	FORCE/LOAD (lb)		FREQUENCY	MOVING DISTANCE (in)
		Avg.	Max.	N/R/O/F/C	
Lifting					
Low Level Lifting		15	20	R	8
Waist Level Lifting		30	35	F	8
Above Shoulder Lifting		-	-	N	-
Carrying					
Front Carry					
Side Carry – Right Hand					
Side Carry – Left Hand					
On Shoulder					
Pushing/Pulling					
Pushing (tools/objects)					
Pulling (tools/objects)					
Grasping & Pinching					
Hand Use					
Dominant					
Non-Dominant					
Forceful Gripping					
Dominant					
Non-Dominant					

N: Not Required (0% of shift), R: Rare (1–5% of shift), O: Occasional (6–33% of shift), F: Frequent (34–66% of shift), C: Constant (67–100% of shift)

Body Posture Frequency

ACTIVITY	COMMENTS (Description of the activity, handled objects, coupling)	FREQUENCY OF WORKDAY				
		Not Required (0% of shift)	Rare (1–5% of shift)	Occasional (6–33% of shift)	Frequent (34–66% of shift)	Constant (67–100% of shift)
Mobility						
(by checking “X”)						
Walking	(terrain/surface)		X			
Standing	(flooring/surfaces)			X		
Sitting/Driving	(type of seat/chair)					
Climbing						
<input type="checkbox"/> stair						
<input type="checkbox"/> ladder						
Other Climbing	(stools, etc.)					

Crouching/Squatting	
Kneeling/Crawling	
Back	(by indicating Magnitude and Amplitude, °)
Forward Bending	20°
Backward Bending	10°
Twist/Trunk Rotation	
Shoulder	(by indicating Magnitude and Amplitude, °)
Above Shoulder Reaching	
Forward Shoulder Reaching	
Below Shoulder Reaching	
Sideways Shoulder Reaching	
Behind Shoulder Reaching	
Neck	(by indicating Magnitude and Amplitude, °)
Forward Bending	
Backward Bending	
Twist/Tilt	
Elbow	(by indicating Magnitude and Amplitude, °)
Flex/Extend	
Wrist	(by indicating Magnitude and Amplitude, °)
Flex/Extend	
Bending	(across the midline)
Rotate	
Ankle	(by indicating Magnitude and Amplitude, °)
Flex/Extend	
Rotate	

Sensory Demands

ACTIVITY	COMMENTS (Description of the activity, handled objects, coupling)	FREQUENCY OF WORKDAY (by checking "X")				
		Not Required (0% of shift)	Rare (1-5% of shift)	Occasional (6-33% of shift)	Frequent (34-66% of shift)	Constant (67-100% of shift)
Hearing/Speech			X			
Sound discrimination		X				
Vision: near/far						
Colour Vision						

Environmental conditions: (e.g., indoor/outdoor, noise, cold, heat, chemical exposure, confined spaces, heights, possible violence, moving equipment)

List most frequently handled tools, equipment, and materials:
(e.g., vibration, pneumatic, tool belt, manual or power tools, shop or office equipment, materials/products, etc.)

List safety equipment: (e.g., safety glasses, safety boots, hearing protection, gloves, etc.)

Basic Ergonomic Risks Identified

Risk	Modified Work for Consideration
1.	
2.	

Printed Name: _____
Signature: _____

Date: _____

2.4.1 Implementation method

The information solicited in the PDA form can be obtained by three approaches: data collection, time study, and collection of other supplementary information.

2.4.1.1 Data collection

The existing body posture data collection methods, such as direct observation, self-report (survey, questionnaire, interview), and physiological measurements (direct/indirect), are research-based and serve to complement occupational safety and health practitioner requirements. However, there are limitations in the real-life implementation in the construction and manufacturing industries (David 2005; Li and Buckle 1999). Body posture magnitude/amplitude can be obtained by both direct physiological measurement (such as goniometers, force sensors, accelerometers, electromyography, and optimal markers) and indirect physiological measurement (e.g., Kinect range camera, computer vision-based approach) (Alwasel et al. 2011; Ray and Teizer 2012; Han and Lee 2013). Although physiological measurement has a high level of accuracy and provides information that is more objective than traditional observation methods, several limitations exist: direct physiological measurement may be limited by experimental cost, environment, and technical and ethics issues, while indirect measurement is compromised by its sensitivity to illumination changes, viewpoints, and occlusion. Wang (2015) points out that in this regard that there is an opportunity for researchers to investigate cost-effective methods of risk assessment and of mimicking human behaviour in a laboratory setting.

The data collection for physical demand and ergonomic posture assessment in current practice depends on direct observation. Direct observation and video recording methods are selected in the present research due to their high reliability. Interviews are also included as part of the PDA project, since communication can assist external observers to better understand the tasks being

analyzed. Other data collection methods include manual measurements (e.g., use of weighting machine and materials). Forms for the “strength demands of job”, “sensory demands”, and “environmental conditions” where frequency data is not required are also completed at this juncture.

2.4.1.2 Time study

The frequency of different required body postures is ascertained through a time study. The total durations of given tasks are also recorded. A 60-minute time study is proposed in this methodology for cases in which most tasks involved can be completed within 30 minutes. The time study spreadsheet is attached in the Appendix A (Table A-1). In the time study, body postures are recorded in a spreadsheet at one-minute intervals for each job. A combination of direct observation and video recording observation is used, since video cameras offer the advantage of recording hours of footage for multiple stations simultaneously. This footage is later analyzed to extract the relevant data. It should be noted that video recording may be unsuitable in cases where the workers are highly mobile, since a video camera’s viewing angle is limited. In addition, some stations may be found to have limited working space, resulting in problematic camera positioning. In these cases, manual and direct observation is the recommended method. The workers are informed prior to observation commencing about the nature of the research work and that the observation is going to be carried out. In the case of video recording, observers take into consideration working hours and scheduled breaks in order to avoid collecting footage during breaks.

It should be noted that “frequency” in this study is defined as the number of times a motion is repeated over a specified period by a worker, and this can be estimated using Eq. (2-1). The duration of the activity, such as lifting and carrying an object, can also be indicated by adding up

the continuous checkmarks in the time study spreadsheet. Once the percentage is calculated for each posture, a frequency descriptor is assigned to each percentage range as follows: Never (0%), Rare (1% to 5%), Occasional (6% to 33%), Frequent (34% to 66%), and Continuous (67% to 100%).

$$F = \frac{N}{T} \times 100\% \quad (2-1)$$

where

F: Percentage of shift (%).

N: Number of checkmarks in spreadsheet.

T: Time study period, e.g., 60 min, in this case.

2.4.1.3 Supplementary information

The last step is to collect supplementary information, such as photographs of each task to be included in the form in order to visualize the task. Scheduling this process as the last step in conducting PDA allows for the workers to become more comfortable with the research and for the observers to familiarize themselves with the production process at the plant. Ample photographs ensure accurate representation of the tasks performed and of the inherent ergonomic risks.

After populating the PDA form, researchers can identify ergonomic risks using existing risk assessment tools based on the data collected in previous processes, and can propose corresponding modified work. The objective of this process is to identify ergonomic risk factors, ensure that tasks are within the worker's capacity and limitations, and devise corresponding modified work. However, the risk factors vary from case to case, as shown in the following discussion of risk factors from PDA implementation in a case manufacturing facility. Based on

the risk assessment analysis, temporary modified work can be proposed which sets out any changes to regular job duties to accommodate a work-related injury.

2.4.2 Case study

The improved PDA integrated with different risk assessment tools is implemented in a case manufacturing plant. This section focuses on the window glazing station, in particular on the glazing stop installation task at this station, as an example and further explains the implementation of the improved PDA. REBA and RULA risk assessment tools are integrated with the improved PDA for the window glazing station. Finally, the main ergonomic risks together with risk assessment methods (such as REBA, RULA, IHSA, and NIOSH) from this industrial implementation are summarized in this section, which also serves as a reference for future PDA implementations and modified work investigations.

2.4.2.1 PDA implementation in a window glazing station

In the window glazing station, according to the frequency data collected from PDA, completing the glazing stop installation task involves *frequent* standing, *occasional* kneeling, *frequent* reaching below shoulder, *occasional* reaching above the shoulder, *frequent* neck/trunk bending forward, *occasional* neck bending backward, and *frequent* elbow flexion. This task is divided into two motions for the purpose of risk assessment as illustrated in Figure 2.2: the first motion (a) is to seal the bottom of the glass to the window frame from a kneeling position (Figure 2.2a) in a manner which involves *frequent* bending forward of the neck to less than 20°, *frequent* bending forward of the trunk in the range of 0° to 60°, legs *occasional* kneeling on the floor, *frequent* upper arm reaching forward with a range of 0° to 45°, *frequent* lower arm reaching forward within 60° to 100°, *occasional* wrist bending within 15° from lower arm, and lower arm and wrist *occasionally* bending across the midline. The second motion (b) is to seal the top of the

glass to the window frame while in a standing position (Figure 2.2b), a motion which involves *occasional* bending backward of the neck, *frequent* bending forward of the trunk in the range of 0° to 20°, *frequent* (i.e., prolonged) standing, *frequent* upper arm and lower arm reaching around or above the shoulder up to 45°, *occasional* wrist bending as much as 15° from the lower arm, and lower arm and wrist occasionally bending across the midline.



Figure 2.2: Window glazing station motions

The content of the improved PDA having been completed by utilizing the aforementioned PDA implementation method, the risk ratings from REBA and RULA for both motions are evaluated as summarized in Table 2-4 and Table 2-5. A *coupling score* of 1 is added, as these two motions are acceptable but involve less-than-ideal handling postures. A *force* of 5 to 10 lb is also needed in order to secure the glazing stop pieces; this knocking motion is often repeated more than 4 times per minute, which adds 1 to the *activity score* for REBA, and adds 1 each to the *muscle score* and *force score* in RULA.

From the results of REBA, the glazing task with kneeling posture yields a risk of 5 to 7, categorized under level 3: “*medium risk, further investigation, change soon*”, while the glazing task with standing posture yields a lower risk rating of 2 to 6 depending on the height of the window, scored in level 2 to 3: “*low to medium risk level, further investigation, change may be*

needed, or change soon”. From the results of RULA, which focuses on upper limbs, the two motions both receive the maximum rating of 7—“investigation and changes required immediately”.

Table 2-4: REBA score for glazing task

REBA	Neck	Trunk	Legs	Table A	Force
Kneeling	1	2-3	4	5-6	0
Standing	2	1-2	1	1-3	0

REBA	Upper arm	Lower arm	Wrist	Table B	Coupling
Kneeling	1-2	1	1-2	1-2	1
Standing	2-4	1-2	1-2	1-6	1

REBA	Table C	Activity	REBA
Kneeling	4-6	1	5-7
Standing	1-5	1	2-6

Table 2-5: RULA score for glazing task

RULA	Upper arm	Lower arm	Wrist	Wrist Twist	Table A	Muscle	Force
Kneeling	1-2	1-2	1-3	1	1-3	1	1
Standing	2-4	2-3	1-3	1	3-5	1	1

RULA	Neck	Trunk	Legs	Table B	Muscle	Force
Kneeling	1-2	1-3	1	1-4	1	1
Standing	4	1-2	1	5	1	1

RULA	Table C	RULA
Kneeling	3-7	3-7
Standing	7	7

To lower the rating for each body segment, the work modification of changing the height of the window is suggested in this case to minimize kneeling and reaching above the shoulder, and to reduce neck/trunk bending magnitude as well as the raising height of the upper and lower arm. An introduction of an auto-height-adjustable rack to support the window is recommended so that the window can be adjusted to a comfortable working height based on the height of the worker. Moreover, staggering the task between workers to reduce the time a given worker is exposed to awkward body postures is another effective measure to reduce the potential risk of injury. All the modified work is summarized in the “basic ergonomic risk identified” section in the PDA form. In addition to these awkward body postures, other demands, such as strength demand,

environmental demand, and sensory demand are all within the capacity of workers. Thus, risk is introduced at the glazing task as a result of awkward body postures from frequent hammering as well as kneeling and/or reaching above the shoulder to seal the glass to the window frame.

2.4.2.2 Assessment and identification of ergonomic risks

Four main ergonomic risks are identified for the case manufacturing plant and are described in this section. Some of these ergonomic risks can be mitigated or eliminated by making immediate changes and modifications, while others may require further investigation or development of the working motion and workstation.

a) Static whole body posture

Most of the workstations require prolonged standing throughout the workday (indicated as “frequent” or “constant” standing posture in the improved PDA), which leads to back and foot pain. To counteract this, anti-fatigue matting or footwear memory foam insoles are recommended, as they can significantly decrease the pressure placed on the spine and feet. Providing footrests for the workers is another effective method to decrease the strain that contributes to back and foot pain.

b) Heavy material handling

Workers are occasionally required to lift, push, or pull heavy materials manually (i.e., without the aid of wheeled carts). These actions pose ergonomic risk to the back and shoulders. Heavy lifting also occurs in various production lines. In terms of manual material handling tasks, worker loading capacity guidelines are provided by IHSA. If the material to be lifted exceeds the worker loading capacity, the worker will be exposed to a dangerously high risk of injury. The ergonomic risks related to material handling can be identified based on four factors: (i) the moving distance of the object; (ii) the size of the profiles; (iii) the working height; and (iv) the

approximate frequency (f) which is calculated using Eq. (2-2). The duration and distance an object is to be moved and the working height are obtained from observation, and the description of the profile provides the dimensions and weight. With the results of the 60-minute time study, the weight limitations for manual lifting can be calculated. By comparing the results calculated using this equation against the numbers given in the IHSA table (IHSA 2014), potential high-risk exposure tasks can be identified. Another option for lifting risk assessment is the NIOSH Lifting Equation (Ergonomics Plus Inc. 2015), which requires measured variables such as weighting load, horizontal location of the object relative to the body, vertical location of the object relative to the floor, vertical moving distance, asymmetry angle or twisting requirement, frequency and duration of lifting activity, and coupling or quality of the worker's grip on the object.

$$f = \frac{T_c}{F} \quad (2-2)$$

where

f: frequency, i.e., time interval between moves, in minutes;

T_c : working cycle time (duration) for one lifting activity; and

F: frequency (%) of lifting/pushing/pulling within the observation time, collected in the PDA.

The two central solutions to this type of ergonomic risk are (i) to investigate the potential of the semi-automated machine, and (ii) to supplant the manual material delivery motion with a safer one. Another simple measure which the organization can implement immediately is to stagger the tasks among workers so that specific workers are not disproportionately exposed to certain ergonomic risks.

c) Sensory risks

The third type of ergonomic risk identified through observation is sensory risk, including eye fatigue and hand or arm vibrations. Based on the improved PDA implementation, workers

occasionally need to conduct manual measurements. Avoiding manual measurement can reduce eye fatigue and improve productivity. Another sensory problem involves hand or arm vibration. An array of tools is utilized in each production line. For many of these tools, such as chop saws, power drills, pneumatic staple guns, and air guns, the worker is exposed to a considerable amount of vibration during operation, where frequent use poses a serious health hazard. Carpal tunnel syndrome is one condition that may result from exposure to this hazard (Health and Safety Executive 2014). The symptoms may include only moderate pain, white fingers, and sleep disturbance, but in more serious cases this hazard may lead to numbness and loss of strength in the hands, among other symptoms (Health and Safety Executive 2014). To prevent the onset of carpal tunnel syndrome, or other conditions or injuries, two corrective measures are recommended. One is to provide tools and equipment at the workstations which minimize worker exposure to hazardous vibration. The other is to limit the duration of exposure to this type of hazard for a given task, a measure which can be achieved (as with risk due to lifting of heavy materials) by staggering the work assignments so that no worker is disproportionately assigned to activities which pose this type of ergonomic risk.

d) Awkward body postures

Awkward body posture is another primary ergonomic risk identified in the manufacturing facility. Postures are categorized into five groups: (i) back/neck bending forward or shoulder reaching forward; (ii) reaching above shoulder; (iii) back backward bending; (iv) kneeling, or crouching/squatting; and (v) elbow, wrist flex/extension. Whenever it is necessary for a worker to reach for an item at the workstation, their back bends (backward/forward) and shoulders reach forward/above. The neck is also strained by operations completed on a flat table. There are various suggestions for modified work that can be implemented to correct a worker's posture.

The first work modification is to locate the workstations as close as possible to one another and the materials as close as possible to the relevant workstation. A second work modification is providing a lifter or tilter for material storage or working surface at each workstation in order to ease access to materials by workers during operations. Third, it is recommended to enable the height of the machine, computer, or working table to be adjustable in order to minimize muscle strain, since the heights of workers vary.

Of even greater concern, there are also situations that require workers to kneel or crouch/squat to complete a task, as illustrated in the previous case study. Frequent kneeling causes pain and strain in the low back and knees and poses a high risk to the worker of developing serious muscle and joint problems. In this case, providing a kneeling mat is the simplest form of modified work to protect workers' knees. With the support of machinery, another alternative is to adjust the height of the handling material to a comfortable working level.

Furthermore, a worker must occasionally twist their wrist and elbow to perform a task, and this may cause pain and strain. Adjusting the height of the workstation components (i.e., tables, computers, and machines) can help to solve this problem. In addition, using better-designed tools, such as ergo-friendly pliers, which can themselves bend to a certain degree, will minimize the need to twist the wrist.

After implementing the modified work, another round of the improved PDA can be conducted in the manufacturing plant and the results of the updated PDA can be compared with the older version to realize the ergonomic risk reduction. Moreover, benefits can also be expected in the form of a reduction in the number of insurance claims and injury reports.

2.5 Limitations

More implementations of this proposed improved PDA form are required in order to validate its universality and flexibility to other industries. Moreover, it is recommended that the modified work be implemented followed by an updated PDA to compare the ergonomic risk reduction between the two versions of PDAs. This is one of the next steps of this research.

In addition, the current method of using observation to collect body posture data can be improved in order to obtain more accurate body posture data for risk assessment. Wang et al. (2015) summarize the existing techniques for WMSDs risk assessments, outlining their benefits and limitations. To be more specific, although direct observation involves minimal work disruption and instrumentation requirements, the results are based on subjective evaluation, and inter-rater differences will exist between observers. These methods can be time-consuming and error-prone since the required information, such as back bending position, must be collected accurately in order to analyze the potential risks of tasks and workers. Li et al. (2016) propose a framework to use 3D motion-based ergonomic analysis to obtain human body posture data for risk analysis. This is not within the scope of this chapter but is another potential area of study to improve this framework.

2.6 Conclusion

Ergonomic assessment supports the return-to-work programs administered by WCBs by assessing an existing workplace to determine any changes or modifications necessary to secure the returning worker's safety. This chapter proposes an improved PDA form and describes its implementation. It also discusses a framework capable of integrating the content in the proposed new PDA form with existing risk assessment tools, resulting in a comprehensive and intelligent application of PDA. Proper implementation of this improved PDA enables risk identification and

evaluation, and proactively mitigates risk for workers by providing modified work. This framework is implemented in a manufacturing facility as a case study in which four main ergonomic risks are listed for the modified work investigations. These four main ergonomic risks can also be considered in future studies. The framework is not limited to implementation in manufacturing industries; rather, it has the potential to assist any industry that involves physically-demanding tasks. In addition, as a result of this initiative, health care personnel in an organization's health and safety department can be better informed about workers' job requirements. Ultimately this will lead to reduced insurance claims and injuries in the industry.

2.7 Acknowledgements

The authors would like to acknowledge the assistance and support from the Natural Sciences and Engineering Research Council of Canada (NSERC) through the Industrial Research Chair (IRC) program (File No. IRCPJ 419145-15), as well as the collaborating industry partner, All Weather Windows. The authors wish to give special thanks to Melissa Ristau (Health and Safety Nurse, AWW), Estelle Carson (Occupational Health and Safety Manager, AWW), and all the production line supervisors who aided in the completion of the project. Also, the authors would like to thank Dr. SangHyeok Han (Assistant Professor, Concordia University), Dr. Marwan El-Rich (Associate Professor, University of Alberta) and Dr. SangUk Han (Assistant Professor, Hanyang University) for the brainstorming and discussion that contributed to this research.

CHAPTER 3: EVALUATION OF MUSCLE ACTIVITY DURING REPETITIVE MANUAL MATERIAL HANDLING ²

PREFACE

The work presented in the journal paper appearing as Chapter 3 of this thesis was conducted as a collaboration between Dr. Amin Komeili and the author of this dissertation. The AnyBody Technology modelling presented in Section 3.2.2 was developed by Dr. Komeili.

3.1 Introduction

Manufacturers seek to automate construction processes in order to reduce over-exertion and awkward body postures of workers. However, manual work in construction is inevitable. Repetition of task manoeuvres in particular is a major issue and causes musculoskeletal disorders (Asensio-Cuesta et al. 2012). Hsie et al. (2009) investigate working time and break schedule in order to optimize the operation process by minimizing job duration and workload. A repetitive task during a certain period requires involvement of a specific group of muscles repeatedly, which results in the development of muscle fatigue. Alternatively, working with adequately timed breaks may reduce the risk of injury (Jaffar et al. 2011). In conventional retrospective risk assessment of workstations, workers' compensation claims are evaluated to identify ergonomic problems, so exposure to the causes of injury usually occurs prior to unsafe tasks being identified. However, a prospective ergonomics study of human body interaction with workstation elements could reduce future injury incidents. Therefore, observing the way workers perform their repetitive tasks in a construction company, for instance, is of high importance for health and safety programs as it supports preventive measures to prevent or reduce instances of injury to workers.

² A version of this chapter has been accepted in the *Journal of Automation in Construction*, AUTCON-02194, 10 pages (In press).

Muscle activity is an important metric that provides insight into the load and function of muscle control. Surface electromyograms (sEMG) have been used in past studies to collect the electrical potential when muscles are electrically or neurologically activated. The sEMG signal is altered based on the extent of muscle involvement during the occupational work (Lindström et al. 1977). Analysis of sEMG can thus serve as a non-invasive method to predict muscle activity and development of fatigue (Zajac et al. 2003; Roy et al. 1989). To study muscle fatigue development using sEMG, some parameters, such as Root-Mean Square (RMS), Average Rectified Value (ARV), Mean Frequency (MNF), and Median Frequency (MDF), are suggested in the literature (Cao et al. 2007; Georgakis et al. 2003; Kim et al. 2007; Mananas et al. 2005). Although sEMG technique provides valuable information about muscle activity, its application is limited to superficial muscles. Hence, the state of load distribution throughout the entire human body cannot be assessed using the sEMG technique.

Knowledge of internal loads and moments acting on body segments is important in describing interactions of skeleton components in a wide range of human body-related studies, such as prosthesis design, preclinical testing, and numerical models of the musculoskeletal system. Despite the advancement of technology, *in-vivo* measurements are limited to a relatively small set of applications, as they are invasive methods and are inhibited by technical limitations (Schellenberg et al. 2015; Finni et al. 1998; Komi et al. 1992). It is thus vital to develop musculoskeletal models in order to estimate internal loads. These models consider bones to be rigid segments the degrees of freedom of which are constrained by joints and the motions of which are actuated with contractions of attached muscles. The success of human models in the estimation of muscle forces and joint moments, meanwhile, is widely reported in the literature (Vaughan et al. 1992; Winter 2009). Musculoskeletal modelling, in contrast with *in-vivo* muscle

force measurement, is a non-invasive and a more feasible technique in most muscle activity analysis. Musculoskeletal models calculate the tissue/joint forces/moments level required to complete a task, and help with making judgments about the tissue-level loading condition. They have been used in a variety of applications spanning job safety evaluation, task visualization, and clinical assessments (Wagner et al. 2007). Recognizing their success in estimation of the internal loads, researchers prepare sophisticated and highly accurate human body models and further implement them in industry applications with minimum manipulation. Inverse-dynamics analysis of human body muscles and joints has been undertaken in recent studies to measure real-time muscle forces while performing a task manoeuvre (Vaughan et al. 1992; Winter 2009; Erdemir et al. 2007). The AnyBody Modelling System (AnyBody Technology A/S. 2015), a software for development and analysis of the musculoskeletal system, is used to dynamically assess the human body interaction with workstation elements. The AnyBody Modelling system is able to calculate individual muscle forces and joint moments using advanced optimization techniques in order to solve the muscle redundancy problem (Wagner et al. 2007).

Low back pain (LBP) is extremely prevalent and widespread among construction workers (Hildebrandt 1995). Back-related complaints are more costly than those from any other body part for work-related claims. Hence, in this study, repetitive heavy material lifting manoeuvres are simulated and fatigue development is studied in some of the superficial low back muscles using sEMG experiment and human body modelling. A human body model, including musculoskeletal bones and muscles, is constructed to predict muscle forces and joint moments. The human body model is driven using motion capture data from the experiment in order to replicate the lifting manoeuvre. The objective of this study is to propose a framework to (1) investigate muscle fatigue resulting from repetitive tasks in construction manufacturing operations by analyzing

four sEMG parameters, RMS, ARV, MNF and MDF; and (2) create a human body model which interacts with workstation elements to investigate muscle forces and joint contact forces and moments. The sEMG parameters, calculated from experimental data, and muscle activity, calculated in the human body model, are compared and cross-validated. The long-term objective is to create a proactive ergonomic analysis method to reduce the risk of work-related injuries by identifying overloaded bones and muscles in the musculoskeletal system, and to seek alternatives by modifying and simulating the interactions between the worker and workstation. The methodology of this framework is described in the next section, followed by the results of a case study. The results of fatigue analysis, muscle forces, joint moments and corresponding methodology limitations are discussed.

3.2 Muscle Fatigue Identification Method

The research framework illustrated in Figure 3.1 is implemented and tested in a Canada-based window and door manufacturer, All Weather Windows, and consists of three steps. The first step is plant observation and physical demand analysis, which identifies high-risk tasks such as heavy material lifting (Li. et al. 2015). The next step is to simulate high-risk construction tasks identified from observation both experimentally and numerically. Reflective markers are used to capture the kinematics of the task manoeuvres; the obtained motion capture data from experimentation is used as input to the human body model in order to drive the human body model and confine the degrees of freedom. sEMG sensors are attached to the low back area to experimentally measure the electrical activity of muscles. The sEMG data are used for two purposes: (1) to study the fatigue development in corresponding muscles, and (2) to validate the human body model. The human body model has been extensively used in sport injury prevention and pre/post-operation implant analysis. However, the use of human body models in the

ergonomic design of workstations remains a science under development. Through these kinematic analyses, interactions between worker and workstation can be investigated. Grounded in experimental and simulation modelling results, proactive analysis can be accomplished in order to reduce ergonomic risks. Corresponding corrective measures to modify the existing workstation are tested and optimized experimentally and/or numerically before being proposed to the manufacturer.

The output of this framework is to identify muscle fatigue from sEMG data analysis and to identify muscles and joints that are overloaded during task manoeuvres. The human body model is an effective tool to assess the new proposed workstation prior to implementing any necessary modifications. The ultimate goal is to reduce the rate of worker injuries in the manufacturing plant and ensure a better working environment.

In the case study, a repetitive lifting task is selected and low back muscle performance is investigated via sEMG muscle activity measurement. The experiment is conducted in the Syncrude Centre at the Glenrose Rehabilitation Hospital (Edmonton, Canada). The kinematics of the lifting task is recorded in order to establish a human body model using AnyBody Technology software (Komeili et al. 2015).

Three male volunteers ranging from 27 to 31 years of age, from 173 to 180 cm in height, and from 57.0 to 80.5 kg in body mass with no history of injury on body parts are invited in this study. The test procedure and possible risks of injuries are explained and a written consent form is obtained from each volunteer/subject.

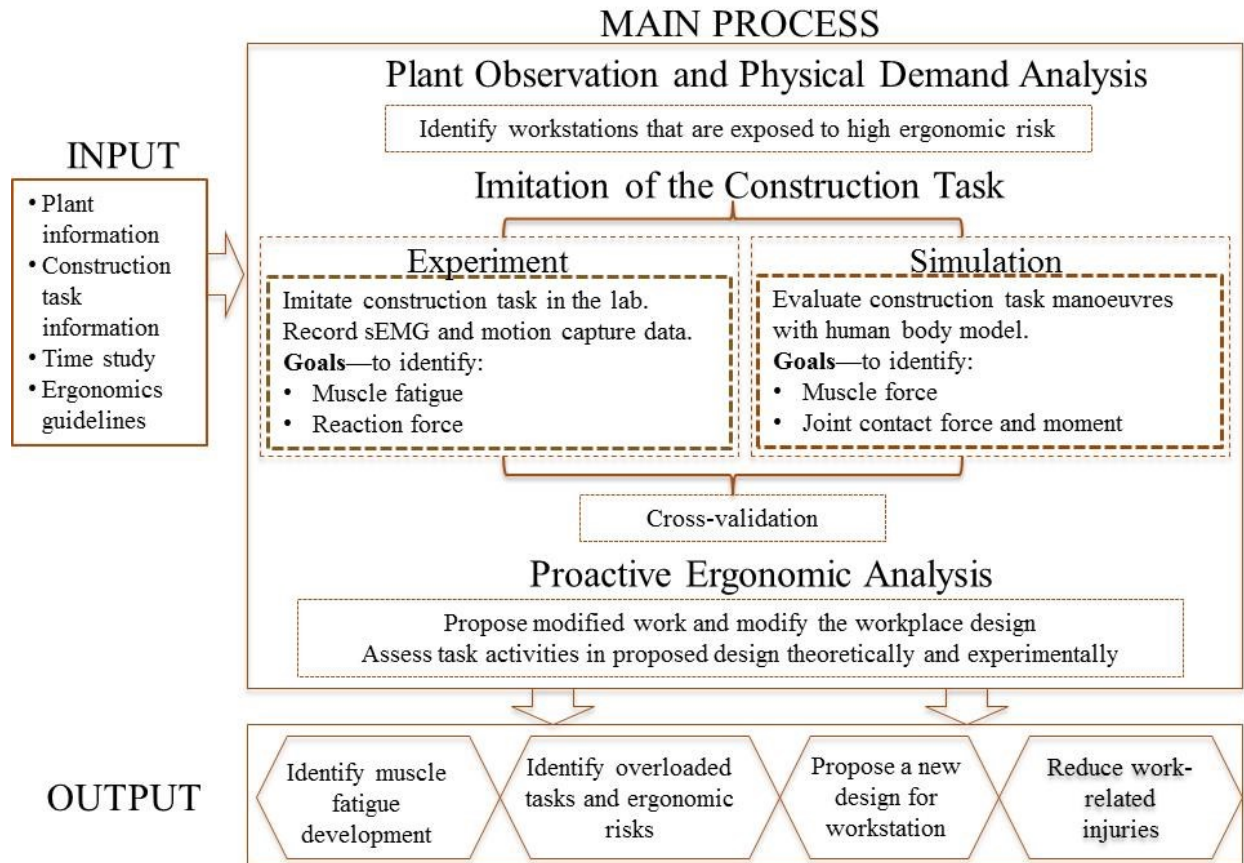


Figure 3.1: Description of research framework

3.2.1 Motion capture and sEMG

3.2.1.1 Data acquisition

The lifting task under study is emulated in the motion capture lab. The sEMG electrodes are attached at specific anatomical locations in order to record electrical muscle activities which corresponds to the amount of force muscles produce. Four pairs (left-right) of sEMG surface electrodes are placed on the skin at the location of the erector spinae muscle group, which includes the iliocostalis (CH7&8), longissimus (CH5&6), multifidus (CH3&4), and rectus abdominis (CH1&2) muscles (Figure 3.2). Areas of electrode placement are shaved and rubbing alcohol is applied to improve conductance. The length of upper and lower limbs including

forearm, upper arm, thigh, shank, and trunk, along with the weight of the subject, are measured in order to develop personalized human body models.

Optical motion capture is a common and effective method for capturing human motion. In addition to sEMG electrodes, thirty-six self-adhesive reflective markers are attached to the subject's skin and are imaged by a set of cameras to record the kinematics of body segments while performing the selected task. The captured marker trajectories are used to drive the human body model. The anatomical positions of the reflective markers and instructions to locate them while the subject performs the lifting task are illustrated in Figure 3.3 and Table 3-1. An 8-camera Eagle Digital Motion Analysis system (Motion Analysis Corp. 2015) sampling at 120 Hz is employed to collect the 3D coordinates of the reflective markers. The subject is surrounded by motion capture cameras to ensure that no marker disappears from camera view at any time. (Nevertheless, it is noted that the location of a missed marker can be interpolated in post-processing.) Either markers are placed directly on the skin or form-fitting clothing is worn to prevent the markers from sliding. As a general rule, markers are to be placed symmetrically to help the motion capture system distinguish the left and right sides. Two Advanced Mechanical Technology Inc. (AMTI) force plates (Advanced Mechanical Technology Inc. 2015) sampling at 2,400 Hz are utilized to capture ground reaction forces under the subject's feet.

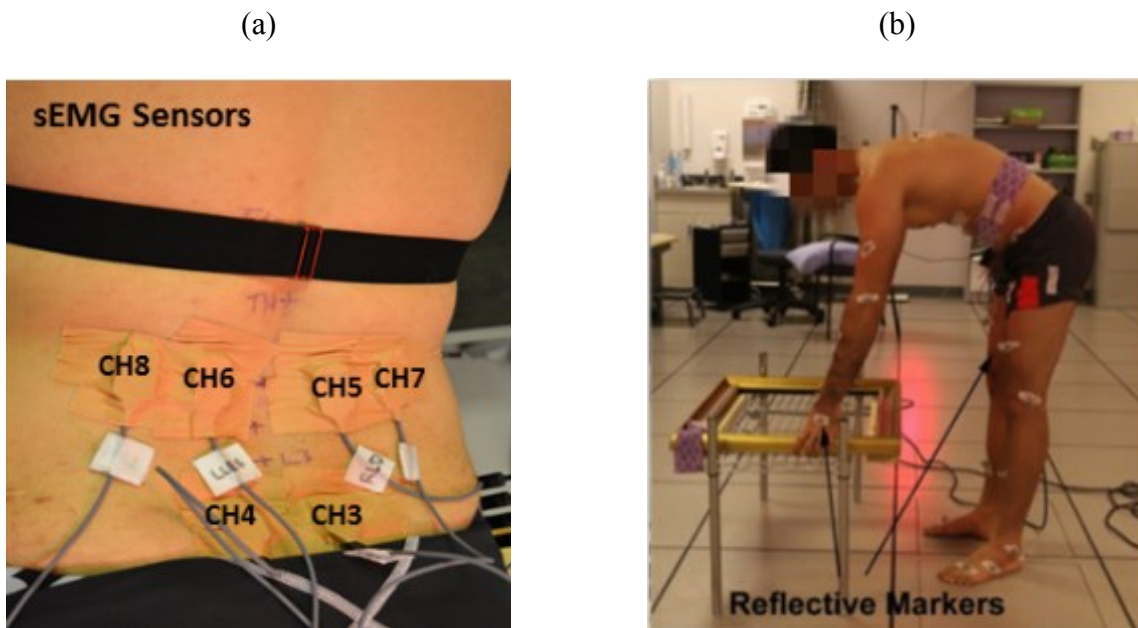


Figure 3.2: (a) sEMG sensors location; (b) Reflective markers attached to specific anatomical locations

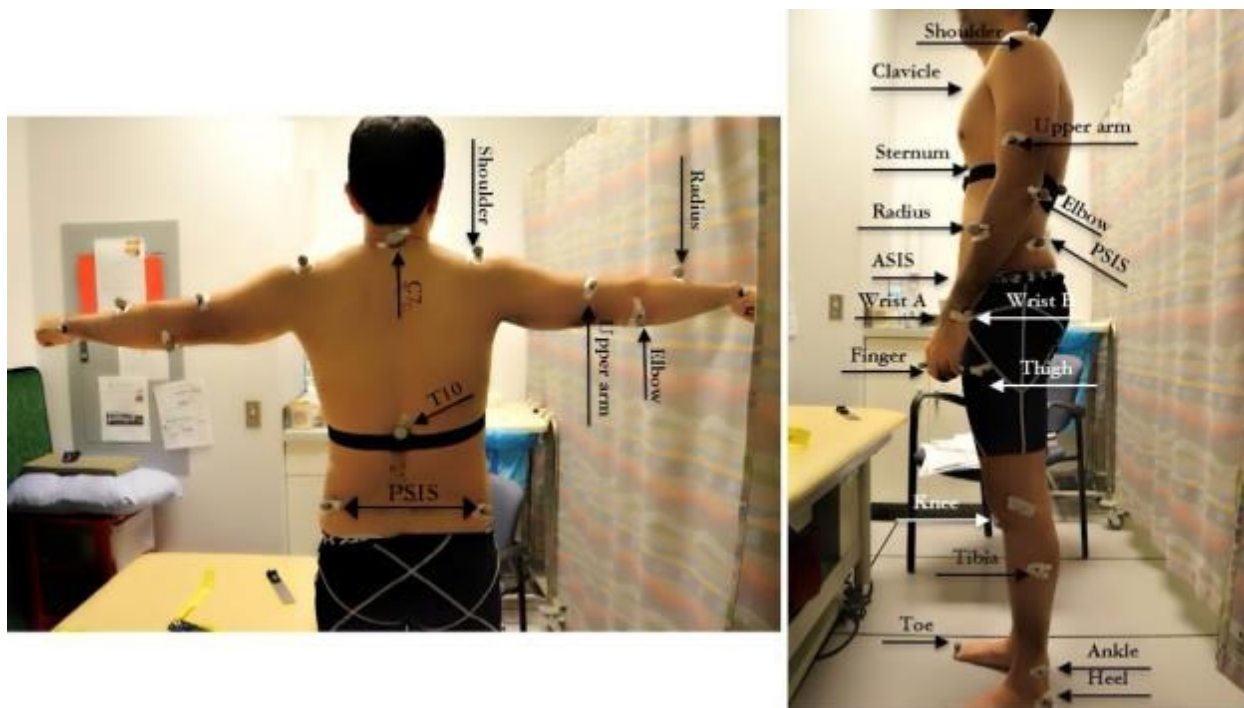


Figure 3.3: Positions of 36 reflective markers used to drive the AnyBody model

Table 3-1: Reflective markers position descriptions and marker names in the AnyBody model.

Marker Positions	Marker Position Descriptions	AnyBody Model Marker Name
Shoulder (Acromion-clavicular joint)	Place markers on each of the left and right acromion-clavicular joint. To identify the acromion-clavicular joint, have the subject move their arm up and down to find the area of the shoulder that remains stationary.	RSHO, LSHO
Upper arm	Place the marker at the middle of the line that connects the shoulder marker to the elbow marker.	RUPA, LUPA
Elbow	Place the marker on the elbow and ensure that it does not move when the arm bends up and down.	RELB, LELB
Forearm	Place the marker on the middle of the radius.	RFRA, LFRA
Wrist	Place markers on the radial styloid process of the ulna and the styloid process of the radius, respectively, for each wrist.	RWRA, LWRA, RWRB, LWRB
Finger	Place the marker on the proximal phalanx of the index finger.	RFIN, LFIN
Clavicle	Find the area between the two collar bones.	CLAV
Sternum	Place a marker at the center of the line that connects the nipples.	STRN
Cervical vertebra 7	Place a marker on C7, which is identified as the bone along the spinal column that projects (where the back of the neck ends) when the subject bends their head down.	C7
Thoracic vertebra 10	Count 10 vertebrae down from C7 while subject bends forward.	T10
Pelvis-anterior superior iliac (ASIS)	Put the marker on the iliac crest, which is the hip bone protruding laterally when viewed from the anterior direction.	RASI, LASI
Pelvis-posterior superior iliac (PSIS)	Find the dimples on the low back area at each side of the spinal column below the waist level.	RPSI, LPSI
Thigh	Place the thigh marker at the middle of the line that connects the ASIS marker to the knee marker.	RTHI, LTHI
Knee	Place the marker on the lateral side of the knee on the lowest area of the upper leg that does not move when the lower leg is swung back and forth.	RKNE, LKNE

Marker Positions	Marker Position Descriptions	AnyBody Model Marker Name
Tibia	Place the tibia marker on the outer edge of the fibula bone at the middle of the line that connects the ankle marker and knee marker.	RTIB, LTIB
Ankle	Put a marker along the line that connects the opposite sides of the ankle bone.	RANK, LANK
Heel	Place a marker on the posterior side of the heel bone at the same height as the toe marker.	RHEE, LHEE
Toe	Place a marker either on the nail of the hallux (i.e., first toe) or on the base of the toe.	RTOE, LTOE
Metatarsal	Place a marker on the lateral side of the foot (on the base of the fifth toe).	RMT5, LMT5

3.2.1.2 Maximum voluntary contraction and test procedure

Maximum Voluntary Contraction (MVC) tests of back flexion and abdominal extension are also conducted before and after each trial in order to normalize the muscle activity (Demoulin 2010). Subjects are instructed to keep their upper body unsupported during MVC trials. In terms of the back flexion MVC test (as indicated in Figure 3.4a), the lower body from the iliac crest is secured to the table while the subject is in the prone position. The test begins while the subject is at 80° flexion, followed by the gradual extension of the torso to the horizontal level of the testing table. For the abdominal extension test (as indicated in Figure 3.4b), the subject sits on the edge of the table with legs pointing straight out and strapped to the table. The subject gradually lowers the torso to the horizontal position while keeping arms across the chest (Demoulin 2010; Demoulin et al. 2006).

(a) Back flexion

(b) Abdominal extension

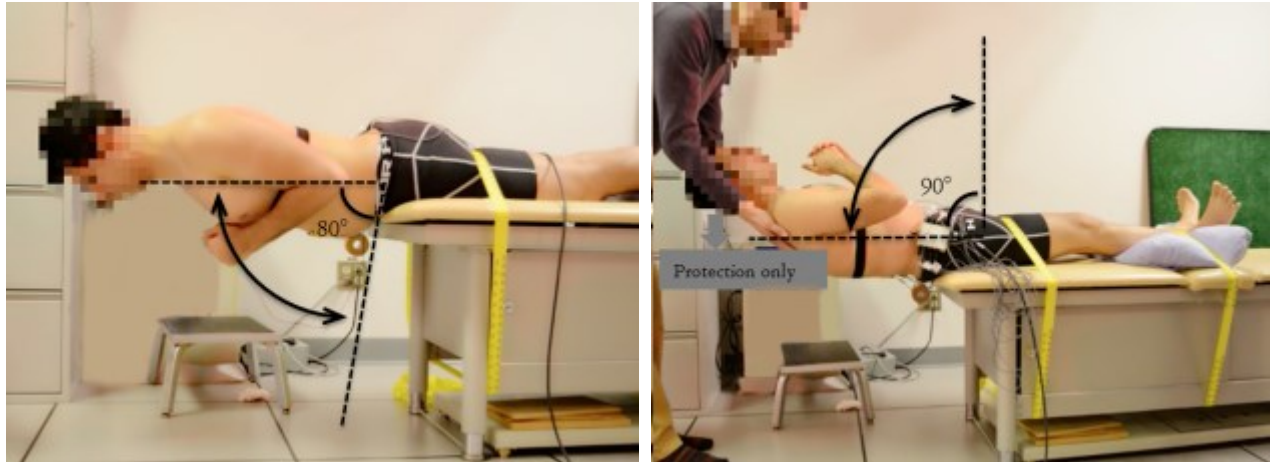


Figure 3.4: Body posture and procedures of maximum voluntary contraction test: a. back flexion; b. abdominal extension

Each cycle consists of an extension and flexion of the spine in a repetitive lifting task. One complete cycle of the lifting task consists of bending forward without twisting the trunk or bending legs, and lifting a 15 lb rectangular window frame from a table at the knee level, holding it close to the body in an upright standing posture, and returning it back to the table as illustrated in Figure 3.5. The weight of the window frame meets the terms of the Workplace Safety & Prevention Services (WSPS) risk assessment procedure. The sEMG graph at the bottom of Figure 3.5 shows experimental raw data for one full cycle of activity corresponding to the posture drawings. Three trials of the lifting task are performed, with 20 cycles in each trial, in order to induce muscle fatigue. One minute of rest time between trials is given to subjects to prevent muscle injury during experimentation.

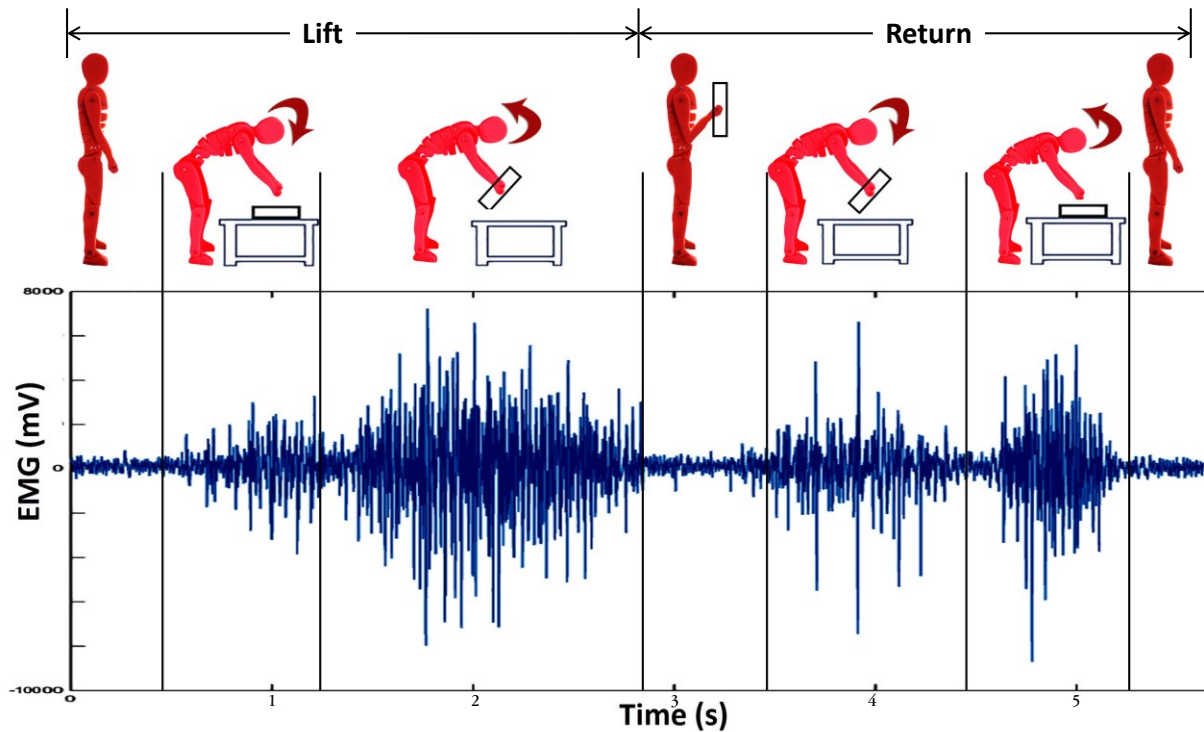


Figure 3.5: Configuration of a full cycle lifting task with two epochs corresponding to experimental sEMG raw data

3.2.1.3 Post-processing

One full cycle of a lifting manoeuvre consists of two epochs; each starts from upright standing posture and ends in the next upright standing posture, either with or without the window frame in hand, as visualized in Figure 3.5. The first epoch represents lifting the load, labelled as “Lift” in the figure, and the second represents returning the load back to the table, labelled as “Return”. Every trial includes twenty full repetitions of lifting tasks. The sEMG signal of each trial is thus segmented into 40 epochs. Eight sEMG channels (CH1-8) record four pairs of muscle activities, as shown in Table 3-2, for both the right and left side of the body, where odd and even numbers are assigned to channels in the right and left side of the body, respectively. The sEMG signal processing is first band-pass filtered (12-1200 Hz) to remove high frequency noises (Cao et al. 2007; Georgakiset al. 2003). The standard deviation of the sEMG over the epoch is calculated

using the empirical cut-off constant, k , where k is equal to 0.6 multiplied by the maximum standard deviation value, as indicated in Eq. (3-1). The sEMG parameters are calculated using the sliding window technique, in which a sliding time window of 1 second is taken and continuously displaced by 10 milliseconds along the hatched windows (Sarmiento et al. 2011). The aforementioned four fatigue parameters are calculated for each time window. All coefficients are then related to time.

$$k = 0.6 \times \max(\sigma(t)) \tag{3-1}$$

where

$\sigma(t)$: standard deviation value of the sEMG

t : time over the epoch

Table 3-2: Four pairs of muscle activities recorded by eight sEMG channels.

Channels	Muscles
CH1	Right Rectus Abdominis
CH2	Left Rectus Abdominis
CH3	Right Multifidus
CH4	Left Multifidus
CH5	Right Longissimus
CH6	Left Longissimus
CH7	Right Iliocostalis
CH8	Left Iliocostalis

A subroutine is developed in MATLAB to calculate four parameters (RMS, ARV, MNF, MDF) for each epoch by following Eq. (3-2) through (3-5) (Georgakis et al. 2003; Kim et al. 2007). The RMS and ARV parameters represent the average amplitude of sEMG signals, which

correlates to the percentage of recruited muscle fibres and, consequently, correlates to the muscle force. The magnitude of sEMG signals correlates to the severity of the stimulation by which muscles are activated. In the other hand, the frequency of the sEMG signal relates to the frequency rate of the neuron motor excitation (Lindström et al. 1977) To handle larger loads or produce faster contractions in muscles, human body utilizes two processes: (1) motor neurons are stimulated with higher frequencies; (2) motor neurons are stimulated with higher intensity. With the frequency analysis, the frequency domain of the sEMG signal is obtained. The MNF and MDF parameters indicate the mean and median frequency at which muscles are activated by the nervous system, where a spectral shift toward lower frequencies in MNF and MDF curves is an indication of muscle fatigue (Kim et al. 2007). The sEMG parameters of RMS and ARV for each sEMG channel are normalized using the MVC values obtained before performing the test while MNF and MDF are not normalized.

$$RMS = \sqrt{\frac{\int_{-\frac{T}{2}}^{\frac{T}{2}} EMG^2(t) dt}{T}} \quad (3-2)$$

$$ARV = \frac{\int_{-\frac{T}{2}}^{\frac{T}{2}} |EMG(t)| dt}{T} \quad (3-3)$$

$$MNF = \frac{\int_0^{\infty} \omega P(\omega) d\omega}{\int_0^{\infty} P(\omega) d\omega} \quad (3-4)$$

$$\int_0^{MDF} P(\omega) d\omega = \int_{MDF}^{\infty} P(\omega) d\omega = \frac{1}{2} \int_0^{\infty} P(\omega) d\omega \quad (3-5)$$

where

T : time window $[-T/2, T/2]$

t : time

P : power spectral density of the sEMG signal

ω : frequency variable

3.2.2 Human body modelling

In this study, the AnyBody modelling system is used to create the human body model that simulates the window frame lifting task. The model contains more than 500 muscles. By using the motion capture data as the driver of human body model, muscle forces in the iliocostalis, longissimus, and multifidus are predicted. Some model configurations can be retrieved from a public-domain repository, which is accessible through the AnyBody modelling system website (AnyBody Technology A/S. 2015), and can be rescaled to eliminate the need to rebuild the human anatomy. The model employed is based on modifications of a standard application from the model repository, MoCap. To account for inter-individual anatomical variations and to minimize co-variance between parameters, a general scale factor (e.g., height of the subject, height of the standard model) is used. (Separate scale factors for groups of bones such as lower limb, upper limb, etc., can be used if a precise model is needed to study individual joints.)

The human body model is subjected to the gravity load, carried load and ground reaction forces under feet. The carrying load (weight of the window frame) is applied to the model with two vertical concentrated loads acting on the left and right finger markers. To ensure stability, some degrees of freedom (DOFs) of bones can be restrained. For example, in the case of the lifting manoeuvre, the markers on the foot, including heel, toe, and metatarsal markers, are connected to make the foot acting as a rigid body. The large number of DOFs, due to the presence of hundreds of muscles and bones in the model, leads to a large system of equilibrium equations that must be formulated and solved. The other challenge is to select among several muscle recruitment scenarios and optimization algorithms for muscle force calculation. In addition to the equilibrium equations, then, a reasonable minimization function in accordance with the physiological assumptions is required in order to constrain the muscle recruitment (De Zee et al. 2007;

Prilutsky et al. 2002; Rasmussen et al. 2001; Van Bolhuis et al. 1999). Therefore, the only viable solution is to use a computer system to solve the equilibrium equations, considering proper muscle recruitment algorithms and inverse-dynamics analysis. With the current technology, it is prohibitive to compute the forward dynamics approach and determine the equilibrium equations. Inverse-dynamics is thus used for such complex systems. Using this inverse-dynamics approach, the body model is fed the kinematics of the body along with the applied external forces needed to predict internal forces. Notably, the inverse-dynamics analysis solver in the AnyBody modelling system is fully dynamic in the sense that the body's inertia and gravity are included in the analysis. Thus, Muscle force, joint contact force and moment can be derived from AnyBody modelling system.

To cross-validate experimental results with simulation modelling results, quantification the correlation between RMS sEMG curves and calculated muscle forces are chosen. The areas under the curve for the normalized RMS sEMG and muscle force are compared. The normalized area at each time point is calculated based on Eq. (3-6). The normalized area parameter related to RMS sEMG and muscle force indicates the total normalized power and activity of the muscle from t_0 to t_i , respectively.

$$A = \sum_{t_0}^{t_i} f \times \Delta t_i \quad (3-6)$$

where

A : normalized area at time t_i

f : normalized RMS sEMG or normalized muscle force

Δt_i : time difference between t_i and t_{i-1}

3.2.3 Proactive ergonomic analysis

Muscles and bones that either developed fatigue or reached maximum capacity in the results of the simulation model are targeted in the revision of the task manoeuvre to mitigate their loading condition. Following suggestions could be used to achieve proactive ergonomic measures: (1) adjusting the working schedule such as limiting the working duration and repetitions, increasing the break time and staggering the task between workers or assigning more workers to carry out the task; (2) implementing ergonomic corrections, such as modifying task manoeuvres and proposing physical alternation of the workstation to reduce the applied loads on the musculoskeletal system. The latter may require capital cost since it includes altering current workplace design and using new equipment.

3.3 Results and Discussion

The physical symptoms of subjects, such as perspiration, respiration rate, heartbeat, and feedback, serve as indicators of the onset of fatigue. Table 3-3 shows the mean heartbeat of subjects during the lifting trials, which increases constantly as subjects perform the test. The increased heartbeat indicates that the test protocol is adequately challenging however safe for subjects.

Table 3-3: Heartbeat rates of subjects during lifting task at the end of each trial.

Heartbeat			
	Trial 1	Trial 2	Trial 3
Subject 1	97	103	109
Subject 2	91	96	107
Subject 3	87	88	103

When the sEMG signals are analyzed to calculate the four parameters mentioned above, the results of the abdominal, multifidus, longissimus, and iliocostalis sEMG parameters show slight

changes for different epochs. The abdominal (CH1&2), multifidus (CH3&4), longissimus (CH5&6), and iliocostalis (CH7&8) sEMG parameters obtained from subject 1 are given in Figure 3.6. The CH1 and CH2 sEMG sensors collect noisy and scattered data in which the epochs cannot be easily identified. Low abdominal muscle activity during the lifting task, and a considerable layer of fat in the abdominal section of the subject, could be the main factors affecting the sEMG signals from these two channels. The RMS and AVR parameters of sEMG signal show slight increase and the MNF and MDF parameters show slight decrease intra-trial (within-trial), as shown in Figure 3.6. However, in this pilot study, a specific pattern for these parameters among three subjects is not identified. This may be attributable to the load being insufficient to initiate fatigue and, to a lesser extent, to the interdependence of the low back muscles in handling loads. Also, the sEMG parameters fail to represent consistent inter-subject behaviour. Figure 3.7 presents the inter-trial (between-trial) variation of CH6 sEMG parameters for subject 1. As can be seen in the figure, the sEMG parameters do not change significantly between trials. The linear regression trendlines of sEMG parameters among three trials do not show any significant difference. A lower magnitude of the RMS in trial 3 is expected in comparison with trial 2 and trial 1, indicating muscle fatigue development due to repetitive material handling.

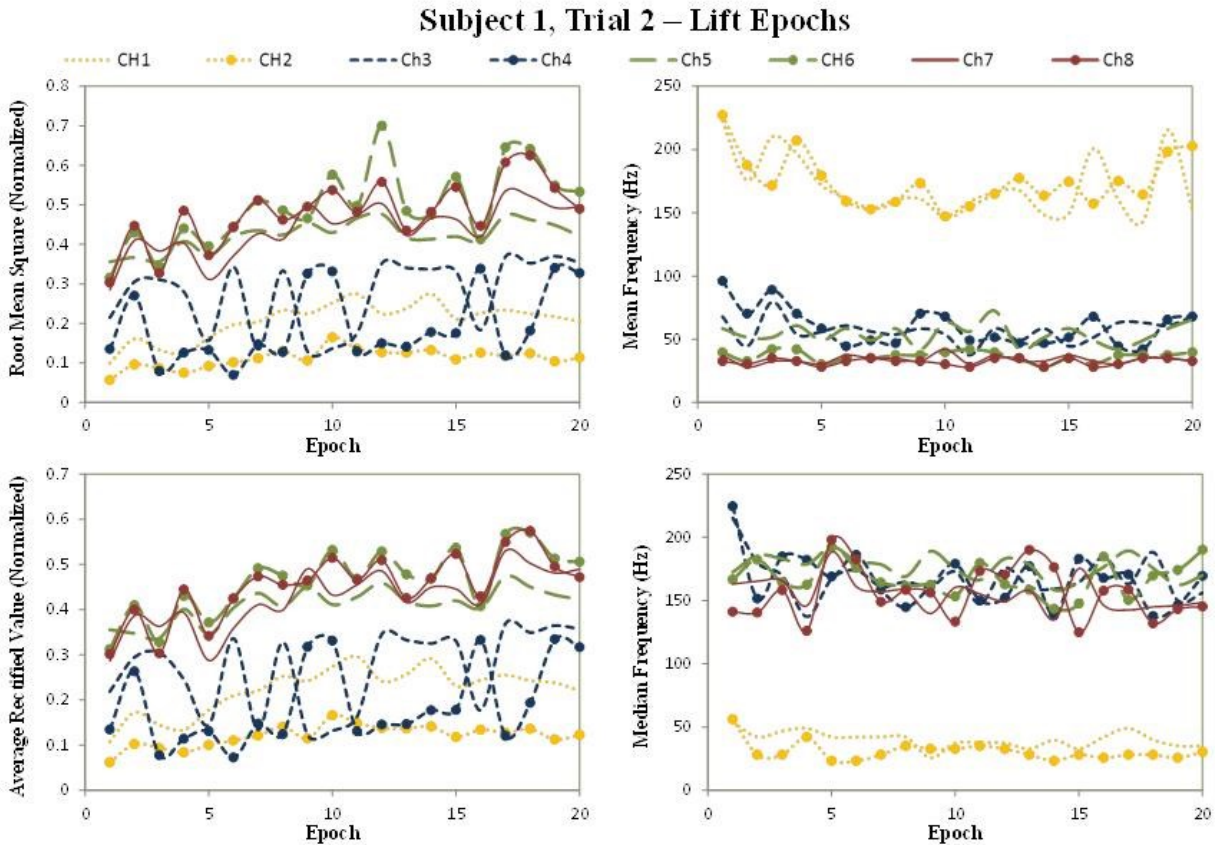


Figure 3.6: Normalized sEMG parameters of CH 1-8 obtained from subject 1 in trial 2. (Curves marked with/without circles represent muscles in the left/right side, respectively)

A shift of the entire power-frequency curve to the lower frequencies is identified in the literature as a fatigue indicator (Demoulin 2010). Figure 3.8 illustrates the power-frequency curve of the sEMG signal of CH5 for subject 3 in trials 1 and 2. The sharp decrease in power at the beginning of the curve is due to the use of the low pass filter in the data processing. As indicated in Figure 3.8, the power-frequency curve shifts to lower frequencies; however, only one of the subjects shows significant change in the power-frequency curve. In addition to the possible causes proposed above, this may be due to the full recovery of the muscles during the break between trials.

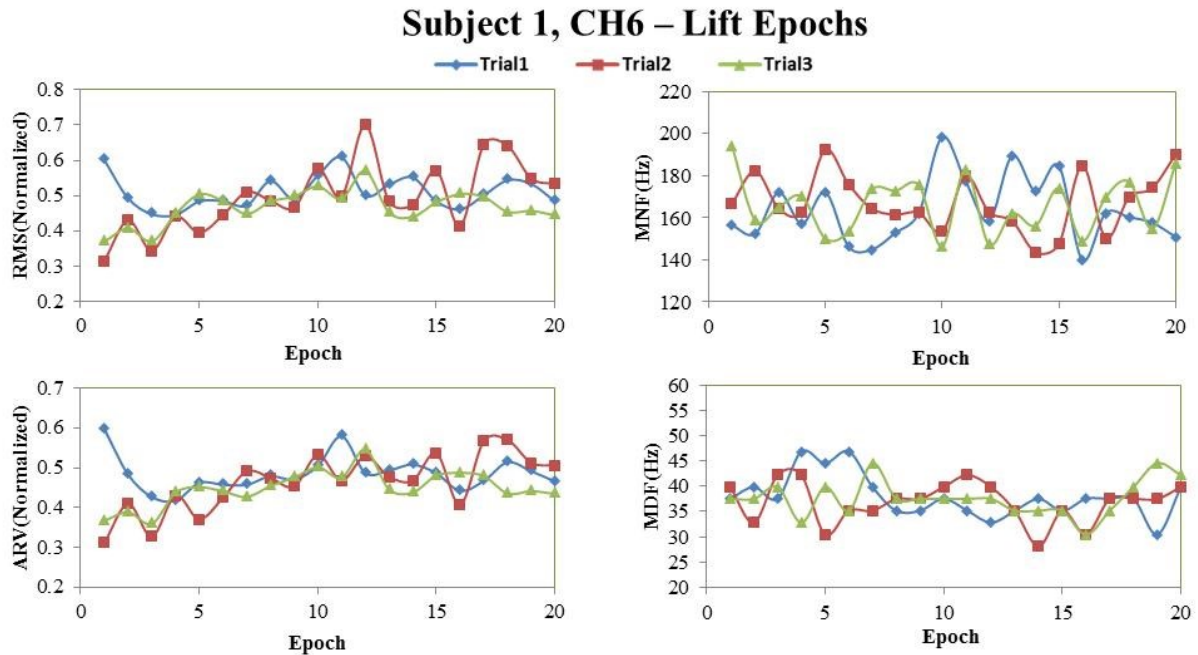


Figure 3.7: Inter-trial variation of sEMG parameters for subject 1 CH6 (left longissimus)

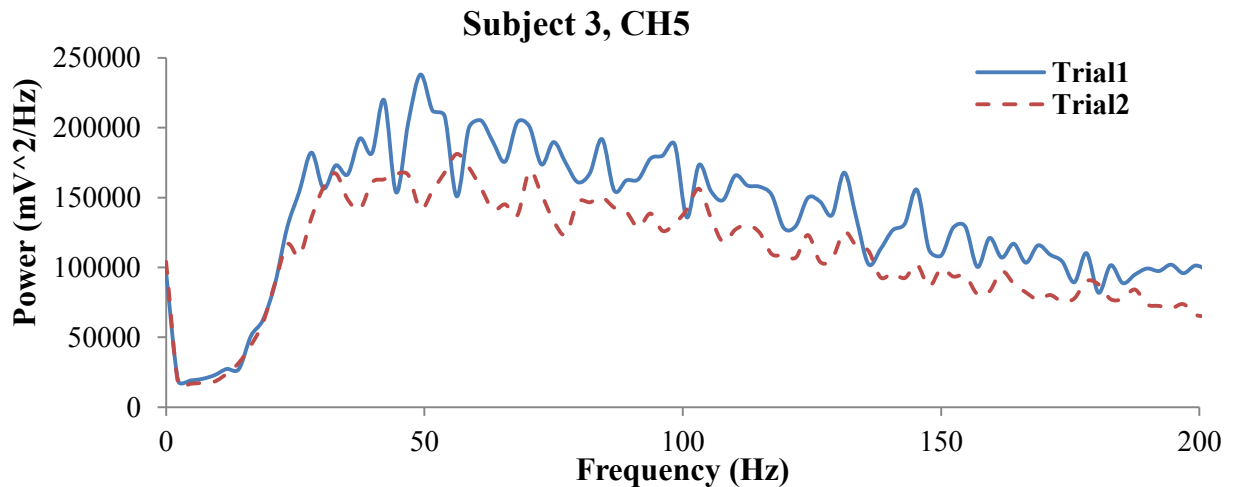


Figure 3.8: Comparison of power-frequency curves of CH5 (right longissimus) in trial 1 and trial 2 for subject 3

To validate the human body model, the computed muscle forces for iliocostalis, longissimus, and multifidus muscles are qualitatively compared with the corresponding sEMG activity in Figure 3.9, taking subject 3, trial 2, cycle 5 as an example. The CH1 and CH2 are excluded from this comparison due to artifacts in the sEMG data. As shown, the patterns of RMS curves and

calculated muscle forces are in good agreement during the lifting manoeuvre for all studied groups of muscles. The calculated multifidus, longissimus, and iliocostalis muscle forces show an equivalent trend in comparison with the sEMG RMS parameter. The peaks in muscle force correspond to the moments at which the subject lifts and returns the load to the table. The magnitude of the calculated muscle force is in agreement with the findings of a study by El-Rich et al. (El-Rich and Shirazi-Adl 2005) in which they employ a similar lifting task experiment. However, there is a time lag between peaks of sEMG RMS and computed muscle force curves, as seen in Figure 3.9. Possible reasons for this discrepancy are as follows: (1) In the lifting phase of the experiment, after the initiation of contact between hands and load, the subject gradually recruits back muscles to lift the load. In the human body model, however, the contact between the load and hands is formed immediately. Therefore, the variation of computed muscle force curve in the human body model is steep compared with the gradual change in the sEMG RMS curve; (2) The low back area contains a multi-layer group of muscles crossing each other, so the recording of sEMG sensors is affected by the activity of adjacent muscles; (3) Muscle forces are calculated using a theoretical minimization technique in the human body model and does not account for the biological factors such as preference of the subject in employing the muscles to perform the task, and chemical and biological reaction time in living tissues. We attempt to minimize this effect by using the superficial muscles for the validation of the human body model; however, better overlap can be expected between sEMG muscle activity and computed force if intramuscular EMG is used. Figure 3.10 illustrates the calculated normalized area for the corresponding curves in Figure 3.9. The correlation coefficient for all investigated muscles are greater than 0.96, representing strong correlation between the trend of RMS sEMG and muscle force curves. This strong correlation suggests that the sEMG experiment and human body

modelling are cross-validated and the results of human body model can be used to assess the loading condition in the musculoskeletal system.

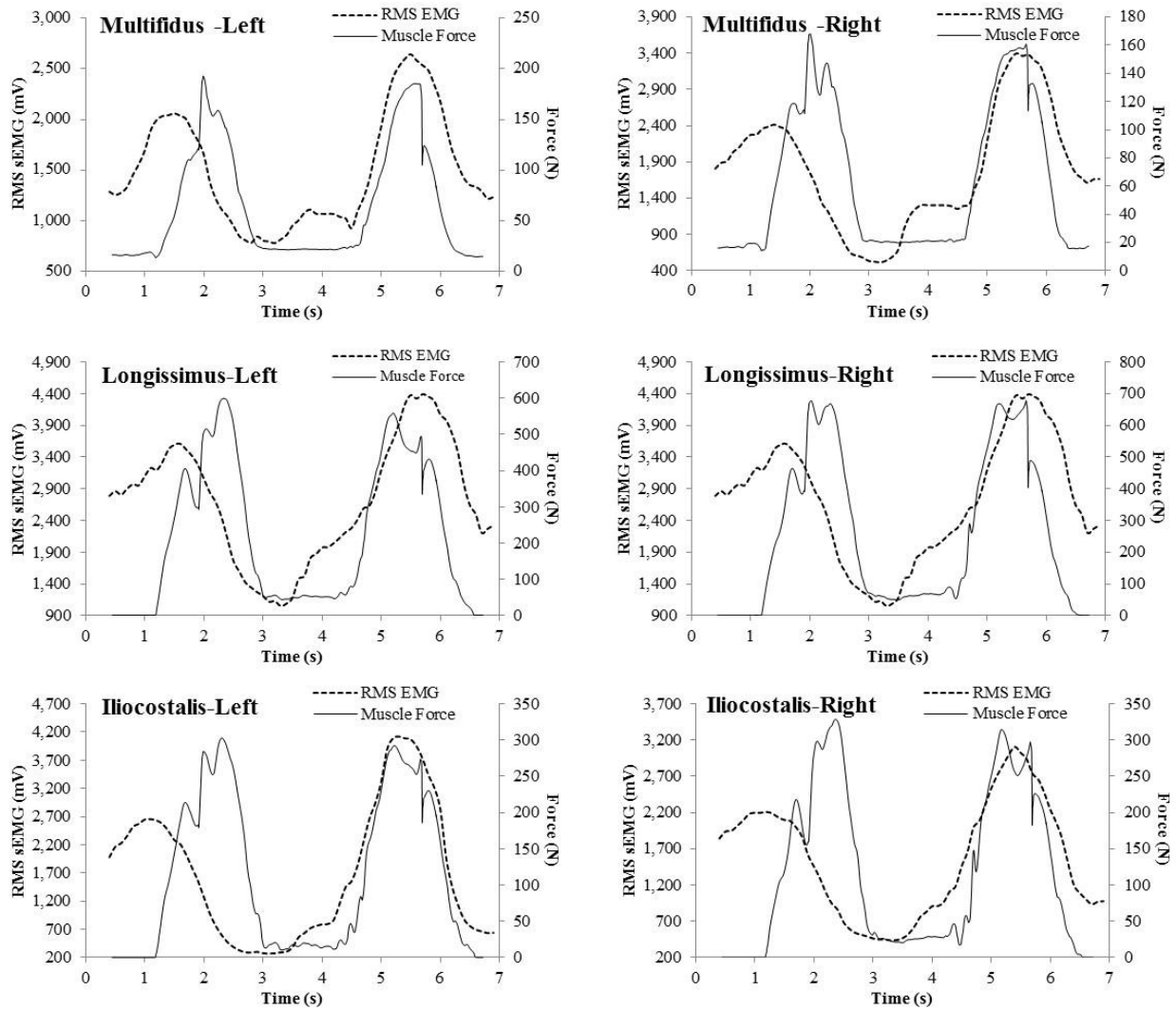


Figure 3.9: Comparison between the sEMG RMS and predicted muscle forces obtained from human body model

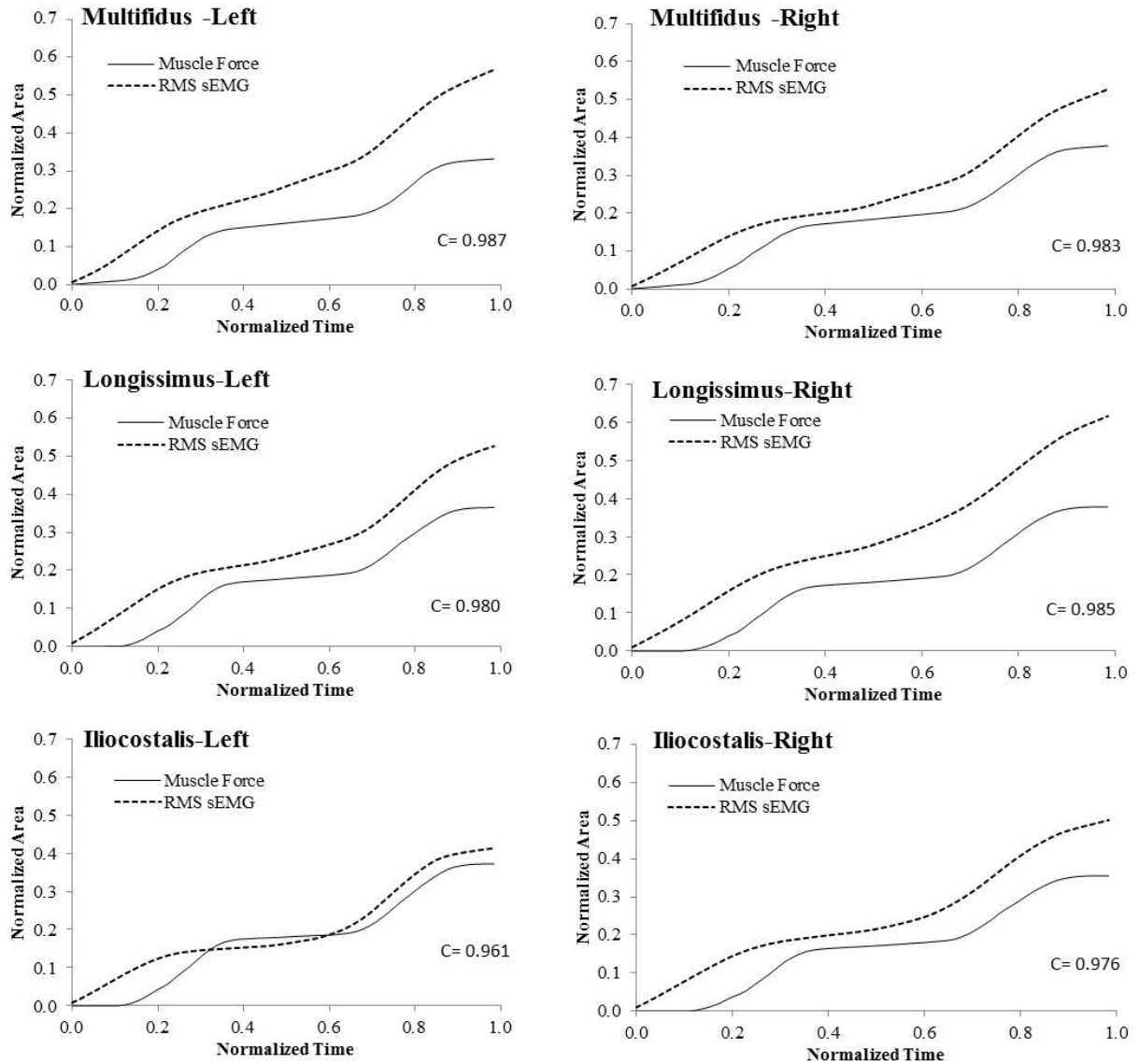


Figure 3.10: Comparison of the calculated normalized area related to RMS sEMG and muscle force curves presented in Figure 3.9; C: Correlation Coefficient

Based on the proactive ergonomic suggestions provided in section 2.3 and considering the workflow of the production line, following solutions are considered to modify the workstation in this study: (a) providing tools, such as a lifter, for workstations where awkward body posture is performed; (b) investing automated or semi-automated machineries to support heavy material handling tasks; (c) adjusting the height of the table to modify the task manoeuvres and

minimizing low back muscles strain; (d) assigning two workers for the lifting task. No severe muscle fatigue is identified in the results of the experiments in this case study. However large muscle forces are obtained in the human body model when the task manoeuvre is simulated. Therefore, without affecting the working schedule, conducting simple ergonomic modifications on the working table of the production line to improve the task manoeuvres and also training workers correct techniques of lifting task are the two proposals. Before implementing the outcomes of proactive ergonomic analysis, the new workstation is analyzed using the human body model. The musculoskeletal working condition is improved in the results of the human body model in terms of reduced maximum muscles forces and joint moments. In the ongoing study, the modified workstation will be implemented in the manufacture production line and rate of injuries related to the back pain will be monitored to assess the effectiveness of the ergonomic modifications.

3.4 Conclusion

This study proposes a framework for assessing muscle activity during repetitive lifting tasks, such as those present in construction work, using *in-vivo* experimental design and numerical modelling. The sEMG analysis in this study quantifies low back muscle activity; however, it has only limited capability to identify symptoms of muscle fatigue from the experimental design. Fatigue development does not alter sEMG signals significantly enough to be observed in the parameters. The experiment protocol lacks the necessary intensity to develop effective muscle fatigue, and the experiment limitations prohibit monitoring fatigue development using sEMG technique. It can be concluded that the effective application of sEMG is limited to superficial muscles in low fat areas in the vicinity of the sensor. There are challenges associated with sEMG technique in quantifying fatigue developed in deep muscles such as the low back area. These

integrated limitations of sEMG technique constrain its application in computing muscle activity and fatigue development for the entire body, thereby justifying the use of human body models in this regard. Human body models enable the measurement of more parameters, such as energy consumption, length, and kinetics of entire body segments with acceptable accuracy. The recorded sEMG data in this study is compared qualitatively with muscle forces predicted by the human body model. The RMS of sEMG and computed muscle forces show similar trends in the full cycle of the lifting task. Although the human body model approach is not effective in quantifying muscle fatigue, it is found to be successful in predicting the variation of muscle force in the body segments at each step of the lifting task. Thus both experimental and numerical simulation analysis facilitate proactive ergonomic analysis and reduce risks to workers by providing modified work and proposing re-design of the workplace. This approach could also be implemented at the design stage of the workstation. Task manoeuvres could be simulated and analyzed to ensure that, in the new designed workstation, muscles and joints will be functioning within their working capacity.

3.5 Acknowledgements

The study is supported by the Natural Sciences and Engineering Research Council of Canada (NSERC) Engage Grant and NSERC Discovery Grant programs. The authors also wish to acknowledge Glenrose Rehabilitation Hospital for allowing the authors to complete the experiment in their motion capture lab. Special thanks are extended to Mr. Justin Lewicke, who assisted in collecting the experimental data.

CHAPTER 4: 3D MOTION-BASED ERGONOMIC RISK ASSESSMENT AND ITS VALIDATION³

4.1 Introduction

Workers in the construction industry are exposed to tasks with higher physical demands—such as overexertion, repetitive motion, and awkward body posture—than those to which workers in other industries are exposed, thereby resulting in a comparatively high rate of work-related musculoskeletal disorders (WMSDs) (Wang et al. 2015; OSACH 2010). Schneider (2001) reports that construction workers are at risk of developing WMSDs, which may affect productivity and increase construction costs. These risks arise from the fact that many workers in this sector are involved in various construction activities such as cleaning, assembling, preparing the construction site, loading and unloading building material, operating power tools, and operating machinery. To some extent, ergonomic analysis prevents the onset of WMSDs and maintains or increases productivity, as it identifies ergonomic risks proactively and reduces inefficient and non-productive motions. Fatigue is another factor related to ergonomics that could result in a loss of productivity. Improvement of the physical condition of the workstation is therefore essential.

Partial ergonomic risk analysis of construction activities has been implemented using existing ergonomic analysis models such as Ovako Working-posture Analysing System (OWAS) (Karhu et al. 1997), Rapid Entire Body Assessment (REBA) (Hignett and McAtamney 2000; Janowitz et al. 2006), and Rapid Upper Limb Assessment (RULA) (McAtamney and Corlett 1993). Inyang and Al-Hussein (2011) propose a comprehensive framework for evaluating and quantifying ergonomic effects on each body segment while the worker is performing construction activities.

³ The manuscript appearing as Chapter 4 of this thesis is under review for publication in the *Journal of Construction Engineering and Management (ASCE)*, as of the time of publication of this thesis.

However, even though workers are greatly affected by their workplaces, these studies have not considered environmental factors as a means to assist in designing productive and safe operations. From a lean manufacturing perspective, the workplace must be organized and standardized to achieve higher productivity by reducing the number of accidents and errors that occur (Dennis 2002). The existing methods for assessing safety risk can provide *a priori* risk estimates and can measure the frequency of unsafe behaviours or conditions, but do not provide a way to assess the potential for accidents based on the actual execution of the operation (Mitropoulos et al. 2009). Thus, it is critical to determine a method that proactively identifies and mitigates WMSD risks. The research presented in this chapter aims to develop a framework to assess ergonomic risks, even in the design phase of manufacturing plants, in order to reduce work-related injuries and claims.

4.2 Literature Review

4.2.1 Existing body motion data collection methods

Existing body motion data collection methods, such as direct observation, self-reporting, and physiological measurements (direct/indirect), are research-based and are typically paired with occupational safety and health practitioner requirements. However, there are limitations in the real-life implementation of these methods in construction manufacturing (David 2005; Li and Buckle 1999). These methods can be time-consuming and error-prone since the required information, such as joint angles of a body, must be collected accurately and efficiently in order to analyze the potential risks of tasks and workers. Wang et al. (2015) summarize the existing techniques for work-related musculoskeletal disorder (WMSDs) risk assessment, outlining their benefits and limitations. As they report, although direct observation can be conducted with minimal disruption to the work and minimal instrumentation, the results are based on subjective

evaluation, and inter-rater differences exist between different observers. The data collection for physical demand and ergonomic posture assessment depends in current practice on this direct observation. Although direct physiological measurement (such as use of goniometers, force sensors, accelerometers, electromyography, and optimal markers) offers a high level of accuracy and provides information that is more objective than traditional observation, it may be limited by experimental cost, environment, and technical and ethical issues for both non-invasive and invasive approaches. Risk assessment tools, including REBA and RULA, require detailed physical data, such as joint angle, in order to complete human body motion analysis. These risk assessment tools have not been fully implemented in construction cases due to the limitations with respect to physiological measurement. Joint angle and body posture can be obtained not only by direct measurement, but also by indirect measurement (e.g., Kinect range camera, computer vision-based approach) (Alwasel et al. 2011; Ray and Teizer 2012; Han and Lee 2013). One way to conduct indirect measurement is to utilize a Kinect range camera; however, the sensitivity of this method to illumination changes, viewpoints, and occlusion detracts from its effectiveness. Wang (2015) points out that there remains an opportunity for researchers to investigate cost-effective methods for risk assessment and mimicking of human behaviour in a laboratory setting.

4.2.2 3D visualization method

Among the various approaches to human body motion data collection, 3D visualization allows its users to imitate and simulate an operational task on the computer screen through careful editing and drawings, a process which is less time-consuming than the existing physiological measurement methods, and helps to prevent human error, technical issues, and the need for costly on-site devices. It can also proactively visualize a proposed design prior to implementation

in the real world. Many researchers (Al-Hussein et al. 2005; Manrique et al. 2007; Staub-French et al. 2008; Han et al. 2014) have demonstrated that 3D visualization is an effective tool for various purposes such as identifying spatial conflicts and designing appropriate operations, site layouts, and construction sequences on heavy industrial construction sites. Dynamic 3D visualization has been proven to benefit construction in both activity and operation planning, in monitoring and controlling aspects with proper machinery, and in resource and material arrangement (Kamat et al. 2011). Feyen et al. (2000) develop a 3D static strength prediction program using an AutoCAD interface as a proactive biomechanical risk analysis tool based on postural and dynamic load analysis functionalities and methods for preventing injury risks at the earliest design stages. However, this and other related studies have used only some aspects of 3D visualization functionalities for their respective objectives. These studies do not provide detailed or complete descriptions of a project, such as the worker's motions and repetitions in regular construction operations or material handling. In order to overcome this limitation, Golabchi et al. (2015) propose a framework for an automated biomechanical simulation approach to ergonomic job analysis for workplace design using 3D visualization. Their research extends the range of applicability of 3D visualization as a support tool in order to collect all engineering information for ergonomic posture analysis in a production line, and as an educational and training tool for junior workers.

This chapter introduces a method which enables automated ergonomic risk assessment for modular construction operations with graphical 3D virtual-based motion capture modelling as a support tool in order to rapidly analyze the potential ergonomic risks and hazards associated with given construction operations. The output can help construction planners to eliminate or mitigate potential risks. Based on the task manoeuvre analysis results, minor or major workplace re-

structuring may be recommended for modified working postures or human body motions. Ultimately, the goal of this research is to secure a healthy and safe working environment for workers and to reduce insurance claims and injuries. 3D visualization is shown in this chapter to be a promising alternative to traditional risk assessment methods, requiring less time on site and thereby leading to both time and cost savings.

4.3 3D Motion-based Ergonomic Risk Assessment Method

As shown in Figure 4.1, the framework consists of the following phases: (1) create 3D model to animate and imitate the operational task; (2) export body posture data from 3D visualization and obtain the joint angle at each frame; (3) conduct risk assessment during the motion by using existing risk assessment tools, REBA/RULA; (4) identify any motions that have a high risk rating based on the assessment in the previous step.

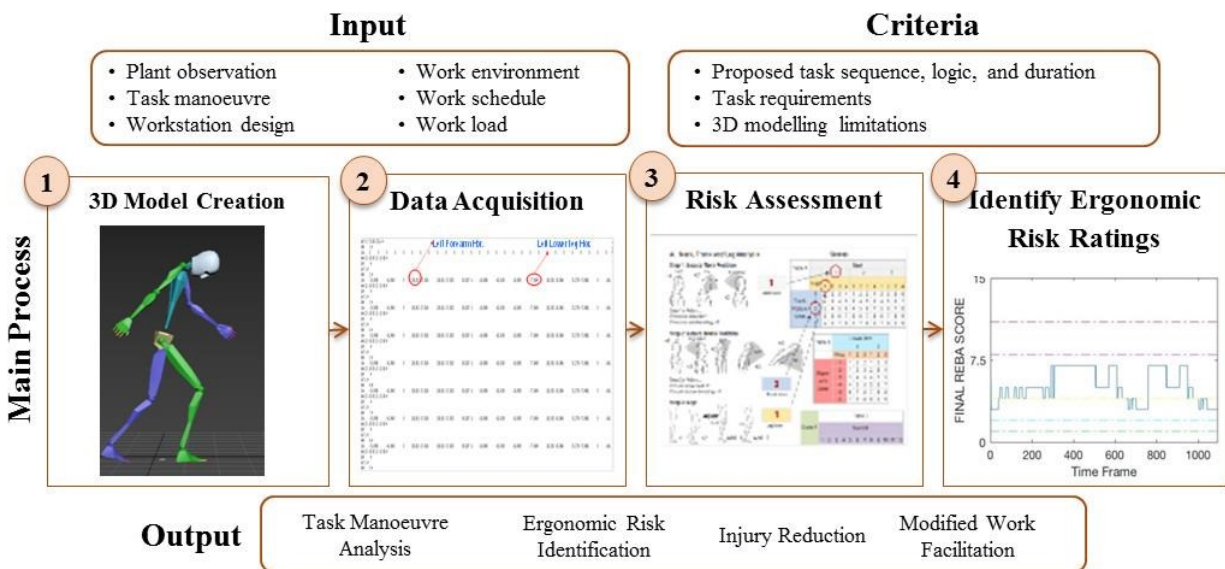


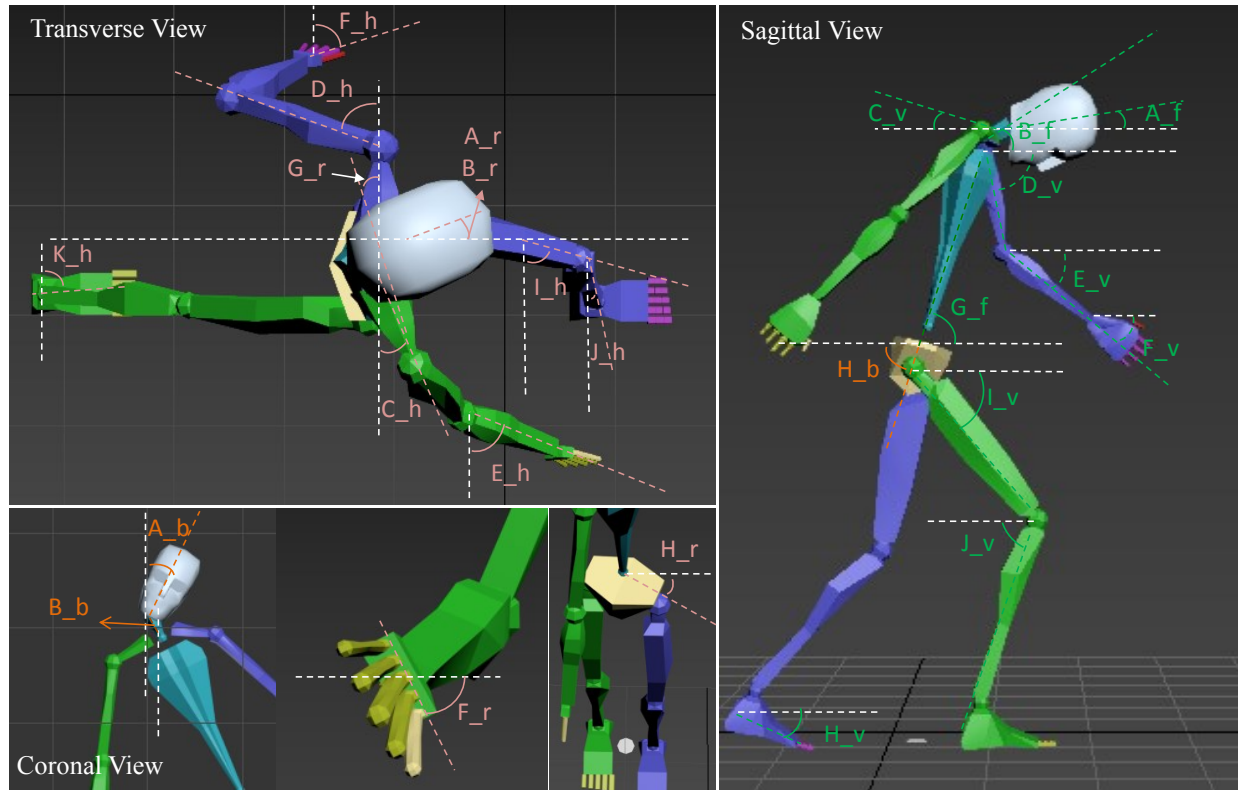
Figure 4.1: Overall methodology and framework of proposed ergonomic risk assessment

In the proposed method, the inputs are the task manoeuvre, workstation design, work environment, and work schedule, which can be obtained from a brief plant observation or a video record in order to thoroughly understand the working process. In order to create a 3D model that

imitates actual operations, one must become familiar with the task manoeuvre. Measurements may also be needed in order to obtain precise dimensions of the machine and equipment and the load to be handled. In this research, 3ds Max (Autodesk 2016) is chosen to create human body working motion animations. Based on the working environment, the first step is to draft or import plant layout, workstations, and work-related elements into the 3D model. Following this, the same motion as performed by the worker in the observation or captured video is animated, including human body model creation, human body movement imitation by controlling footsteps, body posture key frame edition using biped control, and the speed of movement determination that is achieved by defining the frame rate. 3D modelling is capable of representing all the types of body postures, such as bending forward, reaching above shoulder, kneeling and squatting/crouching, that are assumed when the human body model is performing a task. To ensure a precise and accurate human body animation for the physical data extraction, several rounds of modifications may be required.

In phase two, 41 joint angles (e.g., flexion angle on sagittal plane, axial rotation angle, bending angle on transverse plane) are calculated using computer programming by assessing the coordination of related bones in the human skeleton model. The force required by the body segment is also estimated. To obtain the body posture joint angles for various body postures and movements, MAXScript, the built-in language in 3ds Max software (Autodesk 2011), is used in conjunction with the programming code. Referring to the joint angle calculation methodology from the “3D Static Strength Prediction Program” developed at the University of Michigan (2012), joint angles for hand, lower arm, upper arm, clavicle, upper leg, lower leg, foot, head, neck, trunk, and pelvis are calculated and generated (as depicted in the images in Figure 4.2). It should be noted that left and right side, horizontal and vertical, rotation, lateral bend, and flexion

are distinguished and calculated separately. To be specific, the x - y plane is the horizontal plane (transverse plane), where the front of the pelvis is defined as the forward direction, positive y on the y -axis, while the line connecting the iliac crests is defined as the x -axis (perpendicular to the y -axis). Positive x is in the direction of the body segment pointing away from the pelvis. The z -axis is the vertical axis, perpendicular to the x - y plane, where upward is positive. Horizontal angles, which are within the range $[0^\circ, 180^\circ]$ for positive angles and $[-180^\circ, 0^\circ]$ for negative angles, are measured on the x - y plane (transverse plane) between the body segment and the positive x -axis. If the y value is positive, then the horizontal angle is positive, and vice versa. The vertical angles, i.e., those angles falling within the range $[-90^\circ, 90^\circ]$, are defined and measured on the y - z plane (sagittal plane) between the body segment and the positive y -axis. If the segment is above the transverse plane, the vertical angle is positive, and vice versa. In the model, a biped's skeletal structure setting consists of one neck link, one spine link, three leg links, one finger, three finger links, one toe, and one toe link. By selecting the animation frame and running MAXScript to make the calculation, joint angles for body segments can be captured by each frame of the 3D animation in batch files.



In total 41 joint angles:

- A: Head_Flexion (f) / Rotation (r) / Lateral_Bending (b);
- B: Neck_Flexion (f) / Rotation (r) / Lateral_Bending (b);
- C: Clavicle_Left/Right_Horizontal (h) / Vertical (v);
- D: UpperArm_Left/Right_Horizontal (h) / Vertical (v);
- E: ForeArm_Left/Right_Horizontal (h) / Vertical (v);

- F: Hand_Left/Right_Horizontal (h) / Vertical (v) / Rotation (r);
- G: Trunk_Flexion (f) / Rotation (r) / Lateral_Bending (b);
- H: Pelvis_Rotation (r) / Lateral_Bending (b);
- I: UpperLeg_Left/Right_Horizontal (h) / Vertical (v);
- J: LowerLeg_Left/Right_Horizontal (h) / Vertical (v);
- K: Foot_Left/Right_Horizontal (h) / Vertical (v);

Figure 4.2: Schematic drawings of 41 joint angles

In phase three, REBA and RULA are utilized as systematic risk assessment tools for rating each motion, evaluating the body movement during the task by using the body posture, force/load, repetition, and coupling conditions (Hignett and McAtamney 2000; Middlesworth 2012; McAtamney and Corlett 1993). REBA, it should be noted, looks at the entire body working posture while RULA emphasizes the upper limb postures for ergonomic identification and design. These two risk assessment algorithms are integrated with the framework to provide greater flexibility. The user can choose which algorithm to use depending on their purpose of analysis. In phase four, the total risk rating is provided in the final REBA and RULA risk rating chart for a continuous working operation process. Aggregating all the body posture movements, the total

rating is found to fluctuate during the movement. The final REBA and RULA risk ratings both consider the joint angle of each individual body segment, the force/load added to the body, and the frequency of the activity. Five risk severity levels are categorized in the REBA methodology, while four levels are categorized in the RULA methodology. Not all the human body motions evaluated, it should be noted, involve high ergonomic risk. However, the high-risk motions can be identified through this rating algorithm and the plotted chart. Tasks with high ergonomic risk can thus be identified and corresponding analysis can be conducted to help with proposing modified work to reduce the risk of injury.

4.4 Validation Approach

The proposed 3D motion-based risk assessment methodology is compared with two other approaches, the motion-capture experiment and traditional manual observation data collection, in order to evaluate the accuracy of the motion data collected through 3D modelling.

With ethics approval, a lifting task experiment is performed at the Syncrude Centre of the Glenrose Rehabilitation Hospital (Edmonton, Alberta, Canada) (Li et al. 2017). Three male subjects with no history of injury are selected for the experiment, with heights ranging from 173 cm to 180 cm, ages varying from 27 years to 31 years, and body weights varying from 57.0 kg to 80.5 kg at the time of the experiment. The test procedure and risk of injury are explained and a signed consent form is obtained from each subject.

Optical motion capture is a widely used and effective method for capturing human motion. In this study, thirty-six self-adhesive reflective markers are attached to the subject's skin symmetrically to identify the left and right side and are recorded by a set of cameras to capture the kinematics of different body segments while the selected task is being performed. Li et al. (2017) explain the anatomical positions of the reflective markers while the subject performs the

lifting task. The subject is surrounded by an 8-camera Eagle Digital Motion Analysis system (Motion Analysis Corp. 2016) sampling at 120 Hz to collect the 3D coordinates of the reflective markers and to ensure that no marker disappears from camera view at any time. After the experiment, post data processing is carried out in order to clear any data noise. The same 41 joint angles mentioned with regard to phase 2 are calculated based on the coordinates of the markers. Rather than simply using the markers on the two ends of each body segment to calculate the joint angles, depending on the reliability of individual markers during the experiment and the thickness of the body and muscles, minor adjustments are conducted to achieve better joint angle results. However, the joint angles from 3D modelling are estimated based on the two joints of the body segment, a practice which contributes to a slight difference compared with experimental data calculation.

Manual observation is also conducted in order to compare the manual observation results with the 3D motion data collection. Data is recorded for 41 joint angles based on the video captured during the experiment. Based on the duration of each lifting motion by the subject, a half-second in this case is selected as the key time interval to be observed and recorded. The lifting motion durations for the three subjects vary from 6.0 seconds to 8.5 seconds. Thus 13 to 18 groups of body posture data are documented as key motions from the video, and these are later used in joint angle comparisons.

The lifting task contains two extensions (bending backward) and two flexions (bending forward) of the spine. The subject begins from a free-standing posture, then flexion without twisting the trunk or bending legs, and lifting a 15 lb, 18"×24" rectangular window (initially positioned on a table whose center is located 20" from knees), holding the window close to the body while maintaining an upright standing posture, and then returning it back to the table, as illustrated in

Figure 4.3. To improve the accuracy of the 3D motion-based modelling, the sizes of the body segments in the 3D model are adjusted to match the body sizes of the subjects, which are calculated by the coordinates of the markers during the standing posture. The motions in this task are divided into five key postures, beginning from standing posture, bending to reach the window, holding the window, bending to return the window, and ending with another standing posture, as indicated in Figure 4.3. To match the key motions between the 3D modelling and the experiment, a brief time study of these motions is also conducted (i.e., to determine when these key motions occur). In this case, 100 time frames per second is the speed selected for the 3D model. To summarize, in order to develop an accurate animation, the 3D model inputs needed are the size of the body segments, the key motions, the layout and the key time frames of these motions.

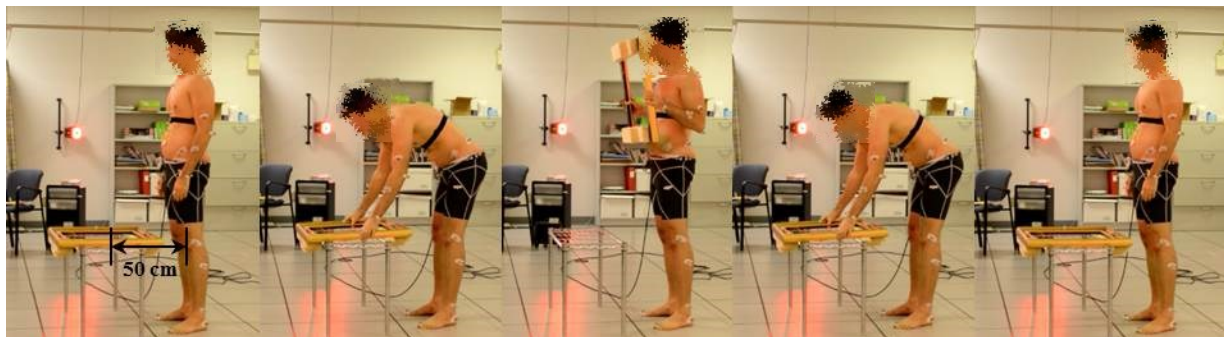


Figure 4.3: Motion capture lifting task and its five key motions

4.4.1 Validation methods

The motion data of this task is collected through the proposed 3D motion-based analysis method, motion capture experimentation, and manual observation from the video captured during the experiment. Validation is based on the assumption that the experiment offers the most accurate and reliable results, these serving as the basis of comparison with the other two methods in order to test the validity of the proposed 3D modelling method. Although, due to the limited data points from manual observation, comprehensive statistical comparison of this method cannot be

conducted, the correlation coefficient can be determined based on the fluctuating trend in the figures of the following analysis. Horizontal and vertical angles for the hand, upper arm, lower arm, upper leg, lower leg, foot, and trunk flexion are selected as the main angles for comparison, and left side and right side are compared separately. The trend of joint angles through the entire motion is compared by using the correlation coefficient given in Eq. (4-1). The accuracy of joint angles collected from the 3D modelling is tested using the difference and error equations given in Eq. (4-2) and Eq. (4-3), respectively. A positive difference and error mean that the 3D modelling results are underestimates, while a negative difference and error signify that the 3D modelling results are overestimates. The accuracy of data collection from manual observation is also roughly estimated using Eq. (4-4) and Eq. (4-5) to compare the cumulative area under the fluctuating curve and its cumulative area difference in percentage (error). For the purpose of comparison, these two equations are specially selected for the method that does not have the same scale of data. In this case these equations are designed for the manual observation method, which includes fewer groups of data. The finding of a positive area difference under the curve and area percentage indicate that the results from the manual observation are underestimates; while a negative area difference under the curve and area percentage demonstrate that the results from the manual observation are overestimates. Moreover, three levels of comparison are selected—joint angle comparison, risk rating comparison for body segments, and REBA/RULA total risk rating and risk level comparison—in order to validate the proposed method. Three data collection methods, each applied to all three experiments (corresponding to the three subjects), are compared using the validation method proposed in this chapter.

$$\text{Correl}(DE_i, DD_i) = \frac{\sum_{i=1}^n (DE_i - \overline{DE_i})(DD_i - \overline{DD_i})}{\sqrt{\sum_{i=1}^n (DE_i - \overline{DE_i})^2 \sum_{i=1}^n (DD_i - \overline{DD_i})^2}} \quad (4-1)$$

$$\overline{\text{Difference}} = \frac{1}{n} \sum_{i=1}^n (DE_i - DD_i) \quad (4-2)$$

$$\overline{Error} = \frac{1}{n} \sum_{i=1}^n \left(\frac{DE_i - DD_i}{D} \times 100\% \right) \quad (4-3)$$

$$Area = \sum_{i=1}^n R_i \times \Delta t_i \quad (4-4)$$

$$Area\ Percentage = \frac{Area_x - Area_y}{Area_x} \times 100\% \quad (4-5)$$

where

DE_i : joint angle collected from experiment at time, i ($^\circ$)

DD_i : joint angle collected from 3D modelling at time, i ($^\circ$)

Correl: correlation coefficient of two arrays in the range, [0,1]

$\overline{Difference}$: joint angle average difference between data collected from experiment and 3D modelling ($^\circ$)

\overline{Error} : 3D modelling joint angle average error compared with experiment (%)

D : the joint angle range for horizontal and vertical angles ($D = 180^\circ$ for horizontal angles; $D = 90^\circ$ for vertical angles, respectively)

Area: cumulative area under the curve

R_i : risk rating at time, i

Δt_i : time difference between t_i and t_{i-1}

Area Percentage: cumulative area difference in percentage of y compared with x through the entire motion (%)

4.4.2 Validation results

The total number of time frames in the 3D simulation models for three subjects varies from 600 to 850. The data collected from the experiment is scaled for the purpose of comparison to match the 3D model time frame, as is the data collected from manual observation.

4.4.2.1 Joint angle comparison

Using subject 3 as an example, 600 data-point groups from the experiment and 3D modelling are selected for statistical comparison, while manual observation provides 13 data-point groups to plot trends for comparison. As expressed in Figure 4.4, 20 main joint angles used in REBA and RULA algorithms are compared. In general, the joint angles from these three methods follow similar trends; however, large gaps can be observed throughout the motion, especially for horizontal angles. The vertical angles perform with higher consistency than do the horizontal angles. Data noise that may have been caused by movement of the markers during the experiment and shaking of the body is observed during experimental data analysis for the upper leg and lower leg motions. Due to the limited data points from manual observation, more detailed statistical analysis is provided in comparing the data collected from the experiment with the 3D modelling later in this section.

The average correlation coefficient between the experimental and 3D extracted vertical angles is 0.80, with the vertical angles for hand, lower arm, upper leg, and lower leg performing at a high average correlation coefficient of 0.94. Only the upper arm has a slight negative correlation. The results from the other two subjects also show a higher correlation coefficient for vertical angles than for horizontal angles. Consistency is observed between the left and right sides of the body segments since the movement is almost symmetrical in this test. Among these 20 main joint angles, 14 angles are found to have less than $\pm 14\%$ error with less than 25° variation.

The results for trunk movement show for each of the three subjects a high correlation coefficient between the experiment and the 3D modelling. For example, the main body movement of the trunk for subject 3 has a high correlation coefficient of 0.96 for flexion with an average difference of 10.24° and an average error of 11%, as expressed in Figure 4.5. The manual

observation results are plotted in a curve, which in turn is compared in the figure to the fluctuating curves of the experiment and of the 3D modelling.

4.4.2.2 REBA/RULA risk rating comparison for body segments

The joint angle results for each body segment having been obtained, REBA/RULA risk assessments are used to evaluate the risk rating for each body segment by defining the rating for certain joint angle ranges. Figure 4.6 plots the ratings for neck, trunk, leg, upper arm, lower arm, and wrist, respectively, for REBA for subject 3 as an example. To be considered acceptable, a given risk rating on average must have a difference of less than 1 when comparing the 3D modelling with the experiment. Moreover, the most crucial rating during the motion is the peak rating, where risk has the highest chance of occurring and thus where further modified work may be necessary to proactively reduce the risk. Thus, five factors are selected for comparison: average rating, maximum rating, minimum rating, rating difference, and error. Table 4-1 takes trunk as an example and shows the comparison of these five factors among the three data collection methods for all three subjects. The ratings are given in Appendix B in Table B-2.

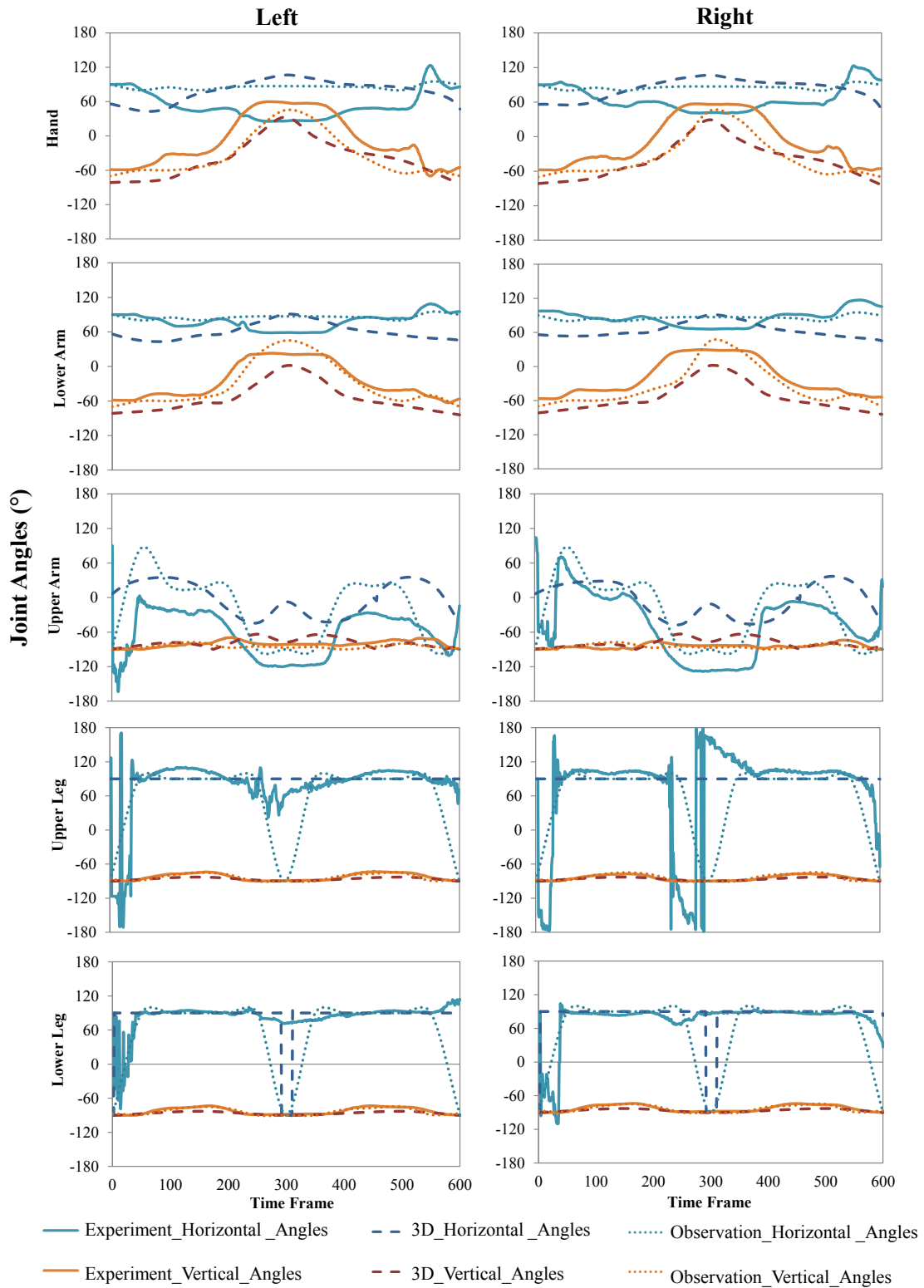


Figure 4.4: Joint angle comparisons of body segment3-subject 3

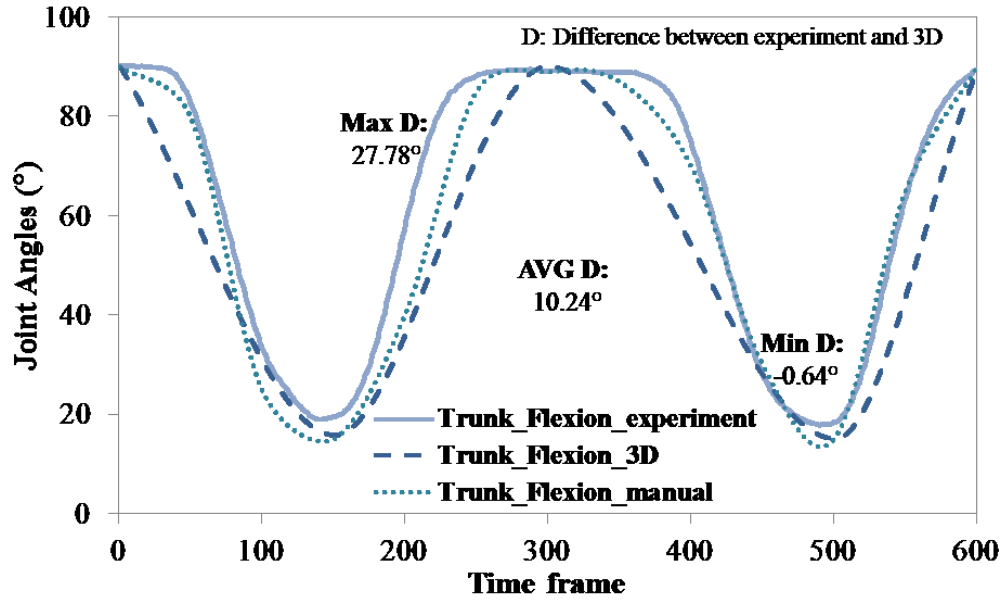


Figure 4.5: Trunk flexion comparisons-subject 3

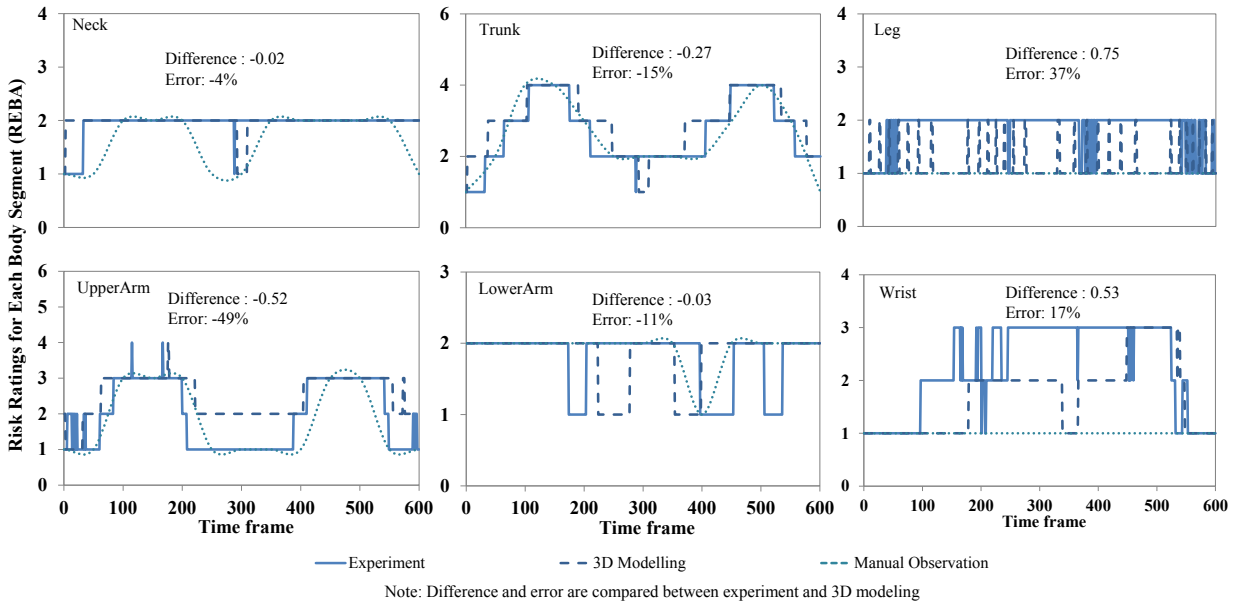


Figure 4.6: REBA risk rating for body segments-subject 3

Table 4-1: REBA/RULA rating comparison of trunk for all three subjects

Rating	Subjects	Subject 1			Subject 2			Subject 3		
	Methods	E	3D	M	E	3D	M	E	3D	M
REBA	Average	2.51	2.93	2.31	2.79	2.97	2.54	2.68	2.95	2.54
	MAX	3	4	3	4	4	4	4	4	4
	MIN	1	1	1	1	1	1	1	1	1
	Difference	-	-0.42	0.21	-	-0.18	0.25	-	-0.27	0.14
	Error	-	-18%	N/A	-	-10%	N/A	-	-15%	N/A
	Average	2.51	2.93	2.31	2.79	2.97	2.54	2.68	2.95	2.54
RULA	MAX	3	4	3	4	4	4	4	4	4
	MIN	1	1	1	1	1	1	1	1	1
	Difference	-	-0.42	0.21	-	-0.18	0.25	-	-0.27	0.14
	Error	-	-18%	N/A	-	-10%	N/A	-	-15%	N/A
	Average	2.51	2.93	2.31	2.79	2.97	2.54	2.68	2.95	2.54

Note: E-experiment; 3D-the proposed 3D modelling method, M-manual observation

4.4.2.3 REBA/RULA total risk rating and risk level comparison

The last point of comparison among the three methods is with respect to total REBA/RULA risk rating and risk level. The risk rating performance and risk level performance for subject 3 are plotted in Figure 4.7 as an example. A force rating of 1 is added to both the REBA and RULA assessments due to the 15 lb load on the hands when the subject lifts the window without the support of the table. The minimum *coupling rating*, *activity rating*, and *muscle rating* are used in this study for REBA and RULA assessment.

In the risk ratings, the 3D motion-based ergonomic analysis generally follows the same trend for both REBA and RULA, as indicated in Figure 4.7. Considering the results of the three subjects, the 3D modelling method is found to provide highly accurate estimation for REBA with a

difference of 0.38 and -0.87% error on average, and for RULA with a -0.44 difference and -13.61% error on average. In terms of the cumulative area under the curve compared with the experimental results, the area percentage of 3D modelling is 6.86% for REBA and -7.54% for RULA on average for all three subjects. Evidently, the manual observation method underestimates the risk of the movement by 34% and 19% of area percentage on average for REBA and RULA, respectively, giving a rough fluctuation trend. In the risk category level, 3D modelling provides accurate estimation with only a 0.11 difference and 0.18% error on average for REBA, and a -0.15 difference and -9.95% error on average for RULA for all three subjects. Furthermore, the experimental data and the 3D extracted data provide almost the same maximum and minimum risk rating and risk level judgment as each other for both REBA and RULA for all three subjects, with only a slight difference for minimum rating in RULA for subject 3. Table 4-2 summarizes the risk rating and risk level judgments of all three subjects for RULA.

Compared with the experiment risk assessment, 3D modelling offers accurate estimation with an average difference of less than 1 for both risk rating and risk level for all three subjects. Furthermore, in both the REBA and RULA assessments, the results for 3D modelling and experiment are found to be more consistent with one another for motions with maximum risk rating than for motions with minimum risk rating, and these two methods are found to yield equal risk levels. Less than half of the minimum ratings and risk levels are underestimated by a difference of only 1.

Both methods—experimental and 3D modelling—conclude that the lifting motion is approaching a maximum risk level of 4 for REBA, a finding which indicates that the motion is exposed to high risk and requires the action of “*investigate and implement change*”. Both methods also

show a maximum risk level of 4 for RULA, again triggering a recommendation to “investigate and implement change”.

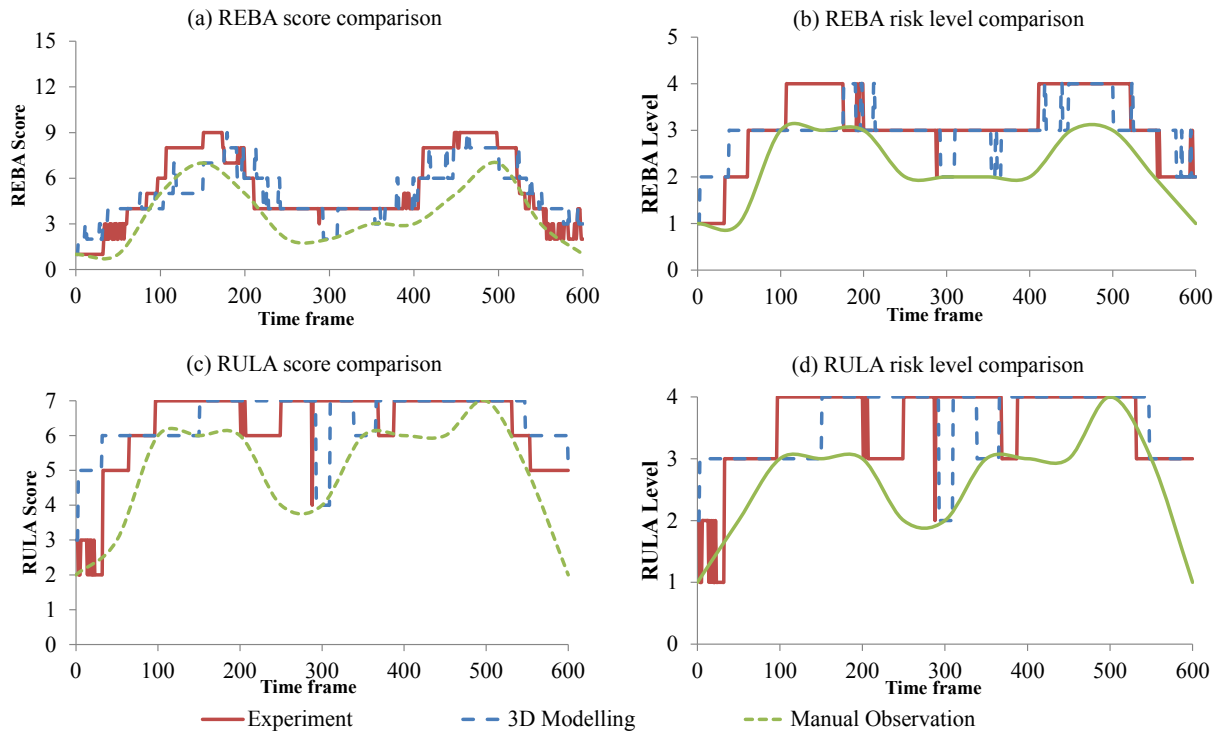


Figure 4.7: REBA/RULA total risk rating and risk level comparison for entire motion—subject 3

Table 4-2: RULA total risk rating and risk level comparison for all subjects

Rating /Risk Level	Subjects	Subject 1			Subject 2			Subject 3		
		Methods	E	3D	M	E	3D	M	E	3D
Rating	Average	5.94	6.40	4.78	5.73	6.43	4.40	6.29	6.47	4.85
	MAX	7	7	7	7	7	7	7	7	7
	MIN	3	3	2	3	3	2	2	3	2
	Difference	0.00	-0.46	1.17	0.00	-0.69	1.33	0.00	-0.18	1.44
	Error*	-	-13.23%	N/A	-	-19.86%	N/A	-	-7.75%	N/A
	Area	5052	5440	4175	4014	4498	3150	3774	3883	3050
	Area percentage [#]	-	-7.68%	17.36%	-	-12.06%	21.52%	-	-2.89%	19.18%
	Average	3.33	3.48	2.61	3.24	3.51	2.47	3.53	3.56	2.54
	MAX	4	4	4	4	4	4	4	4	4
	MIN	2	2	1	2	2	1	1	2	1
Risk Level	Difference	0.00	-0.16	0.72	0.00	-0.28	0.77	0.00	-0.03	0.99
	Error*	-	-7.97%	N/A	-	-15.00%	N/A	-	-6.88%	N/A
	Area	2828	2962	2275	2265	2459	1750	2118	2134	1600
	Area percentage [#]	-	-4.74%	19.55%	-	-8.57%	22.74%	-	-0.76%	24.46%

Note:

*Error refers to the rating difference compared with experiment data in percentage of time frames on average; ratings from manual observation are not compared here due to limited data points.

#Area percentage refers to cumulative area under the curve difference compared with experiment data in percentage.

4.4.3 Validation discussion

There are a few reasons for the differences observed among the three levels of comparison, including joint angle comparison, risk rating comparison for body segments, and REBA/RULA total risk rating and risk level comparison. For the joint angle comparison, joint angles such as

hand vertical angles, lower arm vertical angles, and upper arm horizontal angles are less accurate in subject 3 than in the experiment. This is due to the limitation that the locations of the markers on the joints are slightly different than the locations of the joints in the 3D model, as mentioned above. To be more specific, the hand joint angle calculation in the experiment relies on the marker on the index finger and the one on the midpoint between the two wrist markers, while the hand joint angle in the 3D model is estimated based on the positions of the middle fingertip and the wrist. Lower arm angle is calculated based on the markers on the elbow and wrist B for the experiment, whereas in the 3D modelling the lower arm angle is determined by the joints of the elbow and wrist. The noticeable difference in performance in upper arm horizontal joint angles between the 3D modelling and the experiment is due to the observation direction, which will be further discussed below. Also, the markers are located on the skin of the subjects, which results in different outcomes due to variations in body thickness among the subjects.

The horizontal angle, we infer, is less accurate in this validation due to the limited observation direction (view angle of video captured) in this test, as the subject is captured from the side view during the experiment. If the video captured had also been available from the front view, for instance, then whether or not the upper arm is abducted could have been identified. In this case, the upper arm vertical angles, together with all the other horizontal angles, can be imitated more accurately and realistically. Essentially, in this risk assessment, vertical angles are more sensitive to the final risk rating, as the risk assessment of upper arm varies from 1 to 4 for the rating of vertical angles but has less variation (from 0 to 1) for horizontal angles. Thus, vertical angles are more critical in this risk assessment method.

Another reason for the joint angle difference between the 3D modelling and the experiment is the different speeds of the motion, as indicated in Figure 4.5. The moving speed of the 3D model is

set by default to be constant. However, in the experiment, the subject determines the speed and acceleration of window lifting movement that is comfortable for them. Thus, the speed varies as the subject spends more time holding the window at lifted heights. In the 3D modelling, in contrast, the speed is not an important factor for the current study though it is controllable during creation of the animation. The key motions and the peak joint angles, which are the main ratings to be identified through this method, are vital for risk identification. Thus, the results of the joint angle comparison indicate that the proposed 3D modelling method is valid.

The variations in average rating between the 3D modelling and the experiment are within 1 for all subjects' body segments, a finding which validates the 3D modelling. Due to the different functions of REBA and RULA risk assessments the sensitivity of each body segment is also different, producing results of varying accuracy. Throughout the entire motion, the results from the REBA risk assessment show that 3D modelling provides an accurate outcome (with less than 0.5 difference and less than 30% absolute error) for neck, trunk, and lower arm, while the outcomes for leg, upper arm, and wrist still require improvement. The results from the RULA risk assessment show that 3D modelling provides an accurate outcome (with less than 0.5 difference and less than 20% absolute error) for trunk, leg, and wrist, while the outcomes for neck, upper arm, and lower arm still require improvement. Comparing the peak ratings, including both maximum and minimum rating, the three methods generally demonstrate high consistency with one another. The proposed 3D modelling method shows peak rating estimations that are statistically close to those of the experiment, i.e., with a difference of either 0 (as in most of the cases) or 1. Thus, results from the risk rating comparison for the body segments also indicate that the proposed 3D modelling method is acceptable.

Throughout the entire motion for all three subjects, the 3D motion-based method provides more accurate estimation for the final REBA rating and a slight overestimation for the final RULA rating compared to the experiment. There are two explanations for the finding that the RULA algorithm overestimates risk while the REBA algorithm does not: (1) the movements of neck are underestimated in this experiment due to the absence of markers on the neck; in the experiment, the neck joint angle assumes that the head and neck of the subject always perform vertical to the floor (i.e., the subject is always looking forward); (2) RULA focuses on the upper body, which means neck postures and minor movements by other upper body segments, such as rotation/twist, will be more sensitive to the final risk ratings than they are in REBA. The results from both methods with regard to both REBA and RULA for all three subjects indicate that the motion is associated with a high risk level, a finding which proves the consistency of the framework.

Manual observation is found to generally underestimate the risk rating. In particular, the intricacies of changes in motions such as minor bending and rotation/twist of the body segments are difficult to identify in this method. Manual observation underestimates for the peak risk identification, which in reality may lead to claims or injuries as a result of these unforeseen risks. 3D modelling, on the other hand, provides high accuracy for maximum risk identification. Thus, the proposed 3D motion-based ergonomic analysis is deemed to be acceptable and within the scope of work of this chapter, since identification of the motion with the highest risk (as opposed to identification of the motion with the lowest risk) is the paramount task in this framework.

Additional validation is conducted for the same repetitive lifting task as shown in the example above (using a different cycle) by means of creating an additional 3D model and collecting manual observation data for comparison with the corresponding experimental results. The results

are given in Appendix C in Table C-1, which indicates consistency in the validation analysis as mentioned in this section.

4.5 Conclusion

This research proposes a framework for using 3D visualization to imitate operational motions and to rapidly analyze the ergonomic risks of manufacturing construction activities. The framework eliminates the technical, ethical, and cost issues that would be at play when using other ergonomic analysis methods. The capability of evaluating and identifying ergonomic risk can proactively facilitate the development of modified work for various industries. A more robust return-to-work program can be established with the support of this framework, and a considerable reduction in the number of insurance claims and injuries can be achieved.

4.5.1 Validation summary

The framework is also validated through a motion capture-based experiment for a lifting motion. The results demonstrate high consistency for vertical angles, risk ratings for individual body segments, and REBA/RULA total risk ratings and risk levels. However, due to the limited observation direction of the video, some gaps in the joint angle comparison, especially for horizontal angles, are also observed. Twenty-one main joint angles that have high sensitivity to REBA and RULA algorithms are compared, proving that vertical angles perform with a high correlation coefficient of 0.8. The main motion of trunk flexion has a high correlation coefficient of 0.96 with an average difference of 10.24° and an average error of 11%. The differences in average, maximum, and minimum risk rating for individual body segments and for the entire body between 3D modelling and the experiment are all within 1, and 3D modelling ultimately provides almost the same risk level judgment as the experiment does. To conclude, throughout the entire motion, the 3D virtual-based motion capture method provides accurate estimation for

REBA and a slight overestimation for RULA compared to the experiment. On the other hand, traditional manual observation provides underestimation of risk assessment. Thus, the proposed 3D modelling method has higher accuracy than does the traditional manual observation method, overcomes the limitations of the manual observation method, and is better and faster in this respect because it is automated and capable of reliably analyzing continuous motions. The proposed 3D motion-based ergonomic risk assessment is thus validated and deemed to be reliable for future use.

4.5.2 Limitations and future study

The proposed framework provides less accuracy than the risk assessment from the experiment for the estimation of small movements such as neck and head movement or hand rotation/twist, a limitation which may have a minor effect on the final risk rating results. Thus, this framework is considered to be more reliable for those activities for which the focus is on main body movements than for activities for which the focus is on more the subtle movements of the neck and head mentioned above.

Additionally, to improve the reliability of the proposed 3D motion-based modelling, more experiments, 3D modelling, and manual observations, using this validation approach and different volunteers and researchers, are recommended in order to validate the framework for different movements and occupational tasks.

Furthermore, since continuous work and high physical demand could also result in a loss of productivity, the improvement of physical condition of the workstation can increase worker productivity. Although such improvement measures are not within the scope of this chapter, they constitute a promising area of extension of the proposed method in future study.

Finally, it should be noted that this framework has been implemented in but is not limited to construction manufacturing facilities. Application to other construction areas involving high physical demand may also be feasible.

4.6 Acknowledgements

This study is funded by the Natural Sciences and Engineering Research Council of Canada (NSERC) through the Industrial Research Chair (IRC) in the Industrialization of Building Construction (File No. IRCPJ 419145-15), Engage Grant EGP470391, and Discovery Grants RGPIN 402046, and RGPIN 436051. The authors would also like to acknowledge the support from their industry partner, All Weather Windows, as well as the contributions of Amin Komeili and Justin Lewicke, who assisted with and participated in the experiment. And special thanks are extended to the Glenrose Rehabilitation Hospital for allowing the experiment to be completed in their motion capture lab.

CHAPTER 5: 3D MOTION-BASED PHYSICAL DEMAND AND ERGONOMIC ANALYSIS

5.1 Integration of Physical Demand Analysis and 3D Modelling

Compared with traditional human body motion data collection methods, 3D automation can reduce the time required for motion data collection by exporting human body coordinates from 3D modelling. Moreover, 3D visualization enables the user to adjust and customize the human model and workplace design, thereby providing easy access for researchers to conduct risk assessment comparisons of diverse alternatives, including differences in the design of the workstation and differences in height range of the human body. Ostensibly, 3D modelling, by circumventing the ethical issues associated with carrying out data collection and observation of real-world construction, allows researchers to assess worker motions even in the early design stage of a project or when maximum human body capacity would otherwise be required in order to complete the work. The results can be used to assist health and safety personnel in identifying work-related risks and recommending proper working postures and body motions for operational tasks. The capability of 3D modelling can also be extended to support the re-design of the workplace and the optimization of human body movement accordingly to mitigate ergonomic risks.

This chapter integrates the methods proposed in Chapter 2 and Chapter 4 into a comprehensive physical demand and ergonomic risk assessment framework with the support of 3D modelling for construction operational tasks (Figure 5.1). The inputs to this framework include the summary of worker information, factory layout, and current task manoeuvre with the workstation design and working schedule. To begin (phase one), a manual plant observation and time study are conducted in order to obtain a brief overview of the operation process and physical demands

of operational tasks. Video capture is used to facilitate the completion of phase three. While performing phase one, physical demand data is obtained which serves as the input for conducting a preliminary PDA in phase two. The body posture is recorded minute-to-minute, and strength, sensory, and environmental demands are also measured. All the information is summarized in a PDA form by the end of phase two. In phase three, a 3D animation model for activities in the production line is created based on previous plant observation and preliminary PDA. To make the 3D human body motion modelling more realistic, several rounds of modifications are required. Having an animation that is precise and accurate is critical because it is to be utilized for physical demand data (human body key motions, force/load, etc.) extraction for phase four. In phase four, joint angles are calculated by assessing the coordination of related bones in the human skeleton model. The extracted data from the 3D animation serves as the input for phase five—the risk assessment phase—as well as the input for phase two to complete a comprehensive PDA with risk assessment results. REBA and RULA are selected as two of the current existing risk assessment algorithms for this research to evaluate the ergonomic risk in the manufacturing plant. After evaluating the ergonomic risks for the entire production line, tasks with high work-related risk ratings are identified by comparing the total rating score in phase six. The ratings are categorized into five risk severity levels, based upon which any task with high ergonomic risk can be identified and corrective measures can be proposed accordingly. In this regard, there are two scenarios that may occur:

- a) If the overall rating is not acceptable (i.e., potential ergonomic risks exist in the current production line) the entire process will proceed to phase seven, providing modified work for the identified motion with high associated risk. After modified work has been proposed, the steps are repeated from phase three in order to provide 3D modelling and to

compare the risk rating before and after modified work implementation in the 3D modelling. Lower ergonomic ratings should be expected as a result.

- b) If the overall rating is acceptable (i.e., immediate changes are not required), then either the level of risk associated with the given operational task is deemed to be acceptable or the modified work can be implemented in the plant. A rough productivity test can also be approached for the modified work by comparing the time frames of the modified motion to ensure the duration of the motion is not longer than the existing motion. However, detailed productivity analysis is not within the scope of the current framework, as explained in the limitation section (6.3).

Integrated and systematic PDA is therefore completed with a modified work proposal. Modified work can take any of the following forms, among others: (1) re-structuring of the workstation, such as adjusting the height of work tables; (2) modification of production operations, such as modifications with significant impact on mitigating imposed loads on the musculoskeletal system; (3) revision of human body motion or using braces to support body skeleton; (4) provision for work to be carried out with assistance from other workers; and (5) staggering of a given task between workers (job rotation). However, some of the high-risk workstations cannot be easily modified. The implementation strategy associated with the suggested design may also involve complicated machinery development and employing new tools for task operation. The workstation design should adhere to worker health and safety documentation and guidelines, and should be able to guarantee the productivity of the production line.

The improved PDA is more comprehensive than traditional PDA, with automated risk assessment of rapid body movement. However, the present research must follow ergonomics guidelines and may be limited by certain criteria, such as the risk factors and constraints from the

plant layout itself, 3D model, etc. The output of this framework is an improved systematic PDA, overall task manoeuvre analysis, and an ergonomic risk summary based upon which modified work can be proposed. Analysis of injury reduction and cost effectiveness can then be conducted.

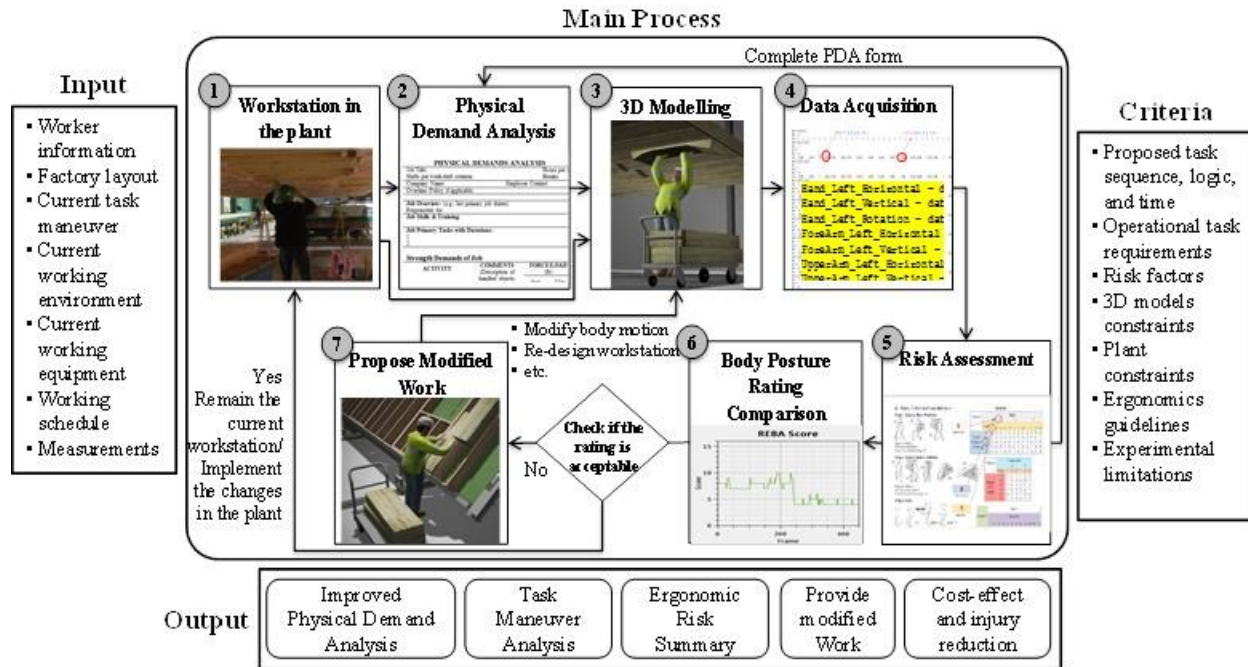


Figure 5.1: 3D motion-based physical demand and ergonomic analysis methodology

5.2 3D Modelling Data Acquisition and Post-data Processing Algorithm

In total, 41 joint angles, as depicted in Figure 4.2 in section 4.3, are obtained from the 3D model. The algorithms for how to generate 41 joint angles from 3D modelling and how to implement these angles for risk assessment are detailed in this section.

5.2.1 3D modelling data acquisition

In the model, a total of 26 bones, as listed in the Table 5-1, must be satisfied and “footsteps” must be selected before running the programmed MAXScript code. The format of the batch files with the list of joint angles in order is presented in Table 5-2. By selecting the range of the animation time frame and running MAXScript to make the calculation (Figure 5.2a), joint angles

for body segments can be captured by each frame of the 3D animation in batch files (Figure 5.2b). The detailed joint angles with schematic drawing are given in Appendix D, Table D-1.

Table 5-1: List of bones in the biped

List of bones in the biped
Pelvis
Spine
Left/Right thigh
Left/Right calf
Left/Right foot
Left/Right toe
Neck
Left/Right clavicle
Left/Right upper arm
Left/Right forearm
Left/Right hand
Left/Right 3 finger bones
Head

a. Obtain joint angles

b. Sample results

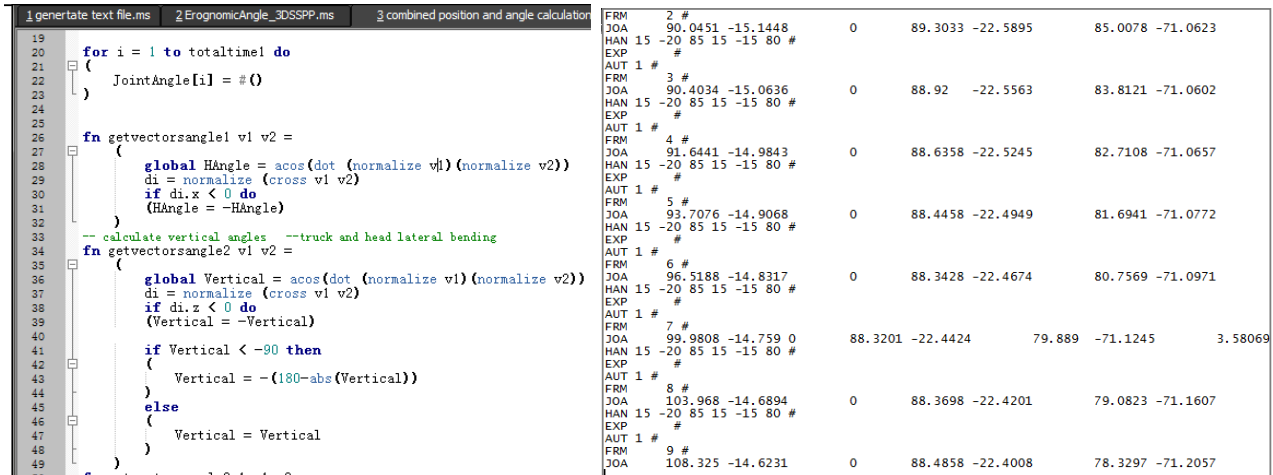


Figure 5.2: Example file of obtaining joint angles and batch file generation

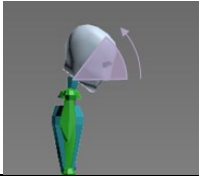
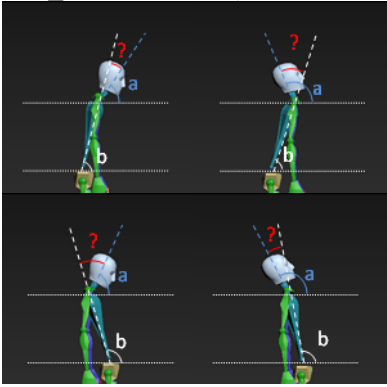
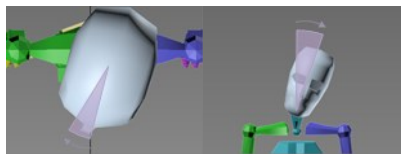
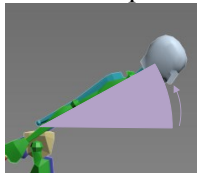
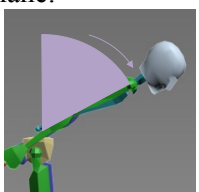
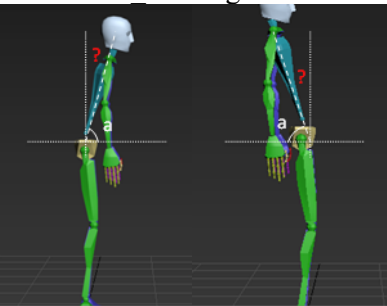
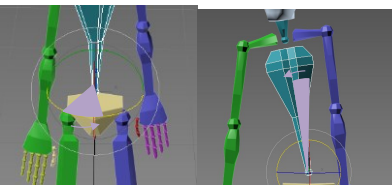
Table 5-2: List of joint angles in order (batch file)

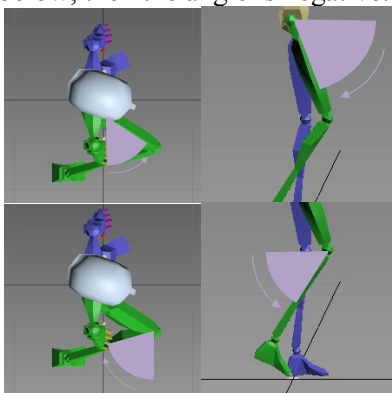
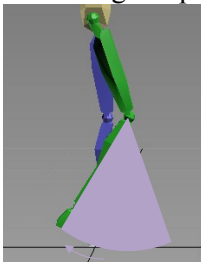
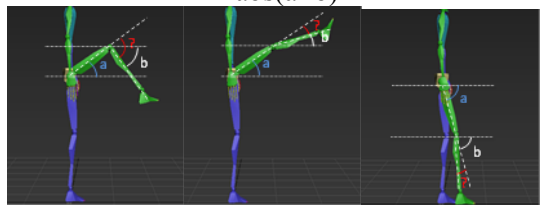
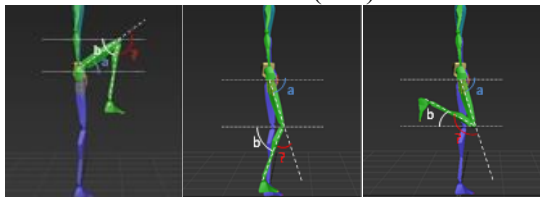
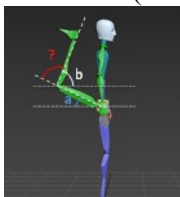
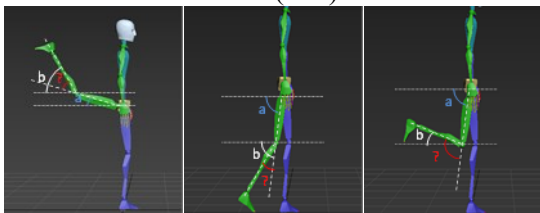
Number	Angle
1	Hand_Left_Horizontal
2	Hand_Left_Vertical
3	Hand_Left_Rotation
4	ForeArm_Left_Horizontal
5	ForeArm_Left_Vertical
6	UpperArm_Left_Horizontal
7	UpperArm_Left_Vertical
8	Clavicle_Left_Horizontal
9	Clavicle_Left_Vertical
10	UpperLeg_Left_Horizontal
11	UpperLeg_Left_Vertical
12	LowerLeg_Left_Horizontal
13	LowerLeg_Left_Vertical
14	Foot_Left_Horizontal
15	Foot_Left_Vertical
16	Hand_Right_Horizontal
17	Hand_Right_Vertical
18	Hand_Right_Rotation
19	ForeArm_Right_Horizontal
20	ForeArm_Right_Vertical
21	UpperArm_Right_Horizontal
22	UpperArm_Right_Vertical
23	Clavicle_Right_Horizontal
24	Clavicle_Right_Vertical
25	UpperLeg_Right_Horizontal
26	UpperLeg_Right_Vertical
27	LowerLeg_Right_Horizontal
28	LowerLeg_Right_Vertical
29	Foot_Right_Horizontal
30	Foot_Right_Vertical
31	Head_Flexion
32	Head_Rotation
33	Head_Lateral_Bending
34	Neck_Flexion
35	Neck_Rotation
36	Neck_Lateral_Bending
37	Trunk_Flexion
38	Trunk_Rotation
39	Trunk_Lateral_Bending
40	Pelvis_Rotation
41	Pelvis_Lateral_Bending

For the data acquisition, *world coordinate system* is used to define the joint angle of the pelvis, *local coordinate system* is utilized to determine the joint angle of the other body segments (vertical angle and horizontal angle), and *gimbal coordinate system* is used in calculating the rotation of the body segments. In addition, *inverse kinematics* method is employed to identify the moving direction of the subject during the animation. It is also applied during the animation creation, as this function reverses the direction of the chain manipulation and facilitates the creation of the animation.

The calculation of joint angles for the proposed method (referring to the “3D Static Strength Prediction Program” developed at the University of Michigan in 2012) differs from the calculation required by REBA and RULA, as summarized in Table 5-3. Thus, a conversion of joint angles among different scenarios is conducted to fit the REBA/RULA requirements, as calculated in the last column of Table 5-3 as well as in Table D-2 of Appendix D.

Table 5-3: Joint angle calculation, schematic drawing, and implementation in REBA and RULA

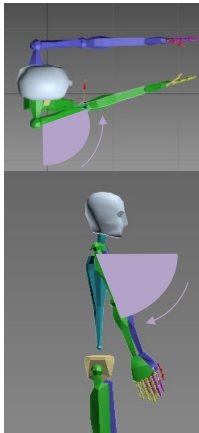
Body Parts	Joint angles from 3D modelling (University of Michigan, 2011)	Joint angle in REBA and RULA	Joint angle conversion to be implemented in REBA and RULA
Neck / Head	<p>Head flexion angle: the axis of the head/neck and a line drawn directly forward from the upper torso in a transverse plane at the C7-T1 spine level.</p>	<p>Head flexion angle: the axis of the head/neck and a line drawn directly upward from the upper torso in a coronal plane at the C7-T1 spine level.</p>	<p>If Neck_flexion ≥ 0 or Neck_flexion < 0, Neck_flexion = $b - a$ (where $b = 90$)</p>
			
Trunk	<p>Head axial rotation angle: the rotation is along the axis of the head/neck.</p> <p>Head lateral bending angle: between the axis of the head/neck and the projection of the same axis on the sagittal plane of the torso.</p>		
	<p>Trunk flexion angle: the angle between the trunk (the center of the hips to the center of the shoulders) and the projection of the trunk axis on transverse plane.</p>	<p>Trunk flexion angle: the angle between the trunk and a line drawn directly upward from the upper torso in a coronal plane.</p>	<p>If Trunk_flexion < 90 or Trunk_flexion > 90, Trunk_bending = $90 - a$</p>
			
	<p>Trunk axial rotation angle: the rotation of the torso is along the axis formed by the line segment from the L5/S1 disc to the center of the shoulders.</p> <p>Trunk lateral bending angle: between the trunk axis and the y-z plane.</p>		

Body Parts	Joint angles from 3D modelling (University of Michigan, 2011)	Joint angle in REBA and RULA	Joint angle conversion to be implemented in REBA and RULA	
Leg	<p>Leg vertical angle: when the body segment is level with the joint (upper leg to pelvis; lower leg to knee), the link is on the plane and the joint angle is 0°. If the link is above the plane, then the vertical angle is positive; if below, then the angle is negative.</p>	<p>Leg angle: the angle between lower leg and upper leg at maximum extension in sagittal plane.</p>	<p>If Upperleg_Horizontal > 0 & Lowerleg_Horizontal > 0, Leg_angle = abs(a-b)</p>	
				<p>If Upperleg_Horizontal > 0 & Lowerleg_Horizontal < 0, Leg_angle = 180 - abs(a+b)</p>
		<p>If Upperleg_Horizontal < 0 & Lowerleg_Horizontal > 0, Leg_angle = 180 - abs(a+b)</p>		<p>If Upperleg_Horizontal < 0 & Lowerleg_Horizontal < 0, Leg_angle = abs(a-b)</p>
				

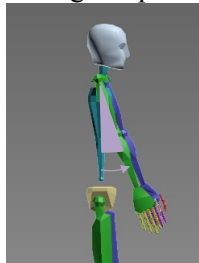
Body Parts	Joint angles from 3D modelling (University of Michigan, 2011)	Joint angle in REBA and RULA	Joint angle conversion to be implemented in REBA and RULA
-------------------	---	------------------------------	---

The **upper arm horizontal angles** and **vertical angles** define the direction of the upper arm but not the axial rotation about the upper arm bones.

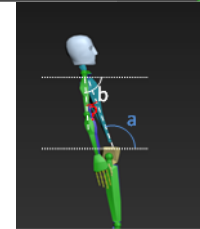
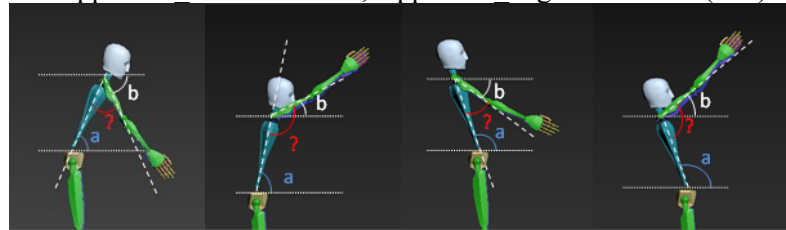
Upper Arm



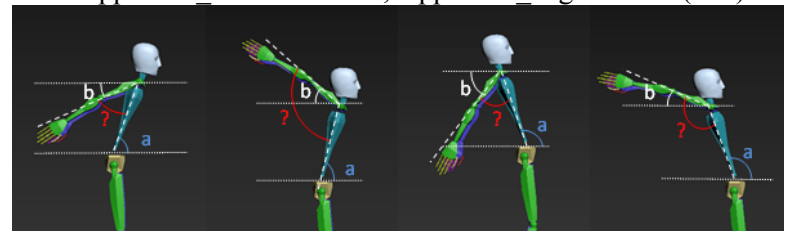
Upper arm angle: angle between upper arm and the trunk on sagittal plane.



If Upperarm Horizontal > 0, Upperarm angle = $180 - \text{abs}(a - b)$



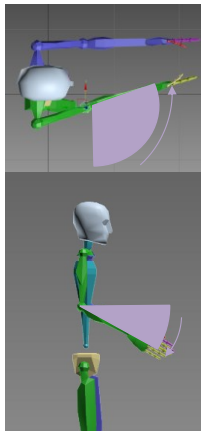
If Upperarm Horizontal < 0, Upperarm angle = $-\text{abs}(a + b)$



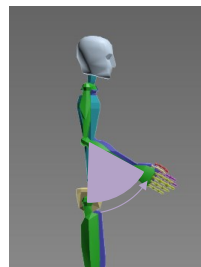
Body Parts	Joint angles from 3D modelling (University of Michigan, 2011)	Joint angle in REBA and RULA	Joint angle conversion to be implemented in REBA and RULA
------------	--	------------------------------	---

The lower arm horizontal and vertical angles design the direction of the lower arm but not the axial rotation about the lower arm bones.

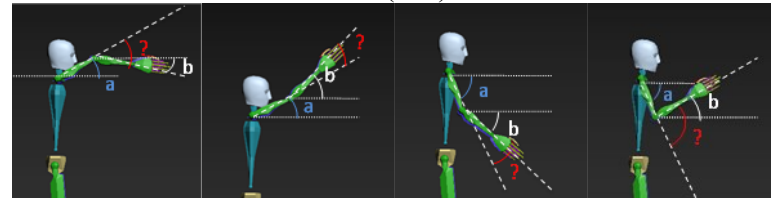
Lower Arm



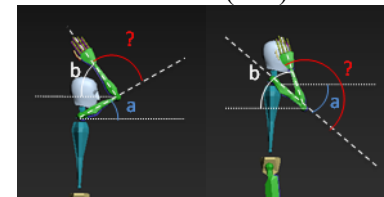
Lower arm angle is the angle between upper arm extension line and lower arm.



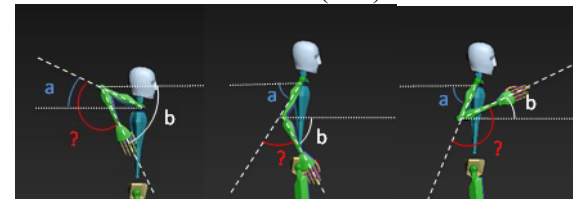
If UpperArm_Horizontal > 0 & LowerArm_Horizontal > 0, Lowerarm_angle = abs(a-b)



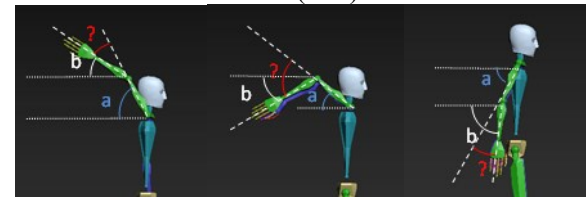
If UpperArm_Horizontal > 0 & LowerArm_Horizontal < 0, Lowerarm_angle = 180-abs(a+b)



If UpperArm_Horizontal < 0 & LowerArm_Horizontal > 0, Lowerarm_angle = 180-abs(a+b)



If UpperArm_Horizontal < 0 & LowerArm_Horizontal < 0, Lowerarm_angle = abs(a-b)



Body Parts	Joint angles from 3D modelling (University of Michigan, 2011)	Joint angle in REBA and RULA	Joint angle conversion to be implemented in REBA and RULA
-------------------	---	------------------------------	---

Hand segment vertical angle:

When the hand is level with the wrist, the joint angle is 0°. If the hand is above the wrist, the vertical angle is positive; if below the angle is negative.



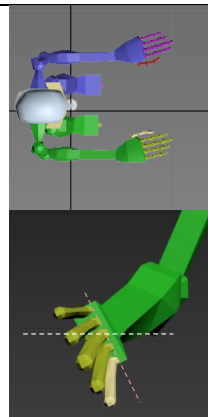
Wrist angle: the angle between the lower arm extension line and the wrist for both horizontal and vertical angles.



Wrist

Hand horizontal angle: between the hand segment and the x-axis constitutes the horizontal angle

Hand rotation angle: the axial rotation of the wrist compared with forearm.



If Lowerarm_Horizontal > 0 & Wrist_Horizontal > 0, Wrist_angle = abs(a-b)

If Lowerarm_Horizontal > 0 & Wrist_Horizontal < 0, Wrist_angle = 180-abs(a+b)

If Lowerarm_Horizontal < 0 & Wrist_Horizontal > 0, Wrist_angle = 180-abs(a+b)

If Lowerarm_Horizontal < 0 & Wrist_Horizontal < 0, Wrist_angle = abs(a-b)

5.2.2 3D modelling post-data processing and risk rating algorithm

A user interface, as displayed in Figure 5.3, is developed for the purpose of conducting data post-processing and further analyzing the results. Initially, printing the raw joint angle data and risk assessment calculations are conducted using MATLAB. With the support of other platforms (to be detailed later in this section), a user interface in 3ds Max is developed. It is not necessary to analyze the entire model in 3ds Max; the analyzed time frames can be defined and selected by the user as needed. The repetitive motion in the animation can also be edited by typing in the time frame range and the number of the repetition, which also generates a repetition score for the motion that needs to be repeated 4 times per minute. Based on Eq. (5-1), if the total duration of the task is less than 60 seconds, then an *activity score* of 1 is added to the total rating.

$$\text{Total duration} = \frac{\text{Total time frame}}{\text{Frame rate}} \times 4 \text{ repeats} \quad (5-1)$$

Note: Frame rate default is set to 30 frames per second and can be customized by the user.

The inputs of the interface are the time frame range of the task, the repetition with the time frame range of the repetitive motion, the handled force (in pounds or kilograms), the time frame range of force implementation, *coupling score*, and *activity score*. To be specific, for the input of handled force, users can also type in multiple entries by inputting force and time frame range data one by one. To check all the force input settings, a function of “show set force information” is also available. The function of clearing all the force input settings in the event of erroneous inputs is also provided. In terms of the *coupling score*, a drop down list is designed for the user to select from: “Well fitting handle and mid-range power grip”, “Acceptable but not ideal hand hold or coupling acceptable with another body part”, “Hand hold not acceptable but possible”, or “No handle, awkward, unsafe with any body part”. Within the *activity score*, a repetition score is calculated as per Eq. (5-1), and check boxes are also included as follows: “1 or more body parts

are held for longer than 1 minute (static)” and “action causes rapid large range changes in posture or unstable base”, as shown in the bottom of Figure 5.3.

Following the joint angle conversion shown in Table 5-3, the angles can be directly implemented in REBA and RULA. The risk rating is calculated using MAXScript programming to read the generated batch file, and is graphically plotted for each individual body segment, including trunk, neck, arm, leg, and wrist, as well as for the total rating of the entire motion at the respective time frame, considering force/load and activity performance. OxyPlot is used as an open source plotting library for .NET. A Dynamic-link Library (DLL) is created to receive information from 3ds Max, and then OxyPlot in conjunction with WindowsForm is applied in order to provide a graphical representation. Windows Media Player is utilized to play the rendered animation of the human body movement. Any high-risk motions can be identified through this rating algorithm and the resulting plotted chart. The peak rating and the corresponding human body motion are identified by comparing the plotted chart with the 3D animation. The plotted chart is displayed based on the time span of the animation (i.e., the next risk rating to be displayed in the chart illustrates the rating of the motion in the animation at the given timeframe). Buttons for pausing the animation and dragging the animation to a certain time frame or footage are also developed for the purpose of viewing the risk at play at a certain time frame. The user can also type in the time frame to check the risk rating accordingly. Moreover, risk ratings are plotted for each body segment, and this assists in providing understanding of which body segments are exposed to higher risks during the given operation, as indicated in Figure 5.4. Modified work can be recommended for the given motion by revising the task manoeuvre of the body segment with a high rating or modifying the task manoeuvre entirely.

A function of plotting joint angle raw data together with its risk assessment method and results is also developed (on the right side of the user interface displayed in Figure 5.3). When the user selects the REBA/RULA calculation method and clicks the body segment button, an interface appears for plotting and displaying raw data of each time frame. This function enables the user to check the raw data and risk assessment results for either REBA or RULA, as indicated in Figure 5.5.

The current model has limitations for joint angle calculations of neck, hand rotation, and clavicle vertical angle. Due to this limitation of the current 3D modelling method, neck flexion is assumed to be 0 in the 3D modelling data acquisition. Thus in the current model neck flexion is replaced by the head for the purpose of risk assessment. All the joint angles are rounded as integers for further analysis because decimals are not needed for these two risk assessments tools. The joint angle conversions and assumptions of implementing REBA and RULA in this 3D modelling are also summarized in the first column of Table 5-4.

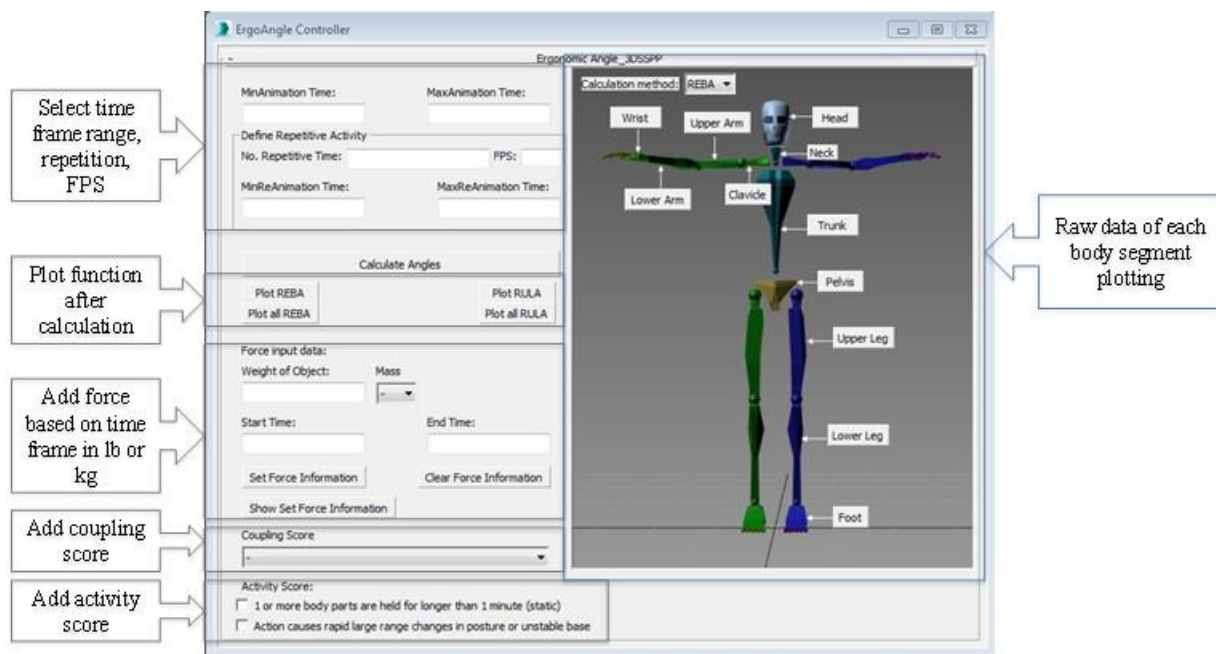
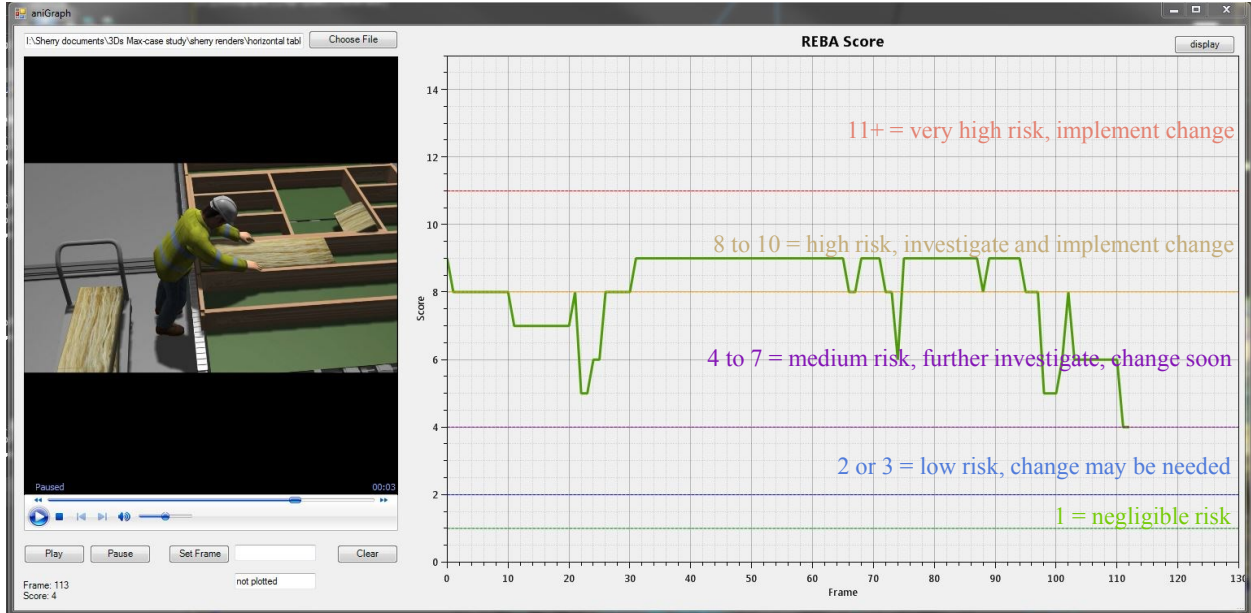


Figure 5.3: Developed user interface of the proposed method in 3ds Max

(a) Total REBA risk rating



(b) Individual rating for each body segment

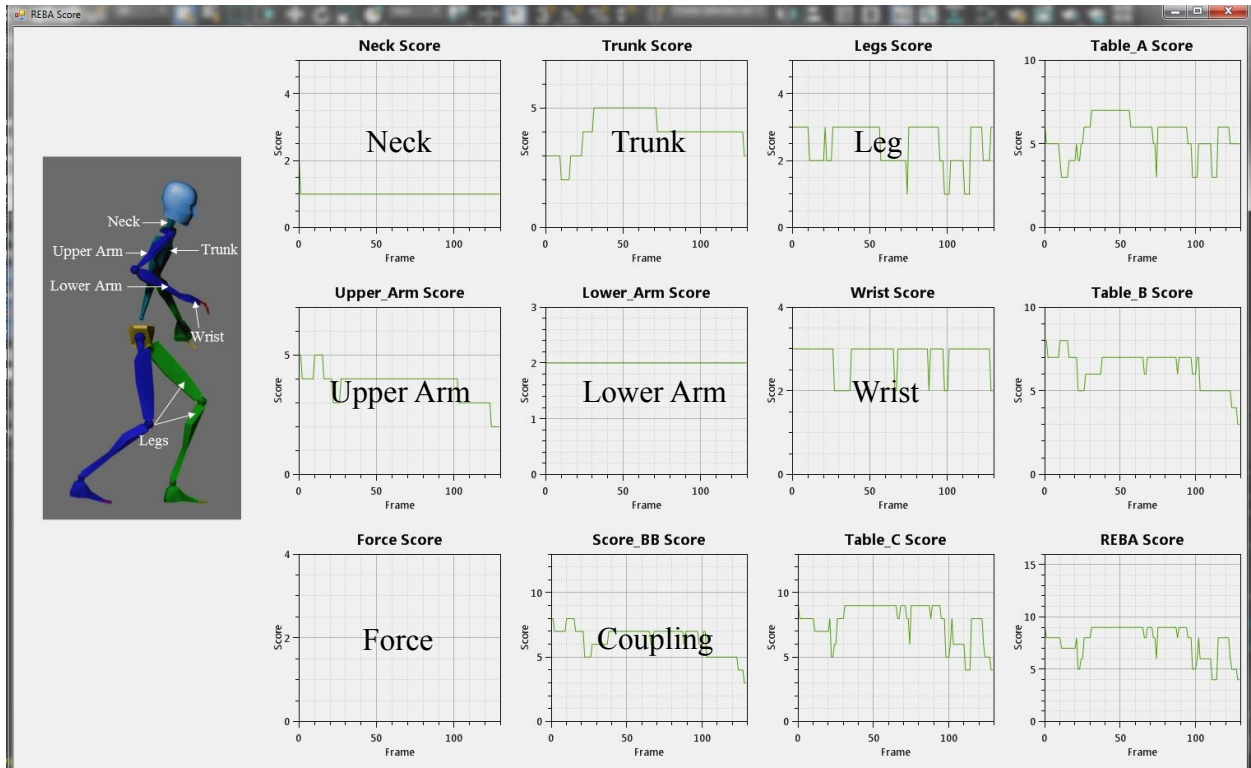


Figure 5.4: Risk assessment sample final REBA risk rating and detailed individual rating for each body segment

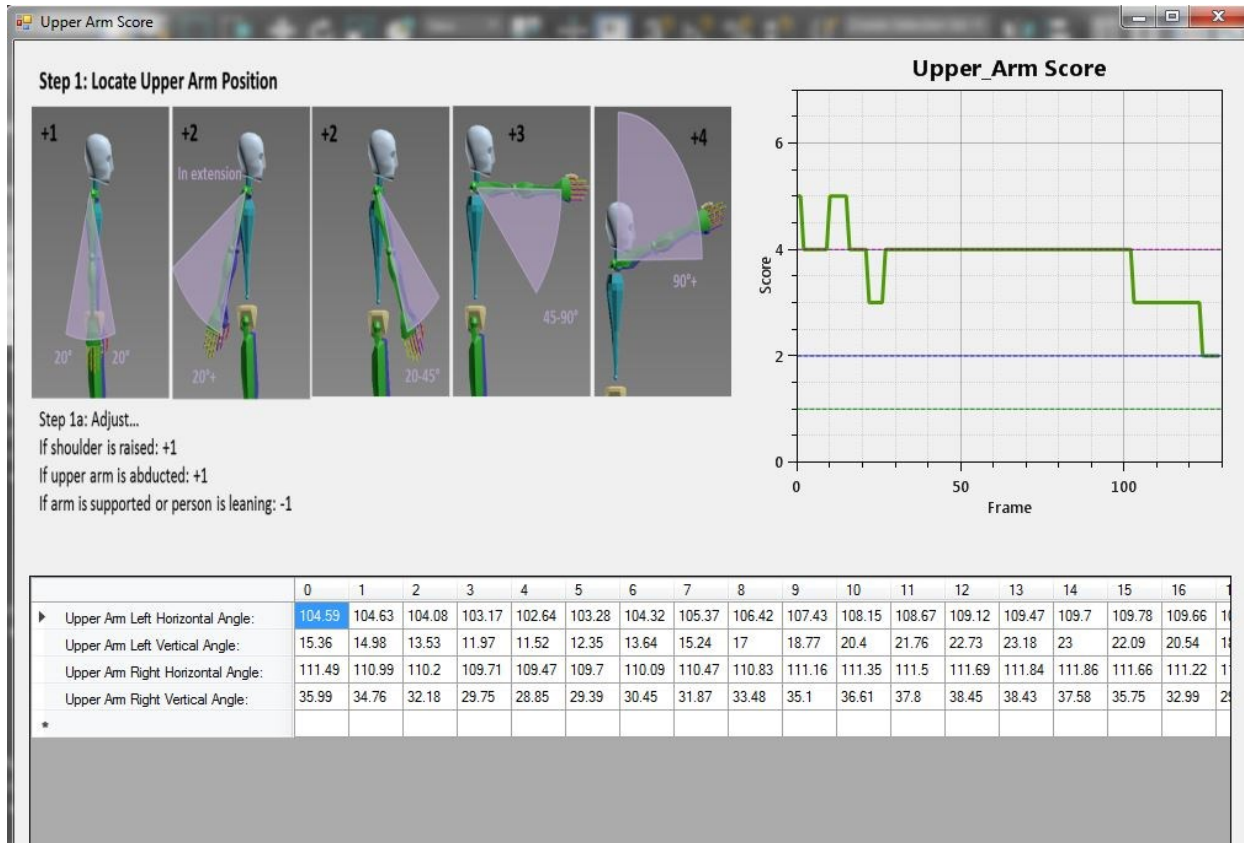
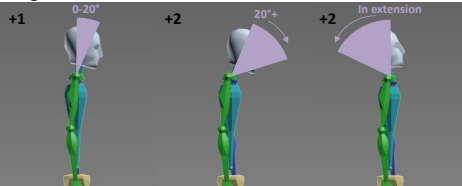
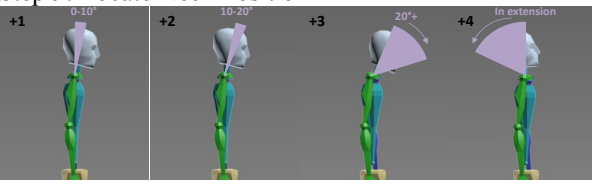
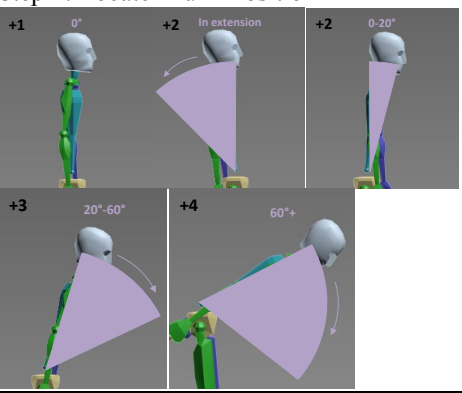
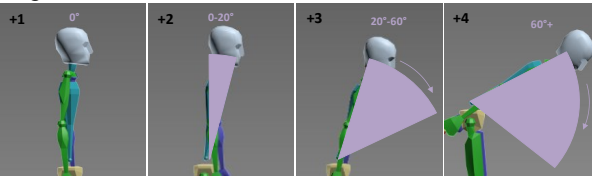
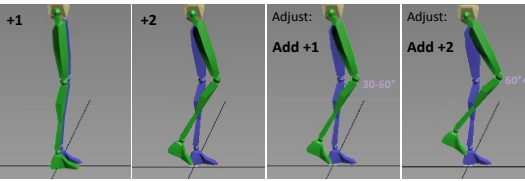
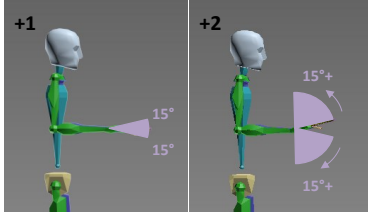
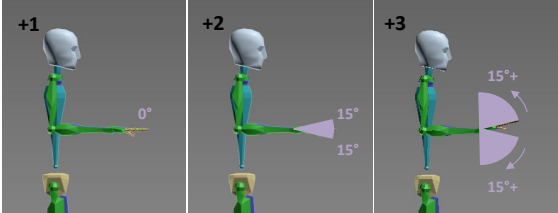
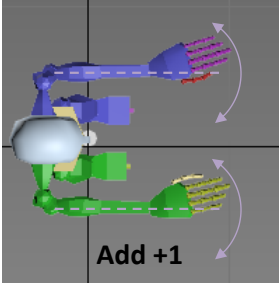
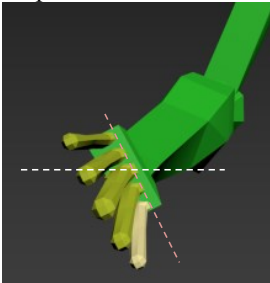


Figure 5.5: Joint angle raw data at each time frame with its risk assessment method (REBA or RULA)

Table 5-4: Implementation of joint angles into REBA and RULA calculations

Body Parts	Converted joint angles and risk assessment assumptions	REBA	RULA
Neck / Head	Neck_Flexion = Head_Flexion; neck_flexion = 90-Neck_Flexion;	Step 1: Locate Neck Position 	Step 9: Locate Neck Position 
	Head_Rotation_Angle > 10,	If neck is twisted: +1	If neck is twisted: +1
	Head_Lateral_Bending_Angle > 10	If neck is side bending: +1	If neck is side bending: +1
Trunk	trunk_flexion = 90-Trunk_Flexion	Step 2: Locate Trunk Position 	Step 10: Locate Trunk Position 
	Trunk_Rotation_Angle > 10	If trunk is twisted: +1	If trunk is twisted: +1
	Trunk_Lateral_Bending_Angle > 10	If trunk is side bending: +1	If trunk is side bending: +1
Leg	$\text{leg_angle} = 180 - \text{abs}(\text{LowerLeg_Vertical} + \text{UpperLeg_Vertical})$ OR $= \text{abs}(\text{LowerLeg_Vertical} - \text{UpperLeg_Vertical})$ Assume the difference between left and right leg_angle larger than 1 as imbalanced posture in Chapter 4; while assume it larger than 5 as imbalanced posture in Chapter 5. Leg is always assumed as being supported in		Step 11: Legs If legs and feet are supported: +1 If not: +2

Body Parts	Converted joint angles and risk assessment assumptions	REBA	RULA
	this model.		
Upper Arm	$upperarm_angle = 180 - \text{abs}(\text{Trunk_Flexion} - \text{UpperArm_Vertical})$ OR $= -\text{abs}(\text{Trunk_Flexion} + \text{UpperArm_Vertical})$	Step 7: Locate Upper Arm Position 	Step 1: Locate Upper Arm Position
	Assume Clavicle_vertical_angle = -1 in the current model Assume UpperArm_Vertical > 10 as raised shoulder	Step 7a: Adjust... If shoulder is raised: +1	Step 1a: Adjust... If shoulder is raised: +1
	Assume $\text{abs}(upperarm_horizontal_angle) \leq 60$ as abducted arm	If upper arm is abducted: +1 If arm is supported or person is leaning: -1	If upper arm is abducted: +1 If arm is supported or person is leaning: -1
	$\text{trunk_flexion} = 90 - \text{Trunk_Flexion}$; Assume $\text{trunk_flexion} > 0$ & $upperarm_angle > 0$ as person leaning	If arm is supported or person is leaning: -1	If arm is supported or person is leaning: -1
Lower Arm	$forearm_angle = \text{abs}(\text{UpperArm_Vertical} - \text{ForeArm_Vertical})$ OR $= 180 - \text{abs}(\text{UpperArm_Vertical} + \text{ForeArm_Vertical})$	Step 8: Locate Lower Arm Position 	Step 2: Locate Lower Arm Position
	Assume $\text{abs}(\text{Lowerarm_Horizontal_angle}) \leq 60$ as working out to side of the body OR $\text{abs}(\text{Lowerarm_Horizontal_angle}) \geq 120$ as working across midline	N/A	Step 2a: Adjust... If either arm is working across midline or out to side of body: Add +1

Body Parts	Converted joint angles and risk assessment assumptions	REBA	RULA
<p>hand_angle = abs(ForeArm_Vertical-Hand_Vertical) OR = 180-abs(ForeArm_Vertical+Hand_Vertical)</p>	<p>Step 9: Locate Wrist Position</p> 	<p>Step 9: Locate Wrist Position</p> 	
Wrist	<p>hand_angle = abs(Hand_Horizontal - ForeArm_Horizontal) Assume hand_angle > 10 as bending hand Hand_Rotation > 10 as twisted hand</p>	<p>Step 9a: Adjust... If wrist is bent from midline or twisted: Add +1</p>	<p>Step 3a: Adjust... If wrist is bent from midline: Add +1</p> 
<p>Assume abs(Hand_Left_Rotation) ≥ 0 & abs(Hand_Left_Rotation) ≤ 90 as rotation in mid-range Hand rotation is assumed to be 0 in the current model.</p>	N/A	<p>Step 4: Wrist twist</p> 	

Although REBA and RULA provide a clear body posture judgement on the main body part for the key rating, minor movements of the body such as hand twisting, trunk lateral bending, and imbalanced leg posture are not explained clearly. Thus some assumptions are made based on the existing experiment as interpreted in Chapter 4. The trunk lateral bending and leg judgment are used as examples in this section to provide a detailed explanation.

Trunk lateral bending occurs when the lateral bending angle exceeds 5° . This judgement is based on the motion capture data collected from the experiment explained in Chapter 3. During the experiment, the subjects are asked to conduct the movement without lateral bending. However, in reality, when a subject performs the lifting task, it is inevitable that the trunk will be tilted to the side at least slightly. As expressed in Figure 5.6, unavoidable bending to a maximum of 4° is performed. Thus 5° is selected as the upper boundary for the lateral trunk position.

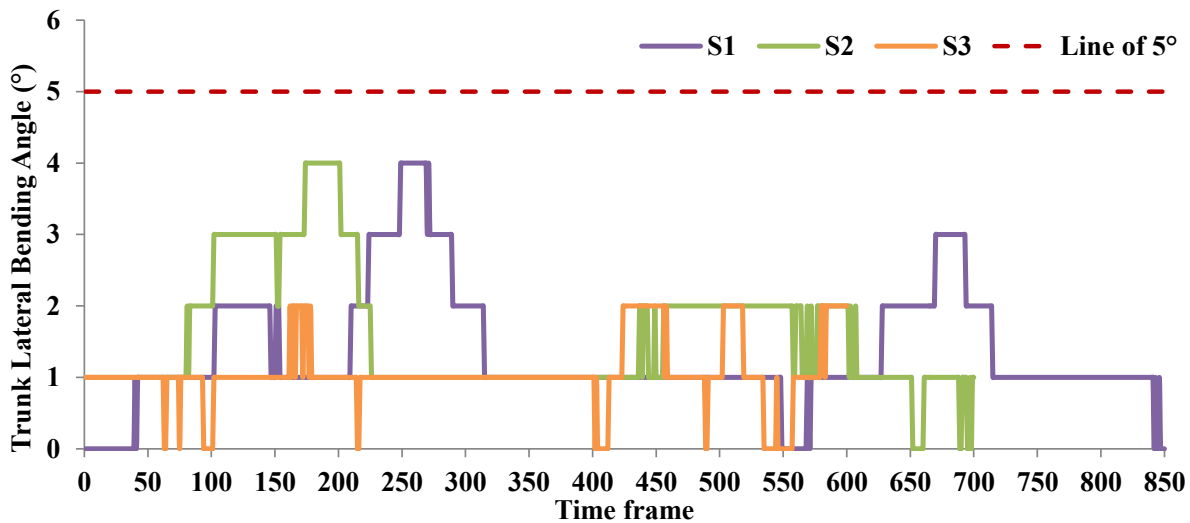


Figure 5.6: Trunk lateral bending angles from the three subjects in the experiment during lifting tasks

In leg risk assessment, the legs are judged with a score of 1 when the legs stand with bilateral weight or during walking or sitting motions. In the proposed model, walking and sitting movement is defined manually by choosing time frames from the 3ds Max animation file. A

score of 2 is assigned to legs when the legs tolerate unilateral weight or imbalanced posture. In this case, the imbalanced posture is judged by the angle formed between the left and right legs. In Chapter 4 it was assumed that a leg is imbalanced when the angle between the left and right legs is larger than 0° , whereas here the angle between left and right legs is assumed to be larger than 5° for imbalanced leg posture. The use of 5° as the threshold is derived from the data collection from the experiment, illustrated in Chapters 4 and 5. In the experiment, although all three subjects are requested to hold the load and carry out the bending motion with straight legs, a difference between two leg angles can still be identified. Figure 5.7 plots the leg angles for both left and right side and Figure 5.8 displays the difference between the two sides for all three subjects. Subject 1 performs the motion with a larger angle difference between his two legs with a maximum angle of 13° . The video captured for subject 1 having been checked, a small gap between the two legs can be identified. Thus the data from subject 1 indicates an imbalanced posture. Based on the angle differences as plotted in Figure 5.8, 5° is identified as the upper boundary for imbalanced leg posture. Thus in the REBA risk assessment a rating of 2 is given for the leg.

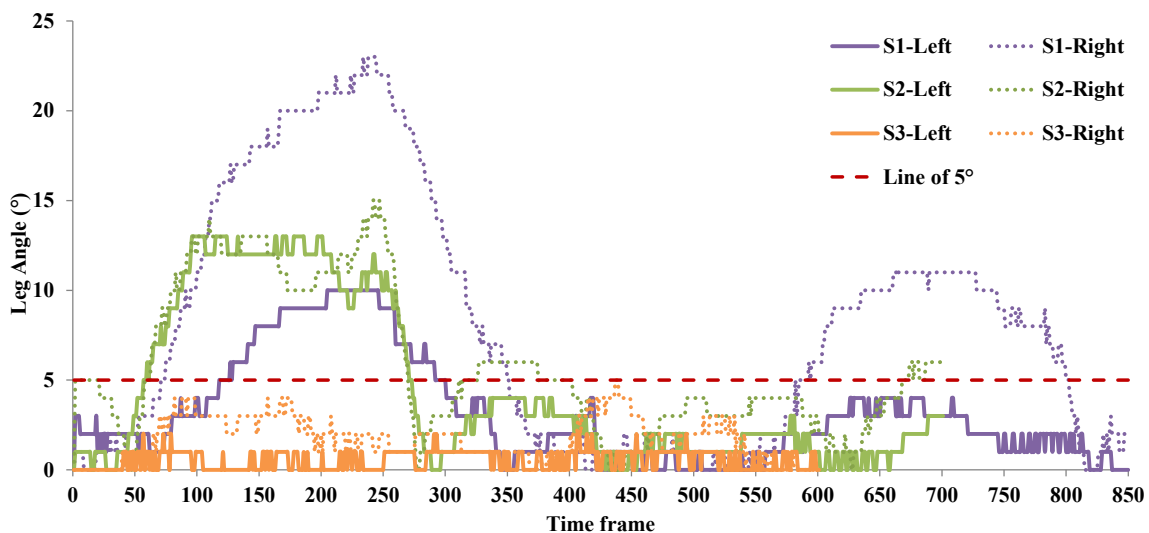


Figure 5.7: Leg angles from the three subjects in the experiment during lifting tasks

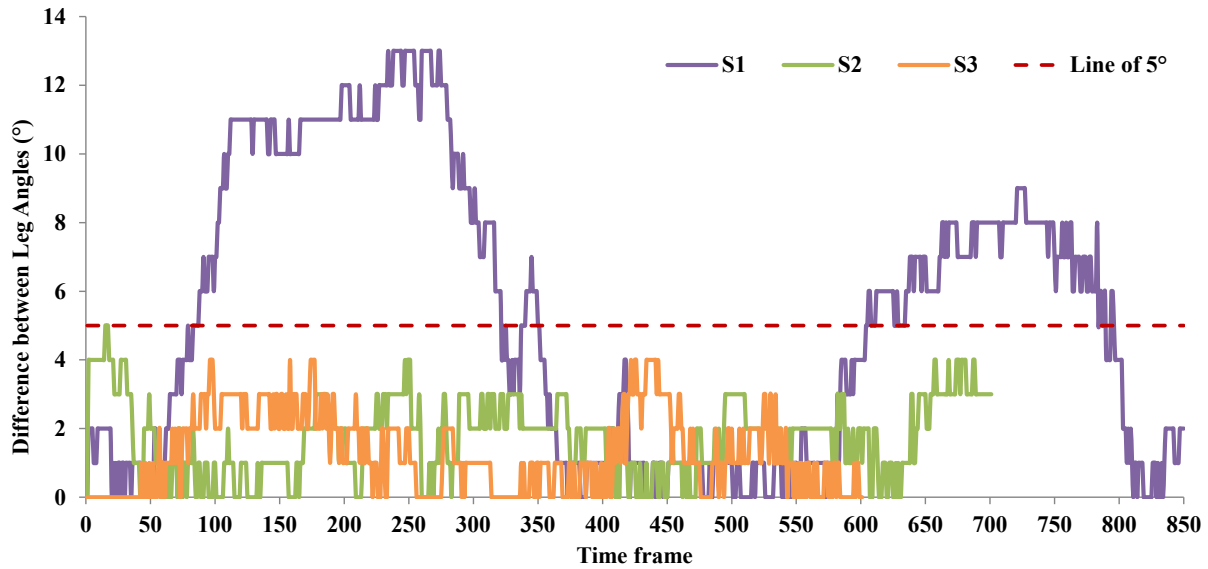


Figure 5.8: Difference between left and right leg angles among subjects in the experiment during lifting tasks

5.3 Implementation of 3D Motion-based Physical Demand Analysis in a Case Study

Although the process of establishing all 3D components from sketching in the early stages of 3D modelling, without any existing 3D component library as support, is highly time-consuming, 3ds Max has a massive inventory of models in an existing library to support this framework and the building of 3D modelling to animate and imitate the working motions in the factory. The ultimate goal of this research is to identify the risk, provide modified work based on the analysis results, and achieve overall risk reduction in the analyzed workstations. It should also be noted that in some industries there may be a variety of supporting equipment/tools available and a number of different worker behaviours that could be exhibited for completing a similar operational task. In this regard, another strength of this framework is that 3D visualization enables the animation and simulation of diverse methods of completing a given task and comparison of the results in order to propose the optimal method.

In this section, the implementation of this framework in a real construction manufacturing task, i.e., placing insulation on the floor or wall panel, is carried out. In this case, the traditional wood frame building envelope is insulated with fiberglass batts, a relatively lightweight type of insulation. Thus the case study focuses on awkward body posture, rather than on the heavy load on the body. Two aspects of the study are completed in this section: (1) comparison among different methods of completing the insulation task; and (2) comparison among different movements based on the change of workstation design. All the data, in regard to the subject movements and workstation design, used in the development of 3D animation is collected from the corresponding PDA of this task. Both REBA and RULA are implemented in the study to complete the risk assessment analysis. The result from the traditional usage of these two methods is given as an integer. However, in this framework, the obtained risk rating result is averaged among a certain range of time frames. Thus, the risk level categories of the two methods are also adjusted to define the average rating for the operational task, summarized in Table 5-5 and Table 5-6.

Table 5-5: Adjusted REBA risk level category

Level of risk	Risk ratings	Instruction
1	[1, 1.5)	Negligible risk
2	[1.5, 3.5)	Low risk, change may be needed
3	[3.5, 7.5)	Medium risk, further investigation, change soon
4	[7.5, 10.5)	High risk, investigate and implement change
5	[10.5, 12]	Very high risk, implement change

Table 5-6: Adjusted RULA risk level category

Level of risk	Risk ratings	Instruction
1	[1, 2.5)	Acceptable posture
2	[2.5, 4.5)	Further investigation, change may be needed
3	[4.5, 6.5)	Further investigation, change soon
4	[6.5, 7]	Investigate and implement change

5.3.1 Installation of insulation by four different methods

Four scenarios of motions collected from the collaborating companies, Kent Homes and ATCO Structures & Logistics, are animated in this case study, as indicated in Figure 5.9. The four scenarios all begin with the subject holding one piece of insulation in their hands and end with one piece of insulation being installed on the panel. The height of the subject is set as 6 ft with the default setting on the size of the body segments. Throughout the motions for this task, risk assessment data are collected based on time frames and are further categorized separately into five risk levels for REBA and four risk levels for RULA. The design and the operation requirements of each workstation obtained from the improved PDA are summarized below.

- 1) The first scenario is to raise the panel using a 7-ft jig, where the subject must reach above the shoulder in order to place insulation above their head on the panel.
- 2) The second scenario is to perform the task from on top of the panel with one leg bending (into a crouched position) and the other leg kneeling in order to place the insulation; the panel is positioned on the floor.
- 3) The third scenario is to provide a supportive table/workstation with a height of 2.4 ft to assist with the insulation task; the panel is designed with a thickness of 0.8 ft and width

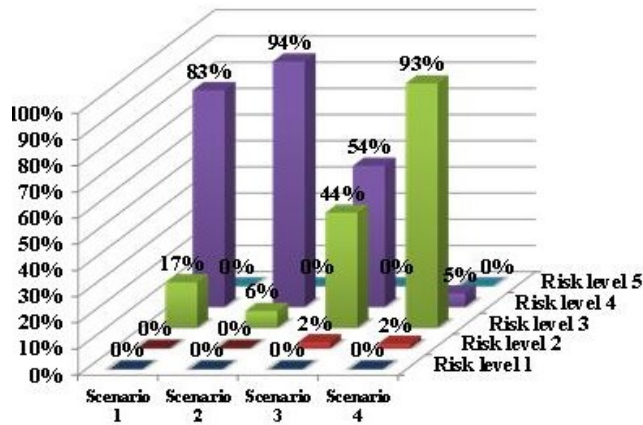
of 9 ft; the workers work on both sides of the table/workstation so that the center of the table is reachable.

- 4) The fourth scenario requires lifting the panel to 14 in from the floor at a perpendicular angle to the floor; the subject then places insulation on the bottom half of the panel within the reachable working height.



Figure 5.9: Four scenarios for placing insulation

a. REBA assessment results



b. RULA assessment results

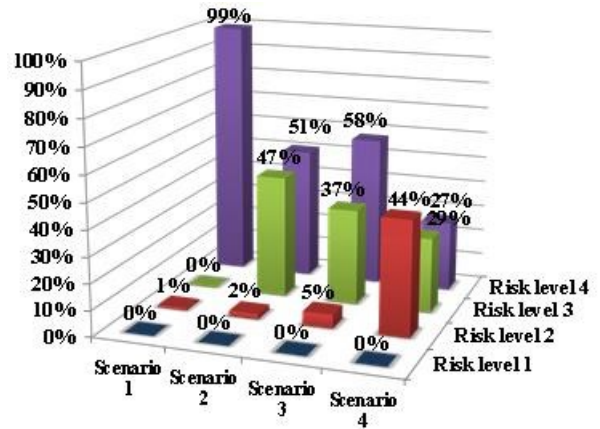


Figure 5.10: REBA and RULA results from four scenarios of placing insulation

Table 5-7: REBA and RULA results from four scenarios of placing insulation with max, min, and mean values

Methods	REBA				RULA			
Scenario	1	2	3	4	1	2	3	4
MAX	10	10	9	8	7	7	7	7
MIN	5	6	3	3	4	4	3	3
MEAN	8.05	8.92	7.24	5.25	6.97	6.37	6.12	5.07
Risk Level	4	4	3	3	4	3	3	3

Table 5-8: REBA and RULA results from three scenarios of placing insulation with risk ratings of each body segment

Risk ratings	REBA				RULA				
	Scenarios	1	2	3	4	1	2	3	4
Neck	1.99	2.00	1.01	1.00	3.97	3.00	1.02	1.00	
Trunk	2.47	3.33	3.66	2.51	2.49	3.66	3.68	2.80	
Leg	2.30	3.77	2.38	2.56	1.00	1.00	1.00	1.00	
Upper arm	4.96	3.14	3.75	3.10	4.96	3.14	3.75	3.10	
Lower arm	1.96	1.84	2.00	1.63	2.05	2.29	2.46	2.34	
Wrist	2.94	2.65	2.84	2.88	3.94	3.64	3.84	3.88	
Wrist Twist	-	-	-		1.00	1.00	1.00	1.00	

Figure 5.10 plots the time frame percentage of each risk level for each scenario. From the REBA assessment, the average risk ratings of the four scenarios are 8.05, 8.92, 7.24, and 5.25, respectively, which correspond to the risk levels of 4, 4, 3, and 3, respectively, as illustrated in Table 5-7. Throughout the collective motions, scenario 2 involves the highest proportion of motions that are exposed to the risk level of 4 (94%); while for scenarios 1, 3, and 4 these proportions are 83%, 54%, and 5%, respectively. Thus scenario 4 involves less risk than do the other three scenarios. In terms of the maximum and minimum ratings, scenarios 3 and 4 have a lower minimum rating (3) than do the other two scenarios. As for scenario 3, due to the width of the panel (9 ft), the maximum rating of 9 occurs since reaching and bending forward is required in order to reach the center of the panel, which is approximately 4.5 ft from the center of the subject's body. The maximum rating and overall average rating of scenario 4 are the smallest when the subject installs the insulation on the bottom of the panel; a ladder, however, may be

required for the insulation installation on the top of the panel, which is not considered in the comparison due to the potential involvement of a falling hazard.

As for the RULA assessment, the average risk ratings of the four scenarios are 6.97, 6.37, 6.12, and 5.07, respectively, and workers are exposed to an average risk level of 4 for the first scenario and an average risk level of 3 for the other three scenarios. Scenario 1 is exposed to the highest risk, with 99% of motions categorized in the risk level of 4. The majority of the motions in scenario 2 are approximately equally distributed between risk levels 3 and 4 (with the remaining 2% distributed in risk level 2); 58% of the motions in scenario 3 are exposed to a risk level of 4. Scenario 4 performs with the least risk among all the scenarios, with 44% of motions exposed to the risk level of 2.

To summarize, REBA assessment indicates that scenario 2 develops higher risk than scenarios 1 and 3, while scenario 4 involves the least risk. The RULA assessment concludes that scenario 1 results in the highest risk of the four scenarios, while scenarios 2 and 3 involves similar levels of risk to one another, and scenario 4 involves the lowest risk. Due to the differing functionalities of the REBA and RULA risk assessment tools, the worst option (i.e., the movement that is exposed to the highest risk) differs for each of the scenarios. However, both assessment methods indicate that scenario 4 involves the least risk and is thus the optimum choice of completing this task. More discussions about the results are given in section 5.3.3.

Moreover, considering the detailed motion of each body segment analyzed from the results of both the REBA and RULA methods (summarized in Table 5-8), scenario 1 has a higher rating for the upper arm and wrist than do the other three scenarios; scenario 2 has a higher rating for the trunk and leg than do the other three scenarios; scenario 3 has a higher rating for the trunk

than do the other three scenarios; and scenario 4 involves a comparably low rating for all the body segments.

5.3.2 Adjust the workstation design

The analysis of scenario 3 is further expanded with ergonomic risk evaluation of the change in workstation design. The current workstation design in scenario 3 involves a horizontal table with the panel positioned horizontally on top. Resulting analysis specifies that the maximum risk exists when the worker bends forward to reach the center of the table. The modified work recommendation for this task may involve tilting the table to a certain degree to reduce the amount of reaching required. The edge of the table nearest to where the work is taking place remains at the same height for the set of modified work scenarios based on scenario 3. The 20° and 45° tilting angles of the table are selected for ergonomic risk comparison, as represented in scenarios 3a and 3b in Figure 5.11. The motions of these three scenarios begin with placing the insulation to the center of the table and end with pressing the insulation at the edge of the table.

Scenario 3 – tilted 0°

Scenario 3(a) – tilted 20°

Scenario 3(b) – tilted 45°



Figure 5.11: Three scenarios with different workstation tilt angles

The risks of the three scenarios are plotted in Figure 5.12. The average ratings from the REBA assessment for the workstations tilted at 20° and 45° are 5.45 and 4.63, respectively, both smaller than the average rating of 7.24 for the motion on the horizontal table. The risk reductions yielded by RULA, which are smaller than those by REBA, are also identified when comparing the

results of these three scenarios using RULA, changing from 6.12 (scenario 3) to 6.07 (scenario 3a) and 5.55 (scenario 3b). To be more specific, the modifications of the workstation offer greater risk reduction on the movement of the trunk, leg, and upper arm than the other body segments, as compared in Figure 5.13. Larger gaps can be identified from the rating of the trunk, leg, and upper arm than the other body segments among the three scenarios in these rebar charts. However, because trunk and leg are more sensitive to REBA assessment than to RULA assessment, which is in agreement with the study by Escobar (2006), it is the REBA calculation that yields the greater risk reduction.

The modified work of tilting the table can thus reduce the ergonomic risk to 2.61 for the entire body according to REBA assessment and 0.58 for the upper body according to RULA assessment. The optimal tilting angle is 45° for the modification of scenario 3, which involves even lower risk than scenario 4 because the working zone is within the comfortable working level of the worker, thereby eliminating the need to bend the legs and trunk as in scenario 4.

The case study underscores the potential of this 3D modelling framework as a supporting tool to evaluate the proposed modified work proactively and to compare the results before and after the implementation of the modified work.

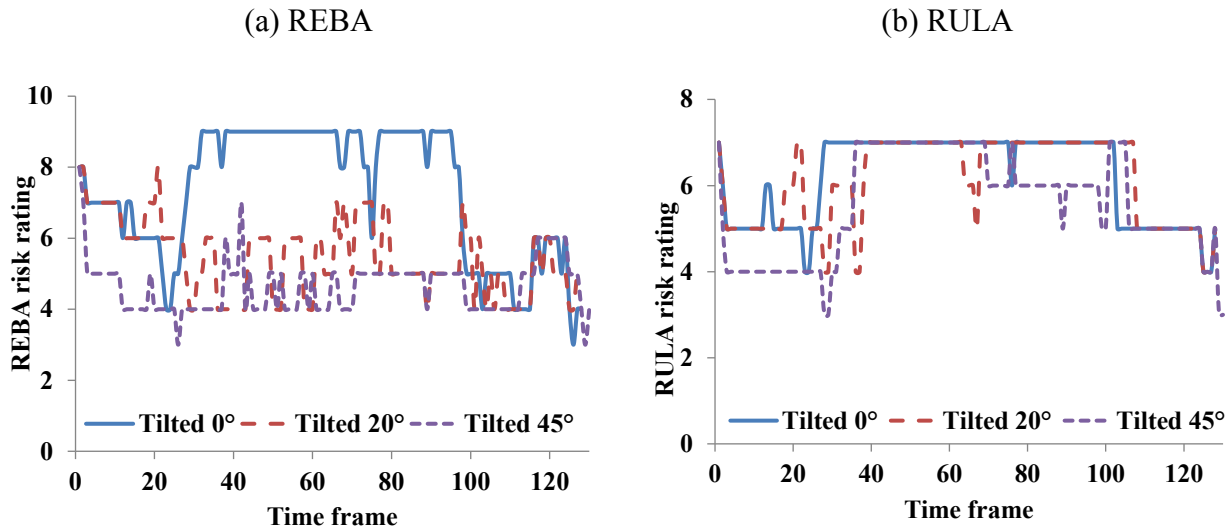


Figure 5.12: REBA and RULA risk comparison for the three scenarios

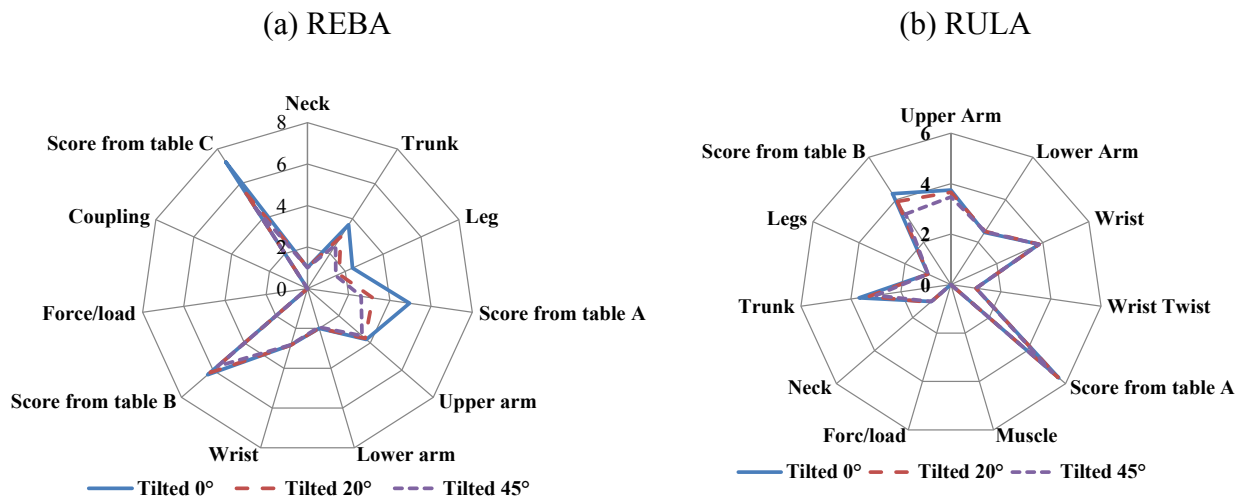


Figure 5.13: REBA and RULA body segment risk comparison for the three scenarios

5.3.3 Case study conclusions

Based on the task manoeuvre analysis results, it is apparent that the worker is exposed to different levels of ergonomic risk when performing the same task under different workstation designs and working environments. Minor or major workplace re-structuring may be recommended for modified working postures or human body motions. In the case study, it is recommended to have the wall or floor panel either positioned on the working table in order for

the subject to work from both sides, or lifted perpendicular to the floor, as given in scenarios 3 and 4. These two scenarios can be recommended as modified work to the other two scenarios for insulation placement in a wall panel or a narrow floor panel, where the worker is exposed to a lower risk rating compared with in the other two scenarios. However, scenario 3 may not be applicable for a wider floor panel where the center of the panel may not be within reach of the subject. In addition, the height of the table in scenario 3 can also be adjusted based on the height of the worker. Ideally, the modified work in scenario 3 will involve an auto-adjustable table for the worker to operate in order to safely complete the task. Tilting the table is another alternative which can effectively reduce the ergonomic risks. To avoid the use of a ladder for scenario 4, it is also recommended to lower the panel to a ditch below the floor to provide the subject easy access to the top of the panel and also ensure that the working zone is within the comfortable working level of the worker.

Results also suggest that if the worker has sustained any previous injuries to the upper arm and wrist they should not be assigned to scenario 1, whereas if the worker has sustained any previous injuries to the trunk, knee and lower body they should not be assigned to scenario 2. Meanwhile, a worker who has sustained any previous injuries to the torso should not work on the station in scenario 3. The motion analysis results can also be implemented in the sheathing placement task, where similar postures are required under the same workstation designs. However, higher risk may occur due to the heavy load of the sheathing board compared with this case study task of insulation installation.

The case study does not involve productivity analysis, as the task involves a short duration and the ergonomic risk is also proportional to the number of repetitions. If the modified work can be finished with higher productivity (a shorter task duration), the repetition of the motion may be

increased due to the fact that, within a certain period of time, more work can be done with higher productivity. However, more repetitions of the work could unfortunately increase fatigue and ergonomic risks. Thus, analysis of work repetitions during a work shift is essential, and for this the reader may refer to the framework developed in Chapter 3. It is expected that a recommendation will be determined for the number of repetitions of various motions in order to avoid potential fatigue development and to ensure safe execution of the given task.

5.4 Conclusion

This chapter automates an integrated framework to assess physical demand and ergonomic risks with the support of 3D modelling. The details of data acquisition and data post-processing are also interpreted mathematically and graphically. The support of the results display platforms can facilitate the analysis of ergonomic risk and can identify the precise moment that is exposed to the highest risk during the continuous movement. A case study of installing insulation in floor and/or wall panels is described to compare multiple scenarios in the manufacturing plant. The framework enables the analysis of entire body movement as well as movement of each body segment under different scenarios, and suggests the optimal alternative. The analysis results also provide recommendations to adjust the existing working conditions based on the performance of each body segment. The optimal options (scenario 3b and 4 in this case) can be introduced as modified work for the existing workstation and can be further implemented in actual practice.

The functionality of the proposed 3D motion-based physical demand and risk assessment modelling is thus proven and expanded. The user of this framework benefits in the following ways: (1) capability to obtain any human body posture data; (2) flexibility to conduct data post-processing; (3) applicability in the design phase of the workstation, such that the actual work can be carried out within safe working conditions; (4) ability to provide visualization of existing

workstations and any changes made to the plant; (5) ability to proactively test any changes made to the plant workstation; and (6) ability to provide comprehensive physical demand analysis documentation for the workstation. The ultimate goal of this research is to achieve overall risk reduction in practice for any construction manufacturing operational tasks. Upon implementing the proposed modified work in real practice, the ergonomic risk rating of the production line can be expected to be lower than before implementation.

CHAPTER 6: CONCLUSIONS

6.1 Research Summary

The importance of investigating physical demands and ergonomic analysis of body movements in the construction manufacturing workplace is increasing, as a high number of lost-time injuries have occurred in recent years. Analyzing the existing workstations enables health and safety personnel to gain a better understanding of the physical demand of each task and to suggest proactive corrections to address high risk body movements or to re-structure the workstation. Considering ergonomic factors for the workstation can also reduce muscle fatigue for the worker and can further improve the productivity of the operation. In this context, this research develops four frameworks for analyzing physical demand and ergonomic factors of human body movements in construction manufacturing as well as for assisting with the development of modified work: (1) an improved physical demand analysis; (2) muscle activity performance evaluation; (3) 3D motion-based ergonomic risk assessment; and (4) 3D motion-based physical demand and ergonomic analysis. The three primary ergonomic risk factors that may cause work-related musculoskeletal disorders (WMSDs) are considered in this research: repetition of the motion, forceful exertion, and awkward body posture. Human body motion data can be collected through direct and indirect measurements. The methods to identify ergonomic risks developed in this research rely on direct observation, physiological measurement, and 3D motion-based modelling.

The research first identifies the gap between the current risk assessment tools and the current physical demand analysis, and develops a framework that enables a comprehensive physical demand analysis encompassing risk identification, risk evaluation, and risk mitigation. This improved physical demand analysis enables recognition of the demands of strength, body posture

with detailed movement magnitude, and sensory and environment, and this in turn also provides the basis for the other three frameworks.

Second, the research develops a framework to assess muscle force and muscle fatigue development due to manual lifting tasks using surface electromyography (sEMG), kinematic motion capture and human body modelling. Muscle fatigue can develop from a task that requires repeated involvement of a specific group of muscles during a certain period, and it is also an ergonomic risk indicator. This framework is thus designed to assist with job recruitment and job rotation by analyzing the four identified fatigue indicators: RMS, ARV, MNF, and MDF. This method is also cross-validated by the muscle force generated from AnyBody Technology modelling for the same task. The limitations of physiological measurements are also identified.

A third framework is designed to enable automated task manoeuvre risk assessment during the construction operation with the support of 3D modelling. Integrated with the REBA and RULA risk assessment tools, the framework is able to identify the tasks that expose workers to high risk. The framework is also validated by the previous physiological measurement method. The fourth framework integrates the first and third frameworks as a comprehensive physical demand and ergonomic risk assessment, and has been implemented in a wall/floor insulation installation case study for the purpose of comparing existing scenarios with the scenarios resulting from workstation design modifications. This method can also be implemented for the design phase of a workstation, proactively analyzing the worker's operation process and ensuring that the work will be carried out in safe conditions. Thus this framework can be implemented in designing the structure and position of the workstation to mitigate potential ergonomic risks.

Ultimately, the goal of this research is to secure healthy and safe work performance and working environment and to reduce injuries and insurance claims. The research has been implemented

with regard to, but is not limited to, construction processes in the manufacturing plant. It can also be applied to on-site operations for heavy industrial construction.

6.2 Research Contributions

The primary contributions of this research are summarized as follows:

- 1) All the proposed frameworks are able to evaluate ergonomic risk proactively and to aid in providing alternatives for modified work to the manufacturing plant. A more robust return-to-work program can be established and a considerable reduction in the number of injuries and in the cost of insurance claims can be achieved, and this will eventually reduce the premium rate paid to WCB.
- 2) The proposed comprehensive physical demand analysis fills the gap between existing risk assessment tools and the existing physical demand analysis, and enables risk identification, risk evaluation, and risk mitigation for operational tasks in the industry.
- 3) The proposed framework for physiological measurement (with sEMG and motion capture), together with the human body simulation modelling, is able to investigate muscle fatigue, muscle forces and joint contact forces, and moments resulting from repetitive tasks in construction manufacturing operations. The results can assist in adjusting job rotation and providing working operation guidelines to limit the load and required force on body parts.
- 4) The research develops a method of using 3D modelling to imitate human motion and extracting human body data for risk assessment. The proposed 3D motion-based modelling method overcomes the limitations of physiological measurement and traditional manual observation methods, providing higher accuracy and effectiveness than the traditional manual observation method in risk assessment because 3D modelling is automated and capable of reliably analyzing continuous motions.

- 5) A user-friendly interface for 3D motion-based physical demand and ergonomic analysis is also established to automate the risk assessment process and visualize the analysis results. This interface can also facilitate the development of modified work.
- 6) The proposed framework of 3D motion-based physical demand and ergonomic analysis allows users to proactively imitate modified work proposed for an existing workstation in 3D modelling without actual changes or investment in the plant, and takes ergonomic concerns into consideration even in the design phase of the workstation.

6.3 Limitations and Future Research

In order to improve the performance of the proposed frameworks, the following can be pursued in future research:

- 1) Further implementation of the proposed improved PDA form from Chapter 2 is required in order to validate its universality and flexibility to other industries. The exported data from the proposed 3D modelling method in Chapter 5 can also serve as the input for the PDA form in future research. Systematic computer-based PDA automation can thus be achieved.
- 2) In this research the effective application of sEMG is limited to superficial muscles in low-fat areas in the vicinity of the sensor. There are challenges associated with the sEMG technique in quantifying fatigue developed in deep muscles such as the low back area. More experiments are needed to demonstrate the validity of this framework.
- 3) Each of the validation methods utilized in Chapter 4 has its own limitations which lead to differences and errors when comparing the experiment to the 3D modelling. During validation, the main causes of difference and error are as follows. (1) Video capture in this experiment is from the side view of the subject. Front view video capture is

suggested for future study to improve the accuracy of the horizontal angles. (2) The marker locations during the experiment are on the skin surface, which may shift during the movements and reduce the accuracy of the joint angle calculations. (3) The locations of the markers in the experiment are not exactly on the joints of the body segment, whereas the joint angles from the 3D modelling are estimated based on the precise coordinates of the joints. This difference may also contribute to the gap between the joint angles identified in the charts. It is also challenging to place a marker on the neck or head to capture motion. (4) The speed of the movement is constant in the 3D modelling, whereas the speed of the subject varies during the movement in the experiment. As a result, the movements between the two methods do not perfectly correspond at each time frame. The validity of this framework can be greatly improved if more experimental applications can be implemented and more 3D modelling can be created by different researchers for comparison.

- 4) Furthermore, for the proposed 3D motion-based physical demand and ergonomic risk assessment method, since continuous work and high physical demand could also result in a loss of productivity, the improvement of physical condition of the workstation can increase worker productivity. Such improvement measures of a dynamic movement, including the speed of the motion (acceleration and deceleration of the movement) and productivity analysis, can be incorporated into the 3D modelling in future work as a promising area of extension of the proposed method.
- 5) Finally, it should be noted that the framework has been implemented in but is not limited to construction manufacturing facilities for both existing workstations and for

workstation design. Application to other construction areas involving high physical demand may also be feasible.

REFERENCES

References for Chapter 1

- Agrawal, D.N. (2011). "Study and validation of body postures of workers working in small scale industry through RULA." *International Journal of Engineering Science and Technology*, 3(10), pp. 7730–7737.
- Alwasel, A., Elrayes, K., Abdel-Rahman, E. M., and Haas, C. T. (2011). "Sensing construction work-related musculoskeletal disorders (WMSDs)." *Proceedings, International Association for Automation and Robotics in Construction (IAARC)*, London, UK, pp. 164-169.
- Ansari, N.A., and Sheikh, D.M.J. (2014). "Evaluation of work Posture by RULA and REBA: A Case Study." *IOSR Journal of Mechanical and Civil Engineering*, 11(4), pp. 18–23.
- Association of Workers' Compensation Boards of Canada (2015). "2015 injury statistics across Canada." <http://awcbc.org/?page_id=14> (accessed January, 2017).
- Bjorksten, M. and Jonsson, B. (1997). "Endurance limit of force in long-term intermittent static contraction." *Scandinavian Journal of Work, Environment & Health*, 3(1), pp 23–27.
- Bureau of Labor Statistics (2016). "Nonfatal occupational injuries and illnesses requiring days away from work, 2015." Department of Labor. <<https://www.bls.gov/news.release/pdf/osh2.pdf>> (accessed February, 2017).
- Canadian Centre for Occupational Health and Safety (2016). "Hazards." <https://www.ccohs.ca/topics/hazards/ergonomic/#ctgt_1-1> (accessed October, 2016).
- Canadian Centre for Occupational Health and Safety. 2017. What are work-related musculoskeletal disorders (WMSDs). <<http://www.ccohs.ca/oshanswers/diseases/rmirsi.html>> (accessed February, 2017).

- David, G. C. (2005). “Ergonomic methods for assessing exposure to risk factors for work-related musculoskeletal disorders.” *Occupational Medicine*, 55(3), pp. 190–199.
- Escobar, C. (2006). Sensitivity Analysis of Subjective Ergonomic Assessment Tools: Impact of Input Information Accuracy on Output (Final Scores) Generation. Graduate Faculty of Auburn University, 54, 258.<<http://etd.auburn.edu/etd/handle/10415/386>> (accessed January, 2017).
- González-Izal, M., Malanda, A., Navarro-Amézqueta, I., Gorostiaga, E.M., Mallor, F., Ibañez, J., and Izquierdo, M. (2010). “EMG spectral indices and muscle power fatigue during dynamic contractions.” *Journal of Electromyography and Kinesiology*, 20(2), pp. 233–240.
- Han, S., and Lee, S. (2013). “A vision-based motion capture and recognition framework for behavior-based safety management.” *Automation in Construction*, 35, pp. 131–141.
- Hignett S. and McAtamney, L. (2000). “Rapid Entire Body Assessment.” *Applied Ergonomics*, 31, pp. 201–205.
- Industrial Accident Prevention Association (2009). “Performing a Physical Demands Analysis Instructions on How to Use the Physical Demands Analysis (PDA) Form.” <www.iapa.ca/Main/documents/pdf/FreeDownloads_PDA_intro.pdf> (accessed January, 2017).
- Inyang, N., Al-Hussein, M., El-Rich, M. and Al-Jibouri, S. (2012). “Ergonomic Analysis and the Need for Its Integration for Planning and Assessing Construction Tasks.” *Journal of Construction Engineering and Management*, 138, pp. 1370–1376.
- Khosrowpour, A., Niebles, J.C., and Golparvar-Fard, M. (2014). “Vision-based workplace assessment using depth images for activity analysis of interior construction operations.” *Automation in Construction*, 48, pp. 74–87.

- Kim, G., Ahad, M. A., Ferdjallah, M., and Harris, G.F. (2007). "Correlation of muscle fatigue indices between intramuscular and surface EMG signals." *Proceedings, IEEE SoutheastCon*, pp. 378–382.
- Levanon, Y., Lerman, Y., Gefen, A., and Ratzon, N.Z. (2014). "Validity of the modified RULA for computer workers and reliability of one observation compared to six." *Ergonomics*, 57(12), pp. 1856–63.
- Li, G. and Buckle, P. (1999). "Current techniques for assessing physical exposure to work-related musculoskeletal risks, with emphasis on posture-based methods." *Ergonomics*, 42(5), pp. 674–695.
- Li, C. and Lee, S. (2011). "Computer vision techniques for worker motion analysis to reduce musculoskeletal disorders in construction." *Proceedings, International Workshop on Computing in Civil Engineering*, Miami, FL, USA, Jun. 19-22, pp. 380–387.
- Mathieu, P.A., and Fortin, M. (2000). "EMG and kinematics of normal subjects performing trunk flexion/extensions freely in space." *Journal of Electromyography and Kinesiology*, 10(3), pp. 197–209.
- Määttä, T. J. (2007). "Virtual environments in machinery safety analysis and participatory ergonomics." *Human Factors and Ergonomics in Manufacturing*, 17(5), pp. 435–443.
- McAtamney, L. and Corlett, E. N. (1993). "RULA: A survey method for investigation of work related upper limb disorders." *Applied Ergonomics*, 24(2), pp. 91-99.
- Middlesworth, M. (2012). "A step-by-step guide to the Rapid Entire Body Assessment (REBA) tool". *Ergonomics Plus*, <www.ergo-plus.com> (accessed January, 2016)

- Ontario Safety Association for Community and Healthcare (2010). Musculoskeletal Disorders Prevention Series Part 1: MSD Prevention Guideline for Ontario. <http://www.osach.ca/misc_pdf> (accessed March, 2015).
- Occupational Safety and Health Administration (1990). “Ergonomic program management guidelines for meatpacking plants” (Publication No. OSHA-3121). Washington, DC, USA: U.S. Department of Labor.
- Plantard, P., Shum, H. P.H., Le Pierres, A. and Multon, F. (2016). “Validation of an ergonomic assessment method using Kinect data in real workplace conditions.” *Applied Ergonomics*, In Press.
- Public Services Health & Safety Association (PSHSA). (2010). “Repetitive work: Could you please repeat that ...again and again and again?” <<http://www.healthandsafetyontario.ca/HSO/media/PSHSA/pdfs/MSDs/RepetitiveWorkInjury.pdf>> (accessed in January, 2017).
- Pah, N. and Kumar, D.K. (2001). “Classification of Electromyograph for Localised Muscle Fatigue Using Neural Networks.” *Proceedings, Seventh Australian and New Zealand Intelligent Information Systems Conference*, Perth, Australia, Nov. 18–21, pp. 271–275.
- Ray, S. J. and Teizer, J. (2012). “Real-time construction worker posture analysis for ergonomics training.” *Advanced Engineering Informatics*, 26(2), pp. 439-455.
- Spielholz, P., Silverstein, B., Morgan, M., Checkoway, H., and Kaufman, J. (2001). “Comparison of self-report, video observation and direct measurement methods for upper extremity musculoskeletal disorder physical risk factors.” *Ergonomics*, 44(6), pp. 588–613.

Syahril, F., and Sonjaya, E. (2015). "Validity, sensitivity, and reliability testing by ergonomic evaluation methods for geothermal task." *Proceedings, World Geothermal Congress*, Melbourne, Australia, Apr. 29-25.

The Center for Construction Research and Training (2012). "Fatal and nonfatal construction injuries in selected industrial countries." <http://www.cpwr.com/sites/default/files/publications/CB%20page%2037.pdf> (accessed in March 2017)

Workers' Compensation Board (2015) "Employers home: Modified work." Accessed from <https://www.wcb.ab.ca/return-to-work/> (accessed in December, 2015)

References for Chapter 2

- Association of Workers' Compensation Board of Canada (2013). "2013 injury statistics." <http://awcbc.org/?page_id=14> (accessed January, 2014).
- Alwasel, A., Elrayes, K., Abdel-Rahman, E. M., and Haas, C. T. (2011). "Sensing construction work-related musculoskeletal disorders (WMSDs)." *Proceedings, International Association for Automation and Robotics in Construction (IAARC)*, London, UK, pp. 164–169.
- British Columbia Municipal Safety Association (2016). "City of Vancouver" <<http://www.bcmsa.ca/resources/physical-job-demand-analysis/>> (accessed March, 2016).
- BLS (Bureau of Labor Statistics). (2014). "Nonfatal cases involving days away from work: Selected characteristics (2011 forward)." <<http://www.bls.gov/data/#injuries>> (accessed January, 2014).
- Bernard T. E. (2010). "Washington state WISHA screening tool (modified)" <http://personal.health.usf.edu/tbernard/HollowHills/WISHA_Checklist_20.pdf> (accessed December, 2016).
- Canadian Centre for Occupational Health and Safety (2016). "Hazards." <https://www.ccohs.ca/topics/hazards/ergonomic/#ctgt_1-1> (accessed October, 2016).
- Christmansson, M., Falck, A.-C., Amprazis, J., Forsman, M., Rasmusson, L., and Kadefors, R. (2000). "Modified method time measurements for ergonomic planning of production systems in the manufacturing industry." *International Journal of Production Research*, 38(17), pp. 4051–4059.
- Deros, B., Khamis, N. K., Ismail, A. R., Jamaluddin, H., Adam, A.M., and Rosli, S. (2011). "An ergonomics study on assembly line workstation design." *American Journal of Applied Sciences*, 8(11), pp. 1195–1201.

- David, G. C. (2005). "Ergonomic methods for assessing exposure to risk factors for work-related musculoskeletal disorders." *Occupational Medicine*, 55(3), pp. 190–199.
- Ergonomics Plus Inc., 2015. "A step-by step guide to using the NIOSH lifting equation for single tasks." <<http://ergo-plus.com/niosh-lifting-equation-single-task/>> (accessed December, 2015).
- Elola, L. N., Clara, A., and Tejedor, P. (1996). "New methods of evaluating physical demand at work areas." *Technovation*, 16(10), pp. 595–599.
- Safety and Health Authority (2006). Ergonomics in the Workplace. <http://www.hsa.ie/eng/Publications_and_Forms/Publications/Manual_Handling_and_Musculoskeletal_Disorders/Ergonomics_in_the_Workplace.html> (accessed March, 2015).
- Finnish Institute of Occupational Health (2009). PEO (Portable ergonomic observation method), Accessed from <http://partner.ttl.fi/en/ergonomics/methods/workload_exposure_methods/table_and_methods/Documents/PEO.pdf> (accessed June, 2016).
- Fransson-Hall, C., Gloria, R., Kilbom, A., Winkel, J., Karlqvist, L., and Wiktorin, C. (1995). "A portable ergonomic observation method (PEO) for computerized on-line recording of postures and manual handling." *Applied Ergonomics*, 26(2), pp. 93–100.
- Getty, R. L. (1994). "Physical demands of work are the common reference for an integrated ergonomics program." *Proceedings, Human Factors and Ergonomics Society 38th Annual Meeting*, Fort Worth, TX, USA, pp. 683–687.
- Golabchi, A., Han, S., Seo, J., Han, S., Lee, S., and Al-Hussein, M. (2015). "An automated biomechanical simulation approach to ergonomic job analysis for workplace design." *Journal of Construction Engineering and Management*, 141(8), 4015020.

- Hales, C. (1995). "Five fatal designs." In V. Hubla (Ed.), *Proceedings, 10th International Conference on Engineering Design Prague, Czech Republic, Aug. 22–24*, pp. 662–667.
- Han, S. and Lee, S. (2013). "A vision-based motion capture and recognition framework for behavior-based safety management." *Automation in Construction*, 35, pp. 131–141.
- Halpern, M., Skovron, M. L., and Nordin, M. (1997). "Employee-rated job demands: Implications for prevention of occupational back injuries." *International Journal of Industrial Ergonomics*, 20(2), pp. 145–153.
- Health and Safety Executive (2014). "Worried about your hands?" <<http://www.hse.gov.uk/vibration/hav/yourhands.htm>> (accessed January, 2017).
- Hignett S. and McAtamney, L. (2000). "Rapid Entire Body Assessment." *Applied Ergonomics*, 31, pp. 201–205.
- Industrial Accident Prevention Association (2009). "Performing a Physical Demands Analysis Instructions on How to Use the Physical Demands Analysis (PDA) Form." <www.iapa.ca/Main/documents/pdf/FreeDownloads_PDA_intro.pdf> (accessed January, 2017).
- Infrastructure Health & Safety Association. (2014). "General Guide for Identifying Ergonomics-Related Hazards." <http://www.ihsa.ca/pdfs/msd/identify_ergonomics.pdf> (accessed July, 2014).
- Karhu, O., Härkönen, R., Sorvali, P., and Vepsäläinen, P. (1981). "Observing working postures in industry: Examples of OWAS application." *Applied Ergonomics*, 12(1), pp. 13–17.
- Karhu, O., Kansu, P., and Kuorinka, I. (1997). "Correcting working postures in industry: A practical method for analysis." *Applied Ergonomics*, 8(4), pp. 199–201.

- Laring, J., Christmansson, M., Kadefors, R., and Örtengren, R. (2005). "ErgoSAM: A preproduction risk identification tool." *Human Factors and Ergonomics in Manufacturing*, 15(3), pp. 309–325.
- Li, G. and Buckle, P. (1999). "Current techniques for assessing physical exposure to work-related musculoskeletal risks, with emphasis on posture-based methods." *Ergonomics*, 42(5), pp. 674–695.
- Li, X., Fan, G., Abudan, A., Sukkarieh, M., Inyang, N., Gül, M., El-Rich, M., and Al-Hussein, M. (2015). "Ergonomics and Physical Demand Analysis in a Construction Manufacturing Facility." *Proceedings, 5th International / 11th Construction Specialty Conference*, Vancouver, BC, Canada, Jun. 8–10.
- Li, X., Han, S., Gül, M., and Al-Hussein, M. (2016). "3D motion-based ergonomic and body posture analysis in construction." *Proceedings, Modular and Offsite Construction (MOC) Summit*, Edmonton, AB, Canada, Sep. 29–Oct. 1, pp. 215–223.
- Määttä, T. J. (2007). "Virtual environments in machinery safety analysis and participatory ergonomics." *Human Factors and Ergonomics in Manufacturing*, 17(5), pp. 435–443.
- McAtamney, L. and Corlett, E. N. (1993). "RULA: A survey method for investigation of work related upper limb disorders." *Applied Ergonomics*, 24(2), pp. 91–99.
- Middlesworth, M. (2012). "A step-by-step guide to the Rapid Entire Body Assessment (REBA) tool". *Ergonomics Plus*, <www.ergo-plus.com> (accessed January, 2016)
- Mitropoulos, P., Cupido, G., and Namboodiri, M. (2009). "Cognitive approach to construction safety: Task demand-capability model." *Journal of Construction Engineering and Management*, 135(9), pp. 881–889.

- Minnesota Occupational Health. (2012) “Job task analysis: Physical demands.”
<<http://www.co.ramsey.mn.us/NR/rdonlyres/82FC98AB-2D47-4E07-BE70-321069D91D80/35969/JobTaskAnalysisElectronicTrffcSignlTech5112.pdf>> (accessed December, 2015).
- Murphy, S., Buckle, P., and Stubbs, D. (2002). “The use of the portable ergonomic observation method (PEO) to monitor the sitting posture of schoolchildren in the classroom.” *Applied Ergonomics*, 33(4), pp. 365–370.
- Nelson, G., Wickes, H., and English, J. T. (1994). “Manual lifting: The revised NIOSH lifting equation for evaluating acceptable weights for manual lifting.” Nelson & Associates, Campbell, CA, USA.
- National Institute for occupational Safety and Health (NIOSH) (1981). “A Work Practices Guide for Manual Lifting.” Technical Report No. 81-122. U.S. Department of Health and Human Services (NIOSH), Cincinnati, OH, USA.
- Occupational Safety and Health Administration (1990). “Ergonomic program management guidelines for meatpacking plants” (Publication No. OSHA-3121). Washington, DC, USA: U.S. Department of Labor.
- Okimoto, M. L. L. R. and Teixeira, E. R. (2009). “Proposed procedures for measuring the lifting task variables required by the Revised NIOSH Lifting Equation: A case study.” *International Journal of Industrial Ergonomics*, 39(1), pp. 15–22.
- Ontario Safety Association for Community and Healthcare (2010). Musculoskeletal Disorders Prevention Series Part 1: MSD Prevention Guideline for Ontario.
<http://www.osach.ca/misc_pdf> (accessed March, 2015).

Occupational Health Clinics for Ontario Workers Inc. (2012) “Guidelines to implementing and performing physical demand analysis handbook.” <<http://www.ohcow.on.ca/uploads/Resource/Workbooks/pdamanualbook.pdf>> (accessed December, 2015).

Occupational Health and Safety. (2015). “Provincial workers’ compensation boards in Canada.” <http://www.ccohs.ca/oshanswers/information/wcb_canada.html> (accessed December, 2016).

Ray, S. J. and Teizer, J. (2012). “Real-time construction worker posture analysis for ergonomics training.” *Advanced Engineering Informatics*, 26(2), pp. 439–455.

Workers’ Compensation Board-Alberta (2014). “Employer – physical demands analysis”. <www.wcb.ab.ca/pdfs/employers/C545.doc> (accessed March, 2016).

Workers’ Compensation Board-Alberta (2015a). “WCB-Alberta worker handbook.” <https://www.wcb.ab.ca/pdfs/workers/WCB-003_Worker_Handbook_2015.pdf> (accessed October, 2015).

Workers’ Compensation Board-Alberta. (2015b) “Millard Health Rehabilitation Centre: Workshops.” <<http://www.wcb.ab.ca/millard/workshops.asp>> (accessed December, 2015).

Workers’ Compensation Board-Alberta. (2015c) “Employers home>Modified work.” <http://www.wcb.ab.ca/employers/mod_work.asp> (accessed December, 2015).

Workplace safety North (2016). “Physical demands analysis”. <<https://www.workplacesafetynorth.ca/subsite/msds-priority-hazards/physical-demands-analysis>> (accessed December, 2016)

Wang, D., Dai, F., and Ning, X. (2015). "Risk assessment of work-related musculoskeletal disorders in construction: State-of-the-art review." *Journal of Construction Engineering and Management*, 141(6), 4015008.

Waters, T. R., Putz-Anderson, V., Garg, A., and Fine, L. J. (1993). "Revised NIOSH equation for the design and evaluation of manual lifting tasks." *Ergonomics*, 36(7), pp. 749–776.

References for Chapter 3

- Asensio-Cuesta, S., Diego-Mas, J. a., Cremades-Oliver, L. V., and González-Cruz, M. C. (2012). “A method to design job rotation schedules to prevent work-related musculoskeletal disorders in repetitive work.” *International Journal of Production Research*, 50(24), pp. 7467–7478.
- AnyBody Technology A/S. (2015). “Case Stories.” Aalborg, Denmark. <<http://www.anybodytech.com/index.php?id=1102>> (accessed in June, 2015).
- Advanced Mechanical Technology Inc. (2015) “Force and motion.” Watertown, MA, USA. <<http://www.amti.biz>> (accessed January, 2015).
- Cao, H., El Hajj Dib, I., Antoni, J., and Marque, C. (2007). “Analysis of muscular fatigue during cyclic dynamic movement.” *Proceedings, Annual International Conference of the IEEE Engineering in Medicine and Biology Society*, pp. 1880–1883.
- Demoulin, C. (2010). “Muscular Performance Assessment of Trunk Extensors: A Critical Appraisal of the Literature.” <<http://cdn.intechopen.com/pdfs-wm/36700.pdf>> (accessed February, 2015).
- De Zee, M., Hansen, L., Wong, C., Rasmussen, J., and Simonsen, E. B. (2007). “A generic detailed rigid-body lumbar spine model.” *Journal of Biomechanics*, 40(6), pp. 1219–1227.
- Demoulin, C., Vanderthommen, M., Duysens, C., and Crielaard, J.-M. (2006). “Spinal muscle evaluation using the Sorensen test: a critical appraisal of the literature.” *Joint Bone Spine*, 73(1), pp. 43–50.
- El-Rich, M. and Shirazi-Adl, A. (2005). “Effect of load position on muscle forces, internal loads and stability of the human spine in upright postures.” *Computer Methods in Biomechanics and Biomedical Engineering*, 8(6), pp. 359–368.

- Erdemir, A., McLean, S., Herzog, W., and van den Bogert, A. J. (2007). "Model-based estimation of muscle forces exerted during movements." *Clinical Biomechanics (Bristol, Avon)*, 22(2), pp. 131–154.
- Finni, T., Komi, P. V, and Lukkariniemi, J. (1998). "Achilles tendon loading during walking: application of a novel optic fiber technique." *European Journal of Applied Physiology and Occupational Physiology*, 77(3), pp. 289–291.
- Georgakis, A., Stergioulas, L. K., and Giakas, G. (2003). "Fatigue analysis of the surface EMG signal in isometric constant force contractions using the averaged instantaneous frequency." *IEEE Transactions on Bio-Medical Engineering*, 50(2), pp. 262–265.
- Hildebrandt, V. H. (1995). "Back pain in the working population: prevalence rates in Dutch trades and professions." *Ergonomics*, 38(6), pp. 1283–1298.
- Hsie, M., Hsiao, W. T., Cheng, T. M., and Chen, H. C. (2009). "A model used in creating a work-rest schedule for laborers." *Automation in Construction*, 18(6), pp. 762–769.
- Jaffar, N., Abdul-Tharim, a. H., Mohd-Kamar, I. F., and Lop, N. S. (2011). "A literature review of ergonomics risk factors in construction industry." *Procedia Engineering*, 20, pp. 89–97.
- Kim, G., Ahad, M., Ferdjallah, M., and Harris, G. (2007). "Correlation of muscle fatigue indices between intramuscular and surface EMG signals." *Proceedings, IEEE SoutheastCon*, Richmond, VA, USA, Mar. 22-25, pp. 378–382.
- Komi, P. V, Fukashiro, S., and Järvinen, M. (1992). "Biomechanical loading of Achilles tendon during normal locomotion." *Clinics in Sports Medicine*, 11(3), pp. 521–531.
- Komeili, A., Li, X., Gül, M., Lewick, J., and El-Rich, M. (2015). "An evaluation method of assessing the low back muscle fatigue in manual material handling." *Proceedings, Modular*

and Offsite Construction Summit & 1st International Conference on the Industrialization of Construction, Edmonton, AB, Canada, May 19-21, pp. 467–475.

Li, X.*, Fan, G., Abudan, A., Sukkarieh, M., Inyang, N., Gül, M., El-Rich, M., and Al-Hussein, M. (2015). “Ergonomics and physical demand analysis in a construction manufacturing facility.” *Proceedings, International Construction Specialty Conference*, Vancouver, BC, Canada, Jun. 7-10.

Lindström, L., Kadefors, R., and Petersén, I. (1977). “An electromyographic index for localized muscle fatigue.” *Journal of Applied Physiology: Respiratory, Environmental and Exercise Physiology*, 43(4), pp. 750–754.

Mananas, M. A., Rojas, M., Mandrile, F., and Chaler, J. (2005). “Evaluation of muscle activity and fatigue in extensor forearm muscles during isometric contractions.” *Proceedings, Annual International Conference of the IEEE Engineering in Medicine and Biology Society*, 6, Shanghai, China, Aug. 31-Sep. 3, pp. 5824–5827.

Motion Analysis Corp. (2015) “Motion analysis.” Santa Rosa, CA, USA. <<http://www.motionanalysis.com>> (accessed January, 2015).

Prilutsky, B. I. and Zatsiorsky, V. M. (2002). “Optimization-Based Models of Muscle Coordination.” *NIH Public Access*, 30(1), pp. 32–38.

Roy, S. H., De Luca, C. J., and Casavant, D. A. (1989). “Lumbar muscle fatigue and chronic lower back pain.” *Spine*, 14(9), pp. 992–1001.

Rasmussen, J., Damsgaard, M., and Voigt, M. (2001). “Muscle recruitment by the min/max criterion - A comparative numerical study.” *Journal of Biomechanics*, 34(3), pp. 409–415.

- Schellenberg, F., Oberhofer, K., Taylor, W. R., and Lorenzetti, S. (2015). “Review of modelling techniques for in vivo muscle force estimation in the lower extremities during strength training.” *Computational and Mathematical Methods in Medicine*, 483921,12.
- Sarmiento, J. F., Benevides, A. B., Moreira, M. H., Elias, A., Bastos, T. F., Silva, I. V, and Pelegrina, C. C. (2011). “Comparative Muscle Study Fatigue with sEMG signals during the Isotonic and Isometric Tasks for Diagnostics Purposes.” *Proceedings, 33rd Annual International Conference of the IEEE EMBS*, Boston, MA, USA, Aug. 30-Sep. 3, pp. 7163–7166.
- Vaughan, C. L., Davis, B. L., and O’Connor, J. C. (1992). *Dynamics of human gait, Volume 2. Human Kinetics Publishers.*
http://books.google.ca/books/about/Dynamics_of_human_gait.html?id=YMFaAAAAYA-AJ&pgis=1 (accessed in June 2014).
- Van Bolhuis, B.M. and Gielen, C.C. (1999). “A comparison of models explaining muscle activation patterns for isometric contractions.” *Biologic Cybernetics*, 81(3), pp. 249-261.
- Winter, D. A. (2009). *Biomechanics and Motor Control of Human Movement* (4th Edition). Wiley. < <http://ca.wiley.com/WileyCDA/WileyTitle/productCd-0470398183.html>> (accessed in June 2014).
- Wagner, D. W., Reed, M. P., and Rasmussen, J. (2007). “Assessing the importance of motion dynamics for ergonomic analysis of manual materials handling tasks using the anybody modelling system.” *SAE Technical Papers*.
- Zajac, F. E., Neptune, R. R., and Kautz, S. A. (2003). “Biomechanics and muscle coordination of human walking: part II: lessons from dynamical simulations and clinical implications.” *Gait & Posture*, 17(1), pp. 1–17.

References for Chapter 4

- Al-Hussein, M., Niaz, M.A., Yu, H., and Kim, H. (2005). "Integrating 3D visualization and simulation for tower crane operations on construction site." *Automation in Construction*, 15(5), pp. 554–562.
- Alwasel, A., Elrayes, K., Abdel-Rahman, E. M., and Haas, C. T. (2011). "Sensing construction work-related musculoskeletal disorders (WMSDs)." *Proceedings, International Association for Automation and Robotics in Construction (IAARC)*, London, UK, pp. 164–169.
- Autodesk Inc. (2016). "Create amazing worlds in 3ds Max." <http://www.autodesk.com/products/3ds-max/overview-dts?s_tnt=69291:1:0> (accessed in January 2017).
- Autodesk Inc. (2011). "MAXScript Introduction" <<http://docs.autodesk.com/3DSMAX/14/ENU/MAXScript%20Help%202012/>> (accessed in January 2017).
- Dennis, P. (2002). *Lean Production Simplified, Second Edition*. Productivity Press, New York, NY, USA.
- David, G. C. (2005). "Ergonomic methods for assessing exposure to risk factors for work-related musculoskeletal disorders." *Occupational Medicine*, 55(3), pp. 190–199.
- Feyen, R., Liu, Y., Chaffin, D., Jimmerson, G., and Joseph, B. (2000). "Computer-aided ergonomics: A case study of incorporating ergonomics analyses into workplace design." *Applied Ergonomics*, 31(3), pp. 291–300.
- Golabchi, A., Han, S., Seo, J., Han, S., Lee, S., and Al-Hussein, M. (2015). "An automated biomechanical simulation approach to ergonomic job analysis for workplace design." *Journal of Construction Engineering and Management*, 141(8), 04015020.

- Han, S. and Lee, S. (2013). "A vision-based motion capture and recognition framework for behavior-based safety management." *Automation in Construction*, 35, pp. 131–141.
- Hignett, S. and McAtamney, L. (2000). "Rapid entire body assessment (REBA)." *Applied Ergonomics*, 31(2000), pp. 201–205.
- Han, S.H., Hasan, S., Bouferguene, A., Al-Hussein, M., and Kosa, J. (2014). "Utilization of 3D visualization of mobile crane operations for modular construction on-site assembly." *Journal of Management in Engineering*, 31(5), 04014080.
- Inyang, N. and Mohamed Al-Hussein. (2011). "Ergonomic hazard quantification and rating of residential construction tasks." *Proceedings, CSCE Annual Conference*, Ottawa, ON, Canada, Jun. 14-17.
- Janowitz, I. L., Gillen, M., Ryan, G., Rempel, D., Trupin, L., Swig, L., ... Blanc, P. D. (2006). "Measuring the physical demands of work in hospital settings: Design and implementation of an ergonomics assessment." *Applied Ergonomics*, 37(5), pp. 641–658.
- Karhu, O., Kansi, P., and Kuorinka, I. (1997). "Correcting working postures in industry: A practical method for analysis." *Applied Ergonomics*, 8, pp. 199–201.
- Kamat, V. R., Martinez, J. C., Fischer, M., Golparvar-Fard, M., Peña-Mora, F., and Savarese, S. (2011). "Research in visualization techniques for field construction." *Journal of Construction Engineering and Management*, 137(10), pp. 853–862.
- Li, G. and Buckle, P. (1999). "Current techniques for assessing physical exposure to work-related musculoskeletal risks, with emphasis on posture-based methods." *Ergonomics*, 42, pp. 674–695.

- Li, X., Komeili, A., Gül, M., and El-Rich, M. (2017). “A framework for evaluating muscle activity during repetitive manual material handling in construction manufacturing.” *Automation in Construction*, AUTCON-02194, 10 pages (In press).
- Manrique, J.D., Al-Hussein, M., Telyas, A., and Funston, G. (2007). “Constructing a complex precast tilt-up panel structure utilizing an optimization model, 3D CAD, and animation.” *Journal of Construction Engineering and Management*, 133(3), pp. 199–207.
- McAtamney, L. and Corlett, E. N. (1993). “RULA: A survey method for investigation of work related upper limb disorders.” *Applied Ergonomics*, 24(2), pp. 91–99.
- Middlesworth, M. (2012). “A step-by-step guide: Rapid Entire Body Assessment (REBA).” Ergonomics Plus, from <www.ergo-plus.com>.
- Mitropoulos, P., Cupido, G., and Namboodiri, M. (2009). “Cognitive approach to construction safety: Task demand-capability model.” *Journal of Construction Engineering and Management*, 135(9), pp. 881–889.
- Motion Analysis Corp. (2016). “Motion analysis.” Santa Rosa, CA, USA. <<http://www.motionanalysis.com>> (accessed in January 2017)
- Ontario Safety Association for Community and Healthcare (2010). “Musculoskeletal disorders prevention series Part 1: MSD prevention guideline for Ontario.” <http://www.osach.ca/misc_pdf> (March, 2015).
- Ray, S. J. and Teizer, J. (2012). “Real-time construction worker posture analysis for ergonomics training.” *Advanced Engineering Informatics*, 26(2), pp. 439–455.
- Staub-French, S., Russell, A., and Tran, N. (2008). “Linear scheduling and 4D visualization.” *Journal of Computing in Civil Engineering*, 22(3), pp.192–205.

Schneider, S.P. (2001). “Musculoskeletal injuries in construction: A review of the literature.” *Applied Occupational and Environmental Hygiene*, 16(11), pp. 1056–1064.

University of Michigan, Center of Ergonomics (2012). “3D static strength prediction program.” http://djhurij4nde4r.cloudfront.net/attachments/files/000/000/284/original/Manual_606.pdf?1406656210 (accessed July, 2016).

Wang, D., Dai, F., and Ning, X. (2015). “Risk assessment of work-related musculoskeletal disorders in construction: State-of-the-art review.” *Journal of Construction Engineering and Management*, 141(6), 4015008.

References for Chapter 5

Escobar, C. (2006). Sensitivity Analysis of Subjective Ergonomic Assessment Tools: Impact of Input Information Accuracy on Output (Final Scores) Generation. Graduate Faculty of Auburn University, 54, 258. <<http://etd.auburn.edu/etd/handle/10415/386>> (accessed January, 2017).

University of Michigan, Center of Ergonomics (2012). “3D static strength prediction program.” <http://djhurij4nde4r.cloudfront.net/attachments/files/000/000/284/original/Manual_606.pdf?1406656210> (accessed July, 2016).

APPENDIX A

Table A-1: Time study table (60-min)

#	Lifting			Carrying			Pushing/Pulling			Grasping & Pinching			#
	Low	Waist	Above shoulder	Front	Side-Right	Side-Left	On shoulder	Push	Pull	Hand dominant	Hand non-dominant	Grip dominant	
1													1
2													2
3													3
4													4
5													5
6													6
7													7
8													8
9													9
10													10
11													11
12													12
13													13
14													14
15													15
16													16
17													17
18													18
19													19
20													20
21													21
22													22
23													23
24													24
25													25
26													26
27													27
28													28
29													29
30													30
:													:
:													:
:													:
50													50
51													51
52													52
53													53
54													54
55													55
56													56
57													57
58													58
59													59
60													60

Job: _____ Job number: _____ Observer: _____ Date: _____

#	Mobility					Back			Shoulder				#	
	Walk	Stand	Sit/drive	Climb	Crouch/Squat	Kneel/Crawling	Forward	Backward	Twist/Rotation	Above	Forward	Below		Sideway
1														1
2														2
3														3
4														4
5														5
6														6
7														7
8														8
9														9
10														10
11														11
12														12
13														13
14														14
15														15
16														16
17														17
18														18
19														19
20														20
21														21
22														22
23														23
24														24
25														25
26														26
27														27
28														28
29														29
30														30
:														:
:														:
:														:
50														50
51														51
52														52
53														53
54														54
55														55
56														56
57														57
58														58
59														59
60														60

Job:

Job number:

Observer:

Date:

#	Neck			Elbow	Wrist		Ankle		Sensory Demand			#		
	Forward	Backward	Twist/Tilt	Flex/Extend	Flex/Extend	Bending	Rotate	Flex/Extend	Rotate	Hear/Speech	Sound discrimination		Vision	Colour
1														1
2														2
3														3
4														4
5														5
6														6
7														7
8														8
9														9
10														10
11														11
12														12
13														13
14														14
15														15
16														16
17														17
18														18
19														19
20														20
21														21
22														22
23														23
24														24
25														25
26														26
27														27
28														28
29														29
30														30
:														:
:														:
:														:
50														50
51														51
52														52
53														53
54														54
55														55
56														56
57														57
58														58
59														59
60														60

Job: _____ Job number: _____ Observer: _____ Date: _____

APPENDIX B

Table B-1 expands the explanation in Chapter 4 regarding which markers are to be used for the calculation: hand is calculated based on the coordinates of the finger and the center of the wrist; upper arm is calculated based on the marker on the shoulder (acromion clavicular joint) and on the upper arm; lower arm is calculated referring to wrist B and the elbow; clavicle is estimated by the shoulder position on each side and the center of the clavicle; upper leg is calculated by the coordinates of the knee and the thigh; lower leg is estimated by the positions of the tibia and the ankle; foot is measured by the markers on the heel and the first toe; trunk flexion is calculated based on cervical vertebra C7 and the Pelvis-Posterior Superior Iliac Spine (PSIS); while pelvis movement is analyzed by the two PSIS on the back of the body.

Table B-2 expands the information in Table 4-1 in Chapter 4 and summarizes the REBA/RULA ratings for all the body segments for all three subjects.

Table B-1: Descriptions of marker positions for motion capture data collection

Body Segment	Marker Positions	Marker Position Descriptions	Abbreviation
Hand (finger, center of the wrist)	Finger	Place marker on the proximal phalanx of the index finger.	Finger
	Wrist	Place markers on the radial styloid process of the ulna and the styloid process of the radius, respectively, for each wrist.	Wrist A, Wrist B
Upper Arm (shoulder, upper arm)	Shoulder (Acromion-clavicular joint)	Place markers on each of the left and right acromion-clavicular joint.	Shoulder
Lower Arm (wrist B, elbow)	Upper arm	Place the marker at the middle of upper arm between shoulder and elbow markers.	Upper Arm
	Elbow	Place the marker on the exterior of the elbow.	Elbow

Body Segment	Marker Positions	Marker Position Descriptions	Abbreviation
	Radius	Place the marker on the middle of the forearm between elbow and wrist B.	Radius
Clavicle (clavicle, shoulder)	Clavicle	Place the marker on two collar bones.	Clavicle
Upper Leg (knee, thigh)	Thigh	Place the marker at the middle of upper leg and on the vertical to the floor line together with the knee marker.	Thigh
	Knee	Place the marker on the lateral side of the knee on the lowest area of the upper leg.	Knee
Lower Leg (tibia, ankle)	Tibia	Place the marker at the middle of lower leg, on the outer edge of the fibula bone, between knee and ankle markers.	Tibia
	Ankle	Put a marker along the line that connects the opposite sides of the ankle bone.	Ankle
Foot (heel, toe)	Heel	Place a marker on the posterior side of the heel bone at the same height as the toe marker.	Heel
	Toe	Place a marker on the first toe.	Toe
Trunk (C7, PSIS)	Cervical vertebra 7	Place a marker on C7, located at the lowest level of cervical vertebra.	C7
Pelvis (PSIS)	Pelvis-posterior superior iliac	Place the marker on the dimples of the low back area at each side of the spinal column below the waist level.	PSIS

1 Table B-2: REBA/RULA rating comparison of each body segment for all subjects

Ratings	Factors	REBA									RULA								
		Subject 1			Subject 2			Subject 3			Subject 1			Subject 2			Subject 3		
	Methods	E	3D	M	E	3D	M	E	3D	M	E	3D	M	E	3D	M	E	3D	M
Neck	Average	1.72	2.00	1.46	1.70	1.97	1.54	1.95	1.97	1.62	3.19	3.99	2.54	3.1	3.90	2.77	3.83	3.91	2.85
	MAX	2	2	2	2	2	2	2	2	2	4	4	4	4	4	4	4	4	4
	MIN	1	1	1	1	1	1	1	1	1	1	1	1	1	1	1	1	1	1
	Difference	-	-0.28	0.26	-	-0.27	0.16	-	-0.02	0.33	-	-0.80	0.65	-	-0.80	0.33	-	-0.07	0.99
	Error	-	-28%	N/A	-	-27%	N/A	-	-4%	N/A	-	-77%	N/A	-	-80%	N/A	-	-13%	N/A
Trunk	Average	2.51	2.93	2.31	2.79	2.97	2.54	2.68	2.95	2.54	2.51	2.93	2.31	2.79	2.97	2.54	2.68	2.95	2.54
	MAX	3	4	3	4	4	4	4	4	4	3	4	3	4	4	4	4	4	4
	MIN	1	1	1	1	1	1	1	1	1	1	1	1	1	1	1	1	1	1
	Difference	-	-0.42	0.21	-	-0.18	0.25	-	-0.27	0.14	-	-0.42	0.21	-	-0.18	0.25	-	-0.27	0.14
	Error	-	-18%	N/A	-	-10%	N/A	-	-15%	N/A	-	-18%	N/A	-	-10%	N/A	-	-15%	N/A
Leg	Average	1.96	1.56	1.46	1.99	1.11	1.00	1.84	1.09	1.00	1.00	1.00	1.00	1.00	1.00	1.00	1.00	1.00	1.00
	MAX	2	2	2	2	2	1	2	2	1	1	1	1	1	1	1	1	1	1
	MIN	1	1	1	1	1	1	1	1	1	1	1	1	1	1	1	1	1	1
	Difference	-	0.40	0.50	-	0.88	0.99	-	0.75	0.84	-	0.00	0.00	-	0.00	0.00	-	0.00	0.00
	Error	-	19%	N/A	-	44%	N/A	-	37%	N/A	-	0%	N/A	-	0%	N/A	-	0%	N/A
UpperArm	Average	2.54	2.51	1.85	2.23	2.42	1.77	1.96	2.48	1.77	2.54	2.51	1.85	2.23	2.42	1.77	1.96	2.48	1.77
	MAX	4	4	3	4	4	3	4	4	3	4	4	3	4	4	3	4	4	3
	MIN	1	1	1	1	1	1	1	1	1	1	1	1	1	1	1	1	1	1
	Difference	-	0.03	0.69	-	-0.19	0.46	-	-0.52	0.19	-	0.03	0.69	-	-0.19	0.46	-	-0.52	0.19
	Error	-	-2%	N/A	-	-22%	N/A	-	-49%	N/A	-	-2%	N/A	-	-22%	N/A	-	-49%	N/A
LowerArm	Average	1.85	1.82	1.92	1.94	1.85	1.85	1.80	1.84	1.92	1.85	1.90	2.00	1.94	1.95	1.77	1.98	2.44	1.92
	MAX	2	2	2	2	2	2	2	2	2	2	3	3	2	3	2	3	3	2
	MIN	1	1	1	1	1	1	1	1	1	1	1	1	1	1	1	1	1	1
	Difference	-	0.04	-0.07	-	0.09	0.10	-	-0.03	0.12	-	-0.06	-0.15	-	-0.01	0.17	-	-0.46	0.06
	Error	-	-0%	N/A	-	3%	N/A	-	-11%	N/A	-	-5%	N/A	-	-2%	N/A	-	-45%	N/A
Wrist	Average	1.70	1.57	1.15	2.25	1.62	1.08	2.25	1.72	1.00	3.46	3.27	1.62	3.37	3.40	1.46	3.48	3.34	1.31
	MAX	3	2	2	3	2	2	3	3	1	4	4	4	4	4	3	4	4	2
	MIN	1	1	1	1	1	1	1	1	1	1	1	1	2	1	1	2	1	1
	Difference	-	0.13	0.55	-	0.63	1.17	-	0.53	1.25	-	0.19	1.84	-	-0.02	1.91	-	0.14	2.17
	Error	-	3%	N/A	-	23%	N/A	-	17%	N/A	-	4%	N/A	-	-4%	N/A	-	2%	N/A

2 Note: E-experiment; 3D-the proposed 3D modelling method, M-manual observation

APPENDIX C

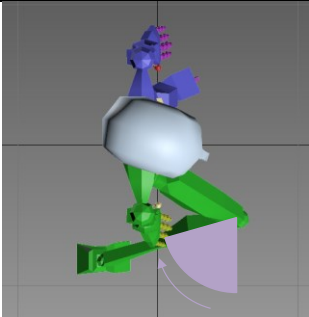
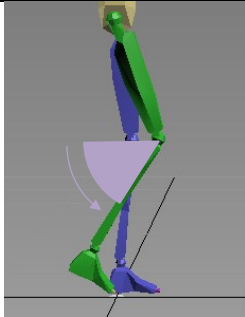
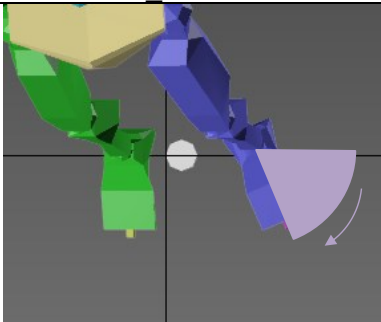
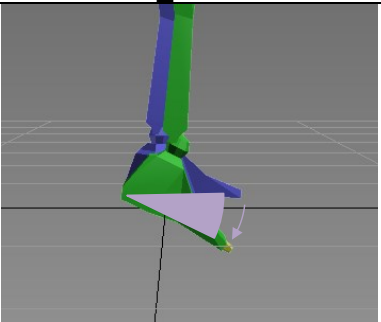
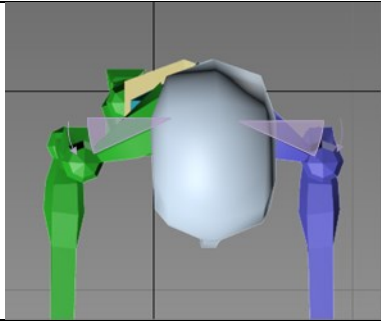
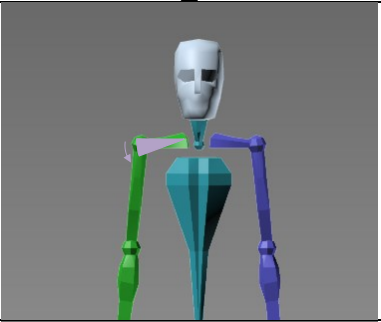
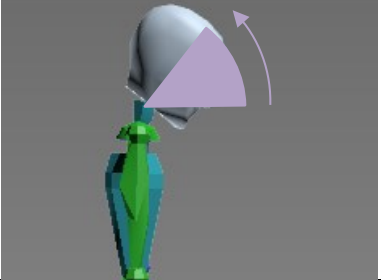
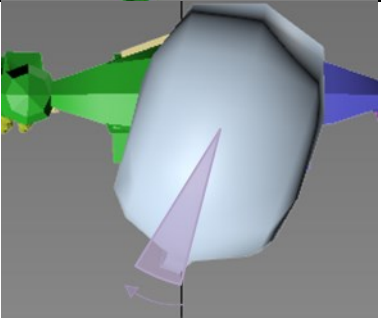
Table C-1: REBA/RULA rating comparison of subject 3-another lifting cycle

Risk rating/ Risk level	Methods	REBA			RULA		
		E	3D	M	E	3D	M
Rating	Average	5.57	5.39	3.47	5.83	6.12	4.60
	MAX	9	9	7	7	7	7
	MIN	1	3	1	4	3	2
	Difference	0.00	0.17	2.10	0.00	-0.29	1.23
	Error*	-	-5.58%	N/A	-	-9.45%	N/A
	Area	1837	1780	1202	1924	2020	1568
	Area percentage [#]	-	3.10%	34.56%	-	-4.99%	18.53%
Risk Level	Average	3.08	3.25	2.20	3.27	3.15	2.47
	MAX	4	4	3	4	4	4
	MIN	1	2	1	2	2	1
	Difference	0.00	-0.17	0.88	0.00	0.12	0.80
	Error*	-	-10.53%	N/A	-	-1.99%	N/A
	Area	1017	1073	754	1079	1041	837
	Area percentage [#]	-	-5.51%	25.83%	-	3.52%	22.45%

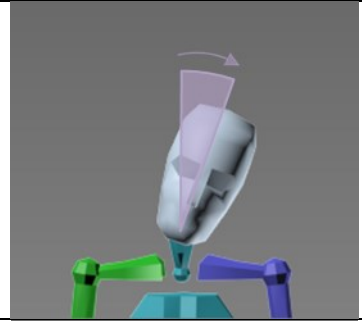
APPENDIX D

Table D-1: 41 Joint angle schematic drawings

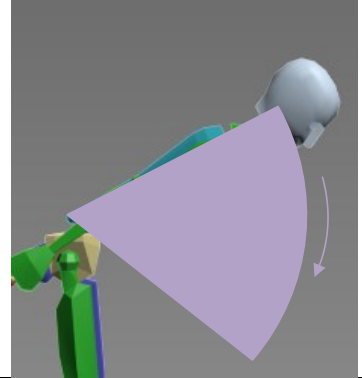
Body Parts	Joint Angle Schematic Drawings	
	Hand_Horizontal	Hand_Vertical
Hand		
Forearm	Forearm_Horizontal	Forearm_Vertical
Upperarm	Upperarm_Horizontal	Upperarm_Vertical
Upperleg	Upperleg_Horizontal	Upperleg_Vertical
Lowerleg	Lowerleg_Horizontal	Lowerleg_Vertical

		
	Foot Horizontal	Foot Vertical
Foot		
	Clavicle Horizontal	Clavicle Vertical
Clavicle		
	<p>Head flexion angle: the axis of the head/neck and a line drawn directly forward from the upper torso in a transverse plane at the C7-T1 spine level.</p>	
Neck / Head	<p>Head axial rotation angle: the rotation is about the axis of the head/neck.</p>	

Head lateral bending angle: between the axis of the head/neck and the projection of the same axis on the sagittal plane of the torso.

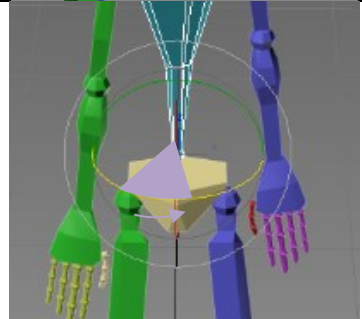


Trunk flexion angle: the angle between the projection of the trunk axis (the center of the hips to the center of the shoulders).



Trunk

Trunk axial rotation angle: the rotation of the torso about the axis formed by the line segment from the L5/S1 disc to the center of the shoulders; the rotation should be measured as the left shoulder location relative to the x -axis. If the left shoulder is rotated behind the x -axis, the angle is positive.



Trunk lateral bending angle: between the trunk axis and the y - z plane.

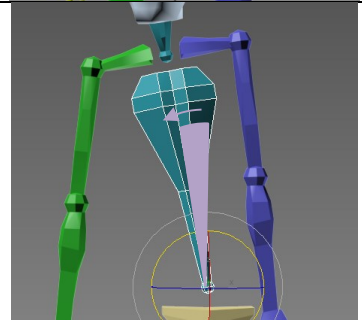
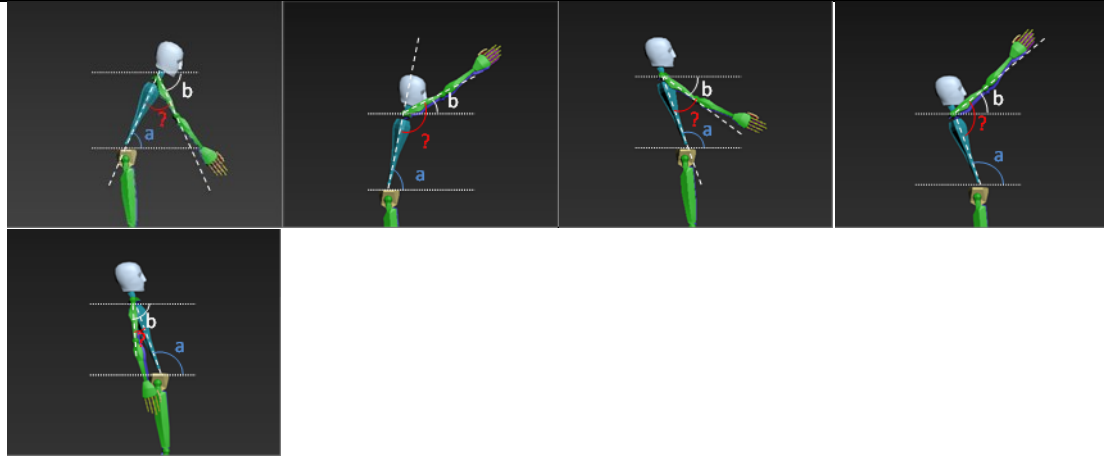
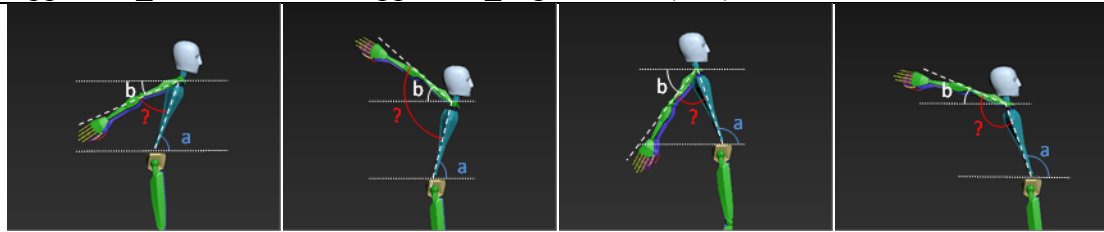


Table D-2: Scenarios covered by the proposed 3D modelling

Trunk	[0,180], [-180,0]
Trunk flexion < 90 or Trunk flexion > 90, Trunk_bending = 90-a	
Neck	[0,180], [-180,0]
Neck_flexion >= 0 or Neck_flexion < 0, Neck_flexion = b-a, where b = 90	
Leg	[0,180]
Upperleg_Horizontal > 0 & Lowerleg_Horizontal > 0, Leg_angle = abs(a-b)	Upperleg_Horizontal > 0 & Lowerleg_Horizontal < 0, Leg_angle = 180-abs(a+b)
Upperleg_Horizontal < 0 & Lowerleg_Horizontal > 0, Leg_angle = 180-abs(a+b)	Upperleg_Horizontal < 0 & Lowerleg_Horizontal < 0, Leg_angle = abs(a-b)
Upper Arm	[0,180], [-180,0]
Upperarm_Horizontal > 0, Upperarm_angle = 180-abs(a-b)	



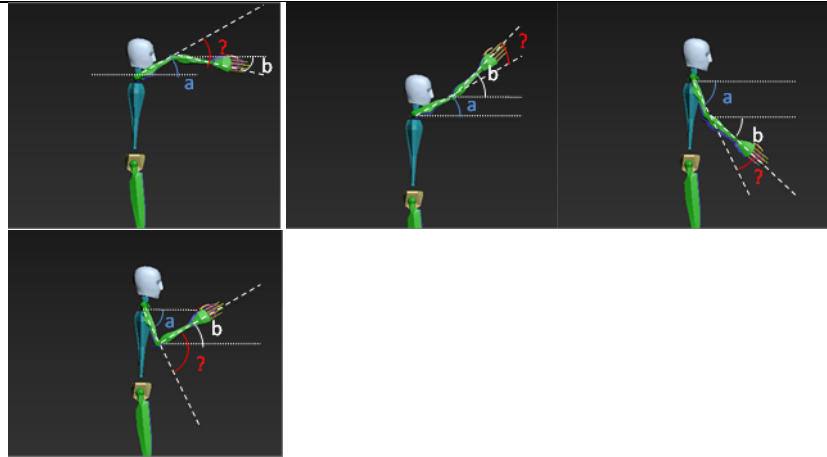
Upperarm_Horizontal < 0, Upperarm_angle = -abs(a+b)



Lower_arm [0,180]

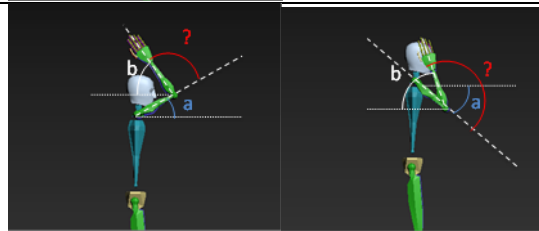
UpperArm_Horizontal > 0
&
LowerArm_Horizontal > 0,

Lowerarm_angle =
abs(a-b)



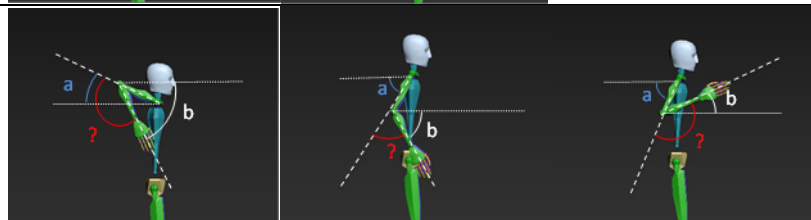
UpperArm_Horizontal > 0
&
LowerArm_Horizontal < 0,

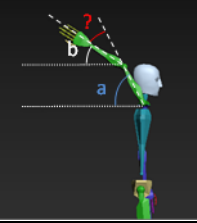
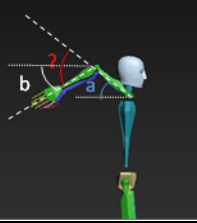
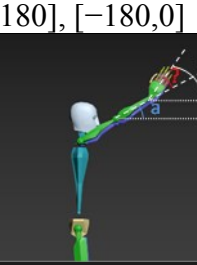
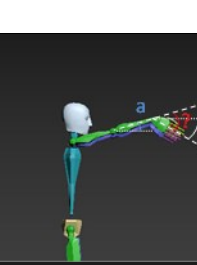
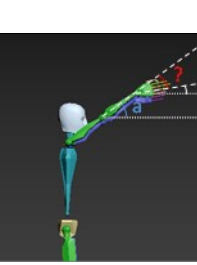
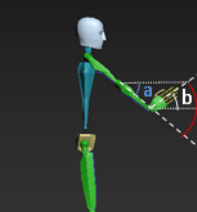
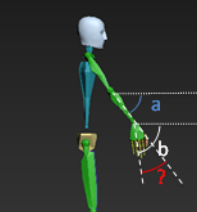
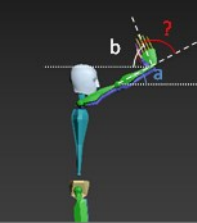
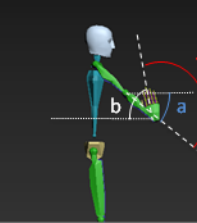
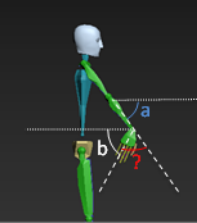
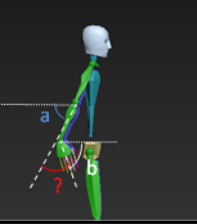
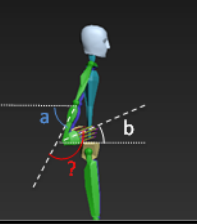
Lowerarm_angle =
180-abs(a+b)



UpperArm_Horizontal < 0
&
LowerArm_Horizontal > 0,

Lowerarm_angle =
180-abs(a+b)



<p>UpperArm_Horizontal < 0 & LowerArm_Horizontal < 0, Lowerarm_angle = abs(a-b)</p>			
<p>Wrist [0,180], [-180,0] Lowerarm_Horizontal > 0 & Wrist_Horizontal > 0, Wrist_angle = abs(a-b)</p>			
			
<p>Lowerarm_Horizontal > 0 & Wrist_Horizontal < 0, Wrist_angle = 180 - abs(a+b)</p>			
<p>Lowerarm_Horizontal < 0 & Wrist_Horizontal > 0, Wrist_angle = 180 -abs(a+b)</p>			
<p>Lowerarm_Horizontal < 0 & Wrist_Horizontal < 0, Wrist_angle = abs(a-b)</p>	